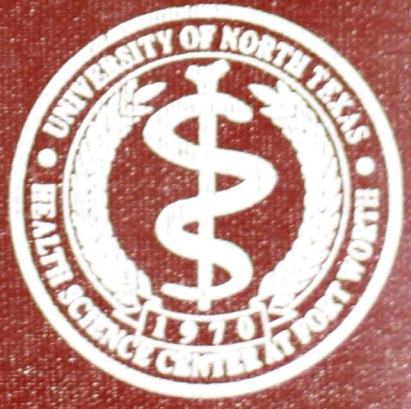
UNIVERSITY OF NORTH TEXAS
HEALTH SCIENCE CENTER AT FORT WORTH
1970

ET-1-induced signaling in ECM remodeling in astrocytes

Shaoqing He, Department of Pharmacology & Neuroscience, University of North Texas Health Science Center, Fort Worth, TX 76107

ET-1 levels are elevated under pathophysiological conditions, including glaucoma, however, ET-1's ocular functions are not fully documented. Therefore, ET-1-induced signaling and ECM remodeling in astrocytes and at the optic nerve head were determined in this study.

Three signaling pathways, including ERK1/2, PKC, and PI3 kinase, were involved in ET-1-mediated cell proliferation of U373MG astrocytoma cells. Blocking one of these pathways completely abolished cell proliferation. It appeared that ERK1/2 activation was involved, but was independent of PKC and PI3 kinase activation by ET-1. It was also determined that the ET_B receptor was the dominant receptor involved in ERK1/2 phosphorylation and cell proliferation. In addition, ERK1/2 phosphorylation was not transactivated by the EGF receptor by ET-1. The studies also indicated that there was no activation of c/nPKC, although PKC was involved in cell proliferation. In U373MG astrocytoma cells, MAPK-ERK, PKC and PI3K pathways appear to exert their roles in parallel without a direct, apparent "cross-talk".

Based on the signaling pathways obtained from U373MG astrocytoma cells, the regulation of MMPs/TIMPs and fibronectin in ET-1-activated human optic nerve head astrocytes (hONAs) was also determined. ET-1 not only induced rapid phosphorylation of ERK1/2 and PKC βI/βII/δ but also increased the activity of MMP-2 and the expression

of TIMP-1 and 2. The activity of MMP-2 was enhanced in the presence of inhibitors of MAPK or PKC in hONAs, whereas the expression of TIMP-1 and 2 was abolished. ET-1 increased the soluble fibronectin (FN) expression as well as FN matrix formation, however, the expression and deposition of FN were MAPK- and PKC-independent, whereas expression and activity of MMPs and TIMPs were MAPK- and PKC-dependent. Therefore, ET-1 shifted the balance of MMPs/TIMPs and substrates that altered the ECM composition and subsequently led to ECM remodeling in activated hONA cells.

ET-1's effects on ECM remodeling at the optic nerve head were also examined following intravitreal administration of ET-1 in rats. The increased expression of MMP-9 and collagen VI was detected in both ET_B deficient rats and wildtype Wistar rats post ET-1 intravitreal injection for 2 and 14 days, whereas the deposition of FN and collagen IV was unchanged. There was no significant difference in staining of MMP-9 and collagen VI between ET_B deficient rats and wildtype Wistar rats. In this study, ECM remodeling was demonstrated in rats injected with ET-1 into the vitreous. Such changes in the ECM seen in the current study provide additional insight into the mechanisms that might explain the glaucomatous changes observed in ET-1-injeciton or perfusion models.

In summary, ET-1 not only activated several signaling pathways in cell proliferation of astrocytes, but also modulated the expression of ECM molecules *in vitro* and *in vivo*, indicating that ET-1 plays a regulatory role in ECM remodeling. These effects coupled with observations that ET-1 levels are elevated in glaucoma patients, suggests that ET-1 may be involved in glaucomatous optic neuropathy.

Endothelin-1-induced Signaling

Involved in Extracellular Matrix Remodeling

APPROVED:

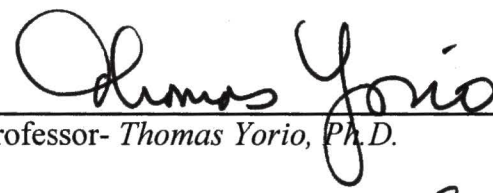

Major Professor- *Thomas Yorio, Ph.D.*

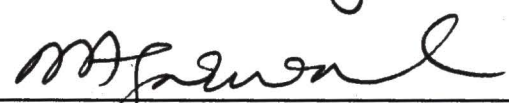

Committee Member- *Neeraj Agarwal, Ph.D.*

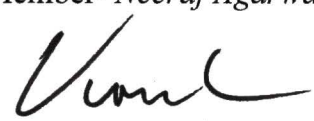

Committee Member- *Peter Koulen, Ph.D.*

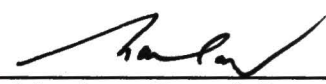

Committee Member- *Ganesh Prasanna, Ph.D.*

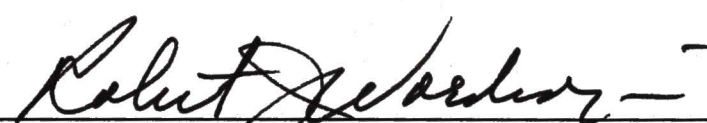

Universtiy Member- *Robert Wordinger, Ph.D.*

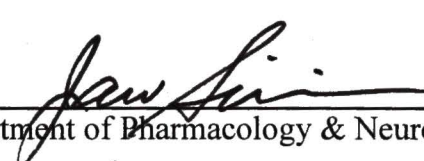

Chair, Department of Pharmacology & Neuroscience- *James Simpkins, Ph.D.*

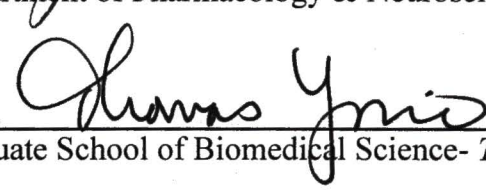

Dean, Graduate School of Biomedical Science- *Thomas Yorio, Ph.D.*

Endothelin-1-induced Signaling

Involved in Extracellular Matrix Remodeling

Ph.D. Dissertation

Presented to the Graduate Council of the University of North Texas Health Science Center at Fort Worth

In Partial Fulfillment of the Requirement for

the Degree of Doctorate of Philosophy

by

Shaoqing He M.S.

Department of Pharmacology & Neuroscience

UNTHSC, Fort Worth, Texas 76107

December, 2006

CONTENTS

ACKNOWLEDGEMENTS

I would like to express my deepest gratitude to my mentor, Dr. Thomas Yorio, for his guidance, instruction and support in many aspects during my graduate study. It is my lucky to have an opportunity to do research under the supervision of Dr. Yorio. I am working in the laboratory like coming into the bosom of a family. I have learnt not only scientific attitude and philosophy, but also life experience.

I also gratefully acknowledge my committee members, including Dr. Neeraj Agarwal, Dr. Peter Koulen, Dr. Ganesh Prasanna and Dr. Robert Wordinger, for their precious suggestions and time. I am deeply indebted to many people who helped me in the study, my colleagues in the laboratory Dr. Ganesh Prasanna, Dr. Raghu Krishnamoorthy, Dr. Adnan Dibas, Dr. Xinyu Zhang and everyone in the lab for their valuable discussions, generous help and kind cooperation.

In 2005, my father was diagnosed with thyroid tumor, which was a bad sign for him because a malignant tumor was removed at same site 32 years ago. My father and mother did not tell me this situation because they did not want me to worry and disturb my study. They knew that if I heard my father was so sick, nothing would stop me to fly all the way back home to take care of them. My tears are still in my eyes while I am writing the dissertation. What a great support they give me for my study aboard.

I would like to thank my wife, Dr. Dongmei Lu, and my lovely son, HongXuan He, who is waiting for my hooding for his doctoral degree in the future. They give me the endless love and continuing support.

LIST OF FIGURES

CHAPTER 1.

CHAPTER 2.

CHAPTER 3.

CHAPTER 4.

LIST OF TABLES

CHAPTER 4.

CHAPTER 1

Introduction

Cells are living in a dynamic environment, in which cells interact with each other and also interact with molecules in the extracellular space, extracellular matrix (ECM). The ECM not only functions as a structural support but also is involved in signal transduction between cells and the receptors on the cell surface. Therefore, the ECM remodeling is essential in many biological functions and physiopathological conditions, such as development, cell proliferation, cell differentiation, migration and disease progression. Numerous proteolytic enzymes are shown to participate in ECM degradation and remodeling, but one class that appears to play the pivotal role is the matrix metalloproteinases (MMPs).

MMPs, tissue inhibitors of matrix metalloproteinases (TIMPs) and ECM components:

MMPs are a large family of zinc-dependent enzymes that degrade the constituents of the extracellular matrix (ECM) [1,2]. More than 26 MMPs are identified in human. MMPs have a great diversity in their domain structure and substrate specificity, although they share some common features and activation mechanisms (Figure 1). They are synthesized as the secreted or transmembrane proproteins, and processed to active enzymes by proteolysis of an N-terminal propeptides. The propeptide inhibits the enzyme activity by binding with the catalytic domain of the enzyme [3]. Disruption of this

interaction triggers the cysteine switch mechanism and results in activation of the enzyme. There are several different domains in MMPs. A signal peptide at the N-terminus is important for secretion of pro-MMPs, a propeptide inhibits the activity of MMPs, a catalytic domain having a zinc binding site is important for the enzyme activity, and a hemopexin-like domain at the C-terminus binds with the catalytic domain. There are also some specific domains found in MMPs, such as fibronectin type II domain in MMP-2 and MMP-9 and a transmembrane domain in MT-MMPs (membrane-type MMPs) (structures depicted in Fig. 1) [4].

MMPs also display differential substrate specificity besides their structural differences. Based on their specificity of degrading the ECM substrates, MMPs are classified into several groups: collagenases, gelatinases, stromylisins, matrilysins, membrane-bound MMPs and other MMPs [3, 5]. MMPs were originally named according to their substrate specificity. Therefore, MMP-1, 8 and 13 are named as collagenases, MMP-2 and 9 as gelatinases, MMP-3, 10, and 11 as stromelysins. However, it is now clear that MMPs display overlapping substrate specificity. Gelatinases, MMP-2 and 9, can degrade collagen IV, V and X beside gelatins. MMP-7 degrades gelatin and collagen IV, and several MMPs degrade fibronectin, laminin, and elastin as well as membrane-bound receptors [3, 6]. MMPs utilize all of ECM molecules as substrates.

ECM consists of a number of proteins that form a dynamic extracellular environment. The major elements include collagens, fibronectin, elastin, laminin, receptors, integrins and glycosylated-macro proteins such as glycosamineglycan.

Figure 1

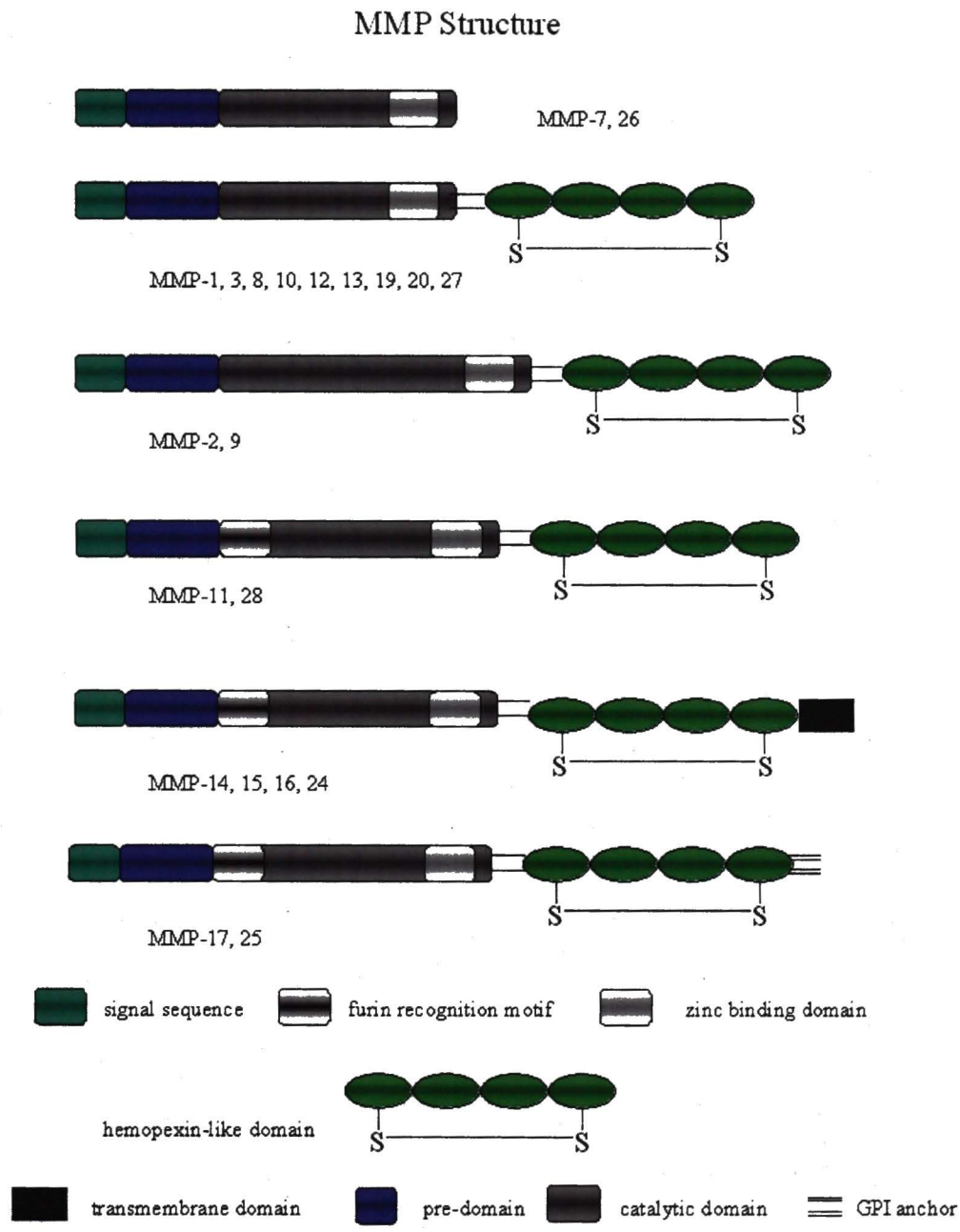

Figure 1. Diagram of structure of MMPs: There are several different domains in MMPs. A signal peptide, a propeptide, a catalytic domain and a zinc binding domain are conserved in all types of MMPs. A hemopexin-like domain is found in most of MMPs except MMP-7 and 26. There are also some specific domains found in MMPs, such as a fibronectin type II domain in MMP-2 and MMP-9 and a transmembrane domain in MT-MMPs (membrane-type MMPs).
(Modified from Stamenkovic, 2003)

Among them, collagens, a class of major structural proteins, provide structural support, protect and support the tissues and connect them. Collagens are ubiquitous proteins responsible for maintaining the structural integrity of vertebrates and many other organisms. Although they have the critical function, the structure of collagens is relatively simple. Three chains of collagens wind together to triple helix.

More than 20 distinct collagens have been identified. In order to resist shear, tensile, or pressure forces in tissue such as tendons and skin, collagens are arranged in fibrils. Only collagen I, II, III, V and VI assemble into fibrils. These "type I" collagen molecules form fibrils functioned as the structural collagens [7, 8]. These fibrils crisscross the space between nearly every cell. Some types of collagen, including collagen IV, VIII, and X, form the extracellular network. A typical example of such a network is the basement membrane, which is mostly made of collagen IV. Type IV collagen has a head and a tail end. Four collagen molecules can bind others with four heads together and four tails projecting outside. The projecting tails bind with tails from other collagen IV molecules. Using these two types of interactions, type IV collagen forms a network. Two other molecules, laminin and proteoglycans, participate in interaction with collagen and occupy the space within network. Networking collagens are associated with fibril surfaces [8].

Fibronectin (FN), an abundantly expressed ECM protein, is broadly expressed by multiple cell types and secreted as a soluble dimer consisting of two similar subunits joined together at the C terminus by disulfide bonds. In plasma, fibronectin exists as a

soluble dimer, but in the ECM it exists as an insoluble multimer. *In vivo*, FN is abundant in blood plasma (pFN) and in tissues where fibroblasts and other resident cells synthesize cellular FN (cFN) and assemble it into a multimeric ECM. As a multifunctional adhesive glycoprotein, FN is widely distributed and important for a variety of biological processes including embryogenesis, wound healing, and oncogenic transformation. These functions are dependent on a variety of cellular interactions of FN with the ECM and plays important roles in cell adhesion, migration, growth and differentiation [9]. FN has a molecular weight of about 230–270 kD and is named type I, type II, and type III based on the composition of homologous repeating units. These repeating modules are organized into functional domains that mediate FN interactions with cells and other ECM proteins, including integrins, heparin, collagen/gelatin, elastin and fibrin, to exert its diverse biological functions. These interactions are also important for communication between cells [10]. For instance, both amino (N)- and carboxyl (C)-terminal fibrin binding regions mediate non-covalent interactions with fibrin. These interaction sites are localized to the N-terminal type I repeats 1–5 and the C-terminal type I repeats 10–12 [11, 12]

FN's structural and functional diversity is achieved by alternative splicing of the FN gene transcript at three sites, EIIIA, EIIIB, and the variable (V) region, to generate over 20 variants of fibronectin [9, 13].

Integrins, the receptors of FN, are the major family of surface receptors that mediate cell adhesion to the ECM. Integrins, located on virtually all cell types, are heterodimers composed of one alpha (α) and one beta (β) subunit, which together

Figure 2

Fibronectin (FN) and Integrins Mediated Signaling

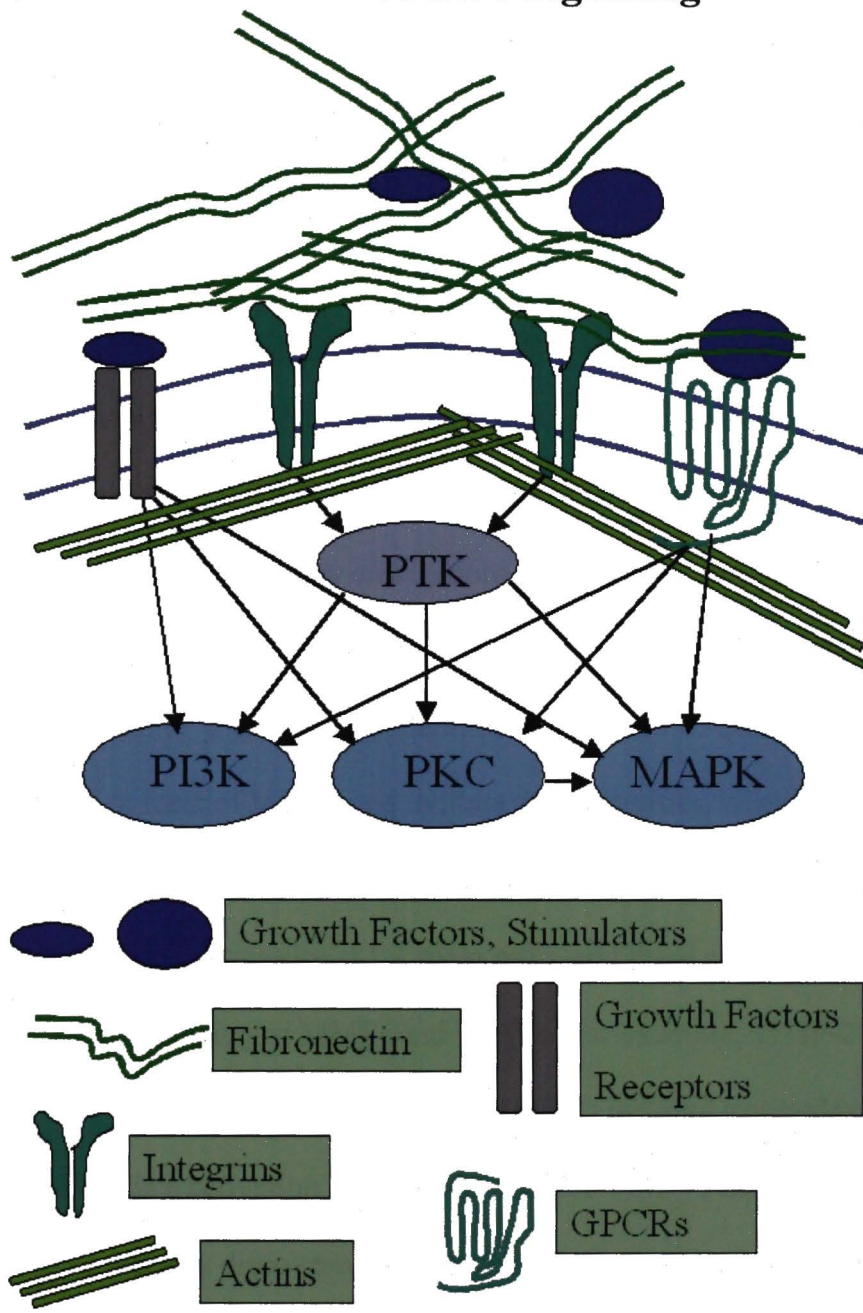

Figure 2: Fibronectin (FN) and Integrins-mediated signaling: FN binds to other ECM molecules, such as collagen I, collagen IV, to form the ECM network. FN also binds to integrins and other receptors (growth factor receptors or GPCRs (G protein-coupled receptors)) leading to formation of the actin scaffold and mediating activation of the intracellular signaling pathways (PTK (protein tyrosine kinase), PKC, MAPK, etc.).

determine the ligand-binding specificity of the intact receptor. For example, $\alpha 5\beta 1$ is the major receptor for FN [14]. Integrins recognize specific sequences present in ECM proteins such as FN, and form a scaffold to propagate signaling transduction not only for FN-integrin interaction but also for signal transduction (Figure 2) [13, 15].

The expression of most MMPs is normally low in tissues and is inducible when ECM remodeling is required. Primarily, MMP gene expression is regulated by growth factors, cytokines and other factors like stress, neurotroma [2, 16]. In addition, to be regulated at the transcriptional and translational level, activity of MMPs is also controlled by zymogen activation and inhibition by endogenous tissue inhibitors of matrix metalloproteinases (TIMPs) on the cell surface or in the extracellular space (Figure 3) [17]. There are four TIMPs (TIMP-1 to TIMP-4) identified in humans [16]. Carboxyl-terminus of TIMPs binds with active form of MMPs and inhibits their activities, whereas N-terminus of TIMPs is considered to possess more biological activities. TIMPs bind tightly with MMPs to inhibit the enzymatic activity at 1:1 mole ratio, and there are some preferences in inhibitory properties in binding of MMPs and TIMPs. For example, TIMP-2 binds tightly with latent form (zymogen) of MMP-2 (proMMP-2) forming a complex that is important in the cell-surface activation of MMP-2, whereas TIMP-1 binds with proMMP-9. TIMP-4 is the most recently discovered, and its function is not clear. TIMP-3 is the inhibitor selective for MT-MMPs (membrane-type metalloproteinases). Unfortunately, there are no studies that show the quantitative data on binding affinity and preferences [18]. TIMPs function not only to inhibit the activity of MMPs, but also to be involved in

activation of MMPs. The activation of MMPs from proMMPs is controlled by the involvement of other MMPs and the plasmin system. For example, MMP-2 binding with TIMP-2 can activate MMP-9; proMMP-9 binding with TIMP-1 is also involved in the activation of MMP-3 [19].

MMPs and TIMPs are required for normal physiological and pathological conditions including embryonic development and growth as well as in tissue remodeling and repairs [6]. An imbalance of MMPs and TIMPs can occur as a result of the abnormal expression of MMPs or TIMPs, it may induce ECM remodeling and turnover in development or pathological conditions. Such remodeling has been shown to cause the pathogenesis of many diseases such as arthritis, tooth decay, cardiovascular diseases (cardiac infarction, cardiac hypertrophy), tumor progression and some lung diseases (chronic obstructive pulmonary disease) [6]. In the central nervous system (CNS), neurons and glial cells both produce MMPs and TIMPs. In fact, MMPs also contribute to the pathogenesis of several CNS diseases such as multiple sclerosis (MS), Alzheimer's disease (AD), and malignant glioma [1]. Combination evidence from CNS and studies on glaucoma, which is an optic neuropathy, indicates that an imbalance of MMPs/TIMPs is also involved in glaucoma formation and progression.

Figure 3

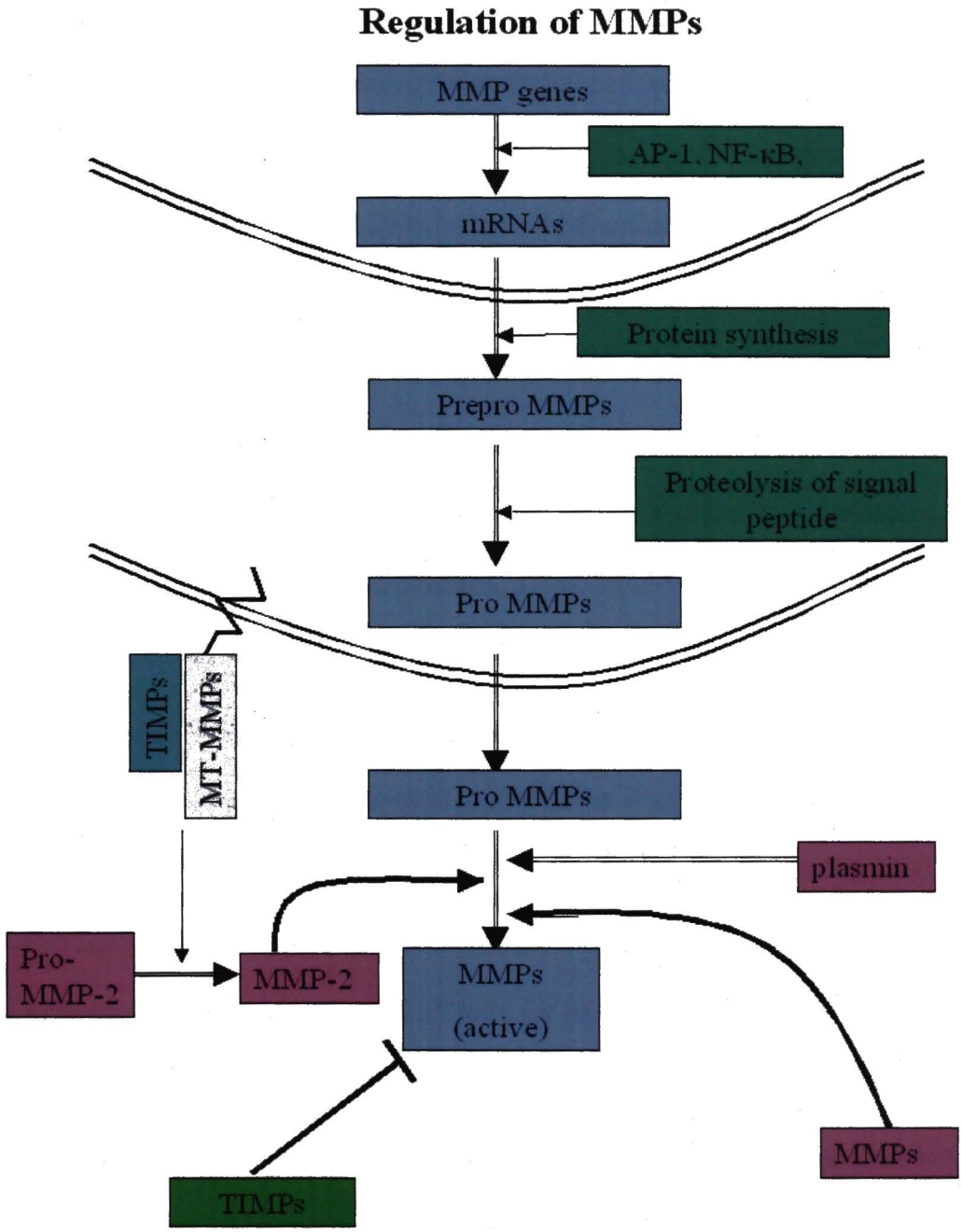

Figure 3. Regulations of MMPs: The expression and activity of MMPs are tightly controlled by multiple key steps. The expression of MMPs is regulated at the transcriptional and translational levels, whereas the activity of MMPs is controlled by zymogen activation. However, The crutial step is that the activity of MMPs is mainly controlled by endogenous tissue inhibitors of matrix metalloproteinases (TIMPs) on the cell surface or in the extracellular space. (Modified from Overall, 2002)

Endothelin-1 and its receptors, ET_A and ET_B

Endothelin-1 (ET-1), a 21-amino acid peptide, was isolated as a potent vasoconstrictor peptide from the pig arterial endothelial cell in 1988 [20]. Two peptides with structural similarity, termed ET-2 and ET-3, were discovered [21]. They share similar structures with ET-1 but differ respectively with 2 and 6 amino acids compared to ET-1. All ET family members have cysteine residues at positions 1, 3, 11, and 15. There are two disulfide bonds formed between 1 and 15 and between 3 and 11.

The maturation of ETs is a process of protein proteolytic cleavage. About 200-amino acid preproendothelin is translated, and this protein is cleaved by a furin-like endopeptidase to form the inactive intermediates, 37-41-amino acid peptides termed big ETs. The big ETs are cleaved by membrane-bound zinc-dependent metalloproteinases, endothelin-converting enzyme 1 and 2 (ECE-1 and 2) to mature 21-amino-acid peptides, the ETs [22, 23]. In humans, the 212-amino-acid prepro-ET is encoded by the endothelin gene, which is located in chromosome 6 with 5 exons and 4 introns [24]. The big ET-1 is cleaved at the Trp-Val position to form the active ET-1. Big ET-1 is at least 100-fold less than ET-1 in vasoconstriction activity and affinity for its receptors [25]. Therefore, the proteolytic processing of big ET-1 by ECE-1 and 2 is important in the function of ET-1.

ET-1 concentration at basal levels is approximately 1.5-2 pg/ml in normal human plasma and increases several folds in many pathological conditions, including myocardial infarction, angina pectoris, acute ischemic cerebral stroke, systemic sclerosis [25] as well as glaucoma and glaucoma animal models[26-30]. Increased ET-1 levels may also be seen in

local tissue with pathological changes. The evidence shows that there are many factors that can induce the production of ET-1, including: 1) cytokines: IL-1, IL-1b, IL-6, etc.; 2) growth factors: epidermal growth factor, fibroblast growth factor, transforming growth factor, etc.; 3) lipids and 4) mechanical stimulation such as pressure, stress, neurotroma [31-38].

Diversity of action of ET-1 can be illustrated in terms of the expression of ET-1, the existence of several receptor subtypes, the differential expression of receptors in cells and tissues, and activation of a variety of different signaling pathways. The main source of ET-1 is endothelial cells, however it is also produced by many other types of cells, including epithelial cells, macrophages, fibroblast, cardiomyocytes, brain neurons and ocular cells [31, 39-41].

Initially discovered as a potent vasoactive peptide, ET-1 has vasoconstriction or vasodilation effects that are dependent on the vessel tissue involved. The growing evidence has shown that ET-1 is involved in development, cell differentiation, cell proliferation, tumor metastasis, angiogenesis, electrolyte balance, matrix formation, mitogenesis, synergism with growth factors, acute or neuropathic pain, apoptosis and anti-apoptosis [24, 32, 33, 35, 37, 39-47].

ET_A and ET_B receptors have the same characteristic of G protein-coupled receptors with seven hydrophobic transmembrane domains. Human ET_A and ET_B receptors are highly conserved in amino acid sequence identity, in which there are 55%-64% similarity in whole sequence, depending on different tissues, and 74% within the

putative transmembrane helices [48]. Besides the transmembrane domains, there are the least sequence similarities in the extracellular NH_2 terminus and the intracellular COOH-terminal tail, whereas the sequences in intracellular loops 2 and 3 are relatively similar [25, 49]. The gene for the human ET_A receptor, encoding 427 amino acids, is located on chromosome 4 [50]. The gene for the human ET_B receptor, encoding 442 amino acids and having molecular weight about 50KD, is located on chromosome 13 [48, 51]. However, the alternative splicing of the human ET_B receptors leads to a variety of mutants with differential amino acid sequence, including 442, 452, 274, 297, 436, 252 amino acids [52]. Generally in the vascular system, the ET_A receptors that are mainly expressed in smooth muscle were thought to function the vasoconstriction effects, and the ET_B receptors that are mainly expressed in endothelial cells in vascular system provide the vasodilation effects.

ET-1 and ET-2 bind the ET_A receptor with high affinities, and ET-3 binds with 70-100-times lower affinity, whereas these three peptides bind the ET_B receptor with similar high affinities [39].

ET-1 and its signaling

G protein-coupled receptors (GPCRs), the largest superfamily of transmembrane receptors, consist of over 1000 members and are involved in diverse responses induced by many types of stimuli, including chemicals, biomolecules, light, odors, lipids, steroids, peptides and stress [53]. These receptors share similar primary amino acid sequences, a

common seven-transmembrane domain, and modulate intracellular metabolism and signaling through the activation of heterotrimeric G proteins, which consists of Gα, Gβγ subunits. The binding of the extracellular stimulant leads to the conformational changes in the receptor subdomains, which transfer the signal to a trimeric G protein complex consisting of Gα and Gβγ. The activation of receptor promotes the exchange of GTP to GDP on Gα subunit protein resulting in dissociation from Gβγ subunits. GPCR activates the heterotrimeric G proteins through activated Gα and Gβγ subunits, which interact with numerous intracellular molecules to trigger the downstream signaling cascades.

ET_A and ET_B receptors are also GPCRs and belong to the rhodopsin family of GPCRs. ET-mediated signaling pathways occur through ET_A and ET_B receptors coupling with $G\alpha_I$, $G\alpha_s$, Gαq and Gα12/13. In addition, other pathways are also activated via Gβγ, tyrosine kinases, transactivation of EGF receptor, PDGF receptor and regulator of G protein signaling (RGS).

1. MAPK, PKC and PI3K are activated through ET_A and ET_B receptors

MAPK signaling pathway is another very important pathway in governing cell proliferation, differentiation and cell death [46, 54]. Each MAPK cascade comprises three components, MEKK (Raf), MEK (MAP kinase kinase) and MAPK, identified as a family of protein Ser/Thr-kinases. In response to diverse stimuli, such as growth factors, stress, etc., the MAPK cascade becomes phosphorylated and activated, consequently triggering additional signaling ultimately resulting in gene transcription [46, 55]. The p44 and p42 MAP kinase/extracellular signal-regulated protein kinase1/2 (ERK1/2) is an important

member of the MAPK family that is involved in cell growth, proliferation and differentiation. MAPK pathways are not only involved in receptor tyrosine kinase-induced signaling, but also involved in signaling induced through activation of GPCR [46, 55, 56]. It is well known that Gαi, Gαs and Gαq trigger downstream Ras, Raf to promote the activation of MAPK.

ET-1 through ET specific receptors (ET_A and ET_B), activates the MAPK pathway by phosphorylation of ERK1/2 in many cell types, including smooth muscle cells, fibroblasts and astrocytes [38, 41, 46, 57]. These studies have indicated that ET_A receptor-mediated mitogenic activity occurs predominantly through two pathways: protein kinase C (PKC)- and phosphoinositide 3-kinase (PI3K)- dependent pathways, both of which stimulate MAPK [58-60], whereas activation of ET_B receptor-mediated mitogenic activity appears to utilize PKC-independent pathways [38, 46, 55, 56]. ET-1-mediated-signals through G-protein coupled receptor (GPCR) activate phospholipase C (PLCβ) and generate inositol 1,4,5-trisphosphate (IP3) and diacylglycerol (DAG) by hydrolysis of phosphatidylinositol 4,5-bisphosphate (PIP2), releasing Ca^{2+} and activating PKC, respectively. PKC can also act upstream of the MAPK pathway via activation of Ras and Raf, to influence cell proliferation through a classical Ras-Raf-MEK-ERK pathway which is also affected by the activation of growth factor receptors [56, 61, 62]. The increased intracellular Ca^{++} can also directly trigger the activation of Ca^{++}-dependent kinases (CaMK, etc.) as well as phospholipase A2, which consequently regulates the release of arachidonic acid [25].

Activation of the MAPK pathway does not depend on Gα alone, but also depends on Gβγ subunits. There are 5 Gβ and 12 Gγ subunits identified in human [63]. This results in the diverse, potential combinations of Gβγ. The different Gβγ dimer implicates the different roles in triggering downstream signaling pathways, including extracellular signal-regulated kinase (ERK1/2), c-Jun NH_2-terminal kinase (JNK) and p38 [64, 65] as well as several calcium channels [66, 67].

Growing evidence indicates that ET-1 also activates the serine/threonine protein kinase Akt/PKB, which plays an important role in cell survival and apoptosis. The anti-apoptotic Bcl-2 family proteins is involved in the activation of Akt, inhibiting apoptosis and promoting cell survival. It was reported that the βγ subunit of activated G proteins of GPCRs has been identified to activate PI3K (same mechanism with interaction between GRK2/3 and Gβγ due to PH domain interaction), subsequently leading to activated PKB/Akt [43, 68, 69]. The studies from other GPCRs have also confirmed the coupling of Gβγ and GPCR to induce activation of PI3K and Akt. In addition, overexpression of inactive, truncated GRK2, which sequestered Gβγ coupling from the receptors, inhibited the phosphorylation and activation of MAPK [68]. Liu et al. found that ET-1 induced NO generation through a PI3 kinase-Akt pathway [43]. However, when the inactive carboxyl terminus of GRK2, which interacted with Gβγ and sequestered the coupling Gβγ from receptors, was overexpressed, NO generation was completely blocked and activation of PI3 kinase and Akt was abolished. The results suggested that Gβγ subunits are involved in activation of PI3 kinase and Akt through GPCRs. In general, the mechanism of Gβγ

interaction with its effectors is not clear, and many effectors containing PH domains interact with Gβγ. However, not all PH domain containing proteins can bind with Gβγ [70].

2. Signaling induced through tyrosine kinase proteins

Signal transduction through the activated GPCR can transactivate receptor tyrosine kinases such as EGFR, PDGFR and nonreceptor tyrosine kinases, such as FAK (focal adhesion kinase) and Src [71]. A variety of studies have reported that activation of Ras-Raf-MAPK pathway by ET-1 occurs through the protein tyrosine kinases (PTK) such as FAK, c-Src, PYK2 (Proline-rich kinase 2), etc. [45, 46, 59, 72, 73]. Several GPCR agonists stimulate EGF-R transactivation, including lysophosphatidic acid, thrombin, ANG II, arginine vasopressin and ET-1 [74]. Transactivation of EGFR by GPCR is also cell type dependent. It has been reported that ET-1 activates ET receptors that then transactivates EGF receptor resulting in phosphorylation of ERK1/2 through the Ras-Raf-MAPK pathway in rat mesangial cells [74], human vascular smooth muscle cells [75, 76], human melanocytes [77] and human ovarian carcinoma cells [78].

Kawanabe et al. found that ET-1 activated Ca^{++}-permeable nonselective cation channels and a store-operated Ca^{++} channel (SOCC) in vascular smooth muscle cells to induce Ca^{++} influx from the extracellular space that was blocked by application of Ca^{++} channel blockers [76]. Blocking Ca^{++} influx inhibited arachidonic acid generation and phosphorylation of ERK1/2. Meanwhile, application of AG1478, a specific inhibitor of EGFR PTK, also inhibited arachidonic acid release and phosphorylation of ERK1/2 induced by ET-1. It has been demonstrated that ET-1-induced EGFR transactivation is

Ca^{++} dependent, whereas arachidonic acid release and phosphorylation of ERK1/2 induced by ET-1 is EGFR tyrosine kinase dependent.

The regulator of G protein signaling (RGS) and activator of G protein signaling and GPCR interacting proteins (GIP) are involved in ET-1-mediated signaling. The different signaling pathways are also connected to differential downstream transcriptional factors to exert ET's function in gene expression. For instance, the phosphorylation of ERK1/2 is a key step in triggering downstream signaling and potential activation of transcriptional factors, such as c-Myc, Elk-1, c-Fos, etc. [79, 80]. PKC and PI3 kinase are also involved in ET-1-mediated activation of transcription factors [79, 81-83]. It has been suggested that some transcription factors, such Elk-1, c-Fos, AP-1, are controlled simultaneously by MAPK-ERK and PKC [45, 79, 84], whereas p38 and JNK share different transcription factors. Some other downstream kinases, including Rsk, p70S6K, are also under control of these three pathways.

Take together, the complicated signaling induced by ETs is partially summarized in Figure 4.

Figure 4 **Major Signaling Pathways Induced by ET-1**

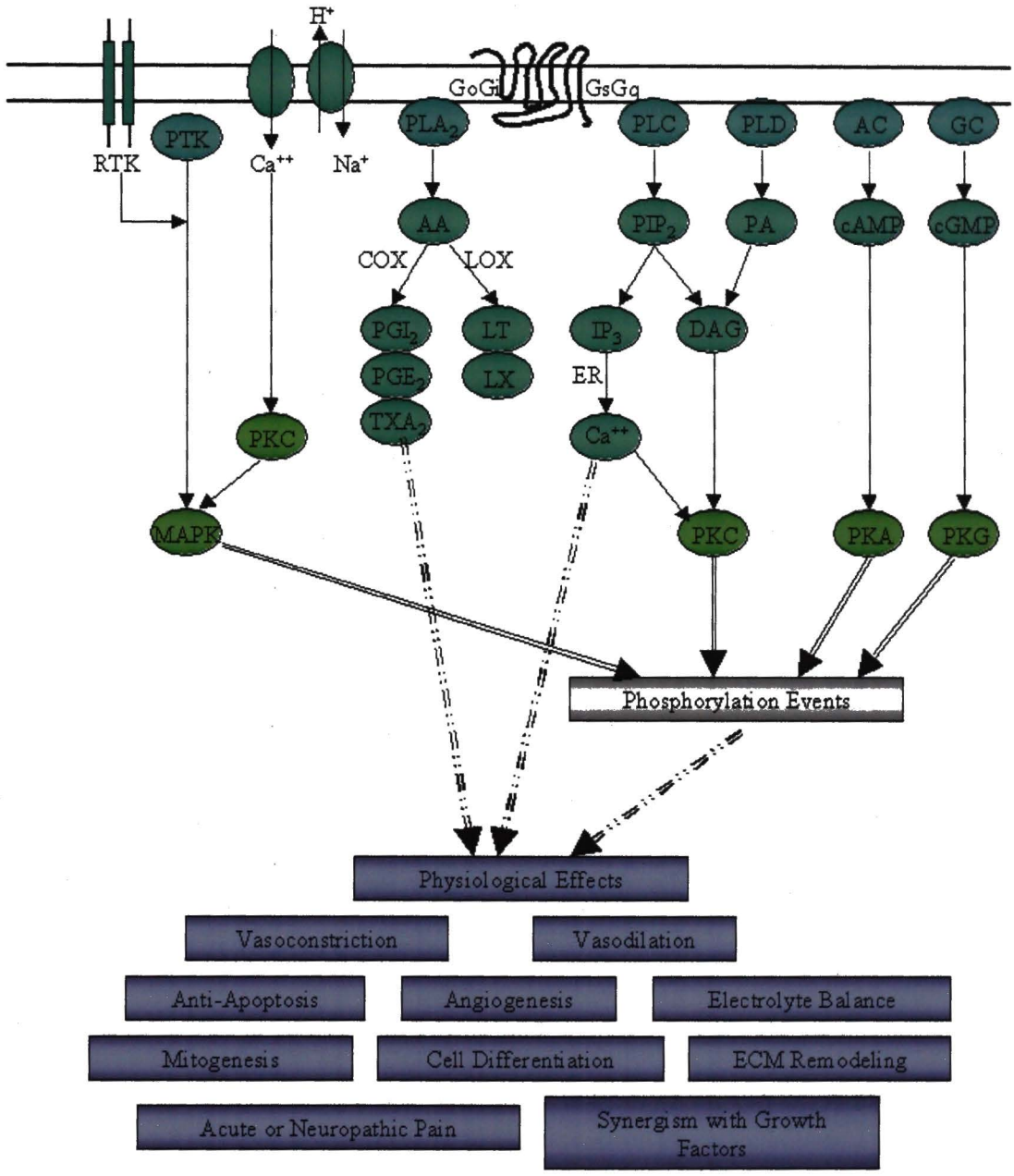

Figure 4. Major Signaling Pathways Induced by ET-1: ET-1 activates phospholipase C (PLC), phospholipase D (PLD), adenylate cyclase (AC) and gualylate cyclase (GC) to generate the secondary messengers, such as IP3, DAG, cAMP and cGMP, to trigger the activation of PKC, PKA and PKG. ET-1 also trigger MAPK and PKC pathways through activation of tyrosine kinases and calcium. Such actions of ET-1 induce a number of physiological effects, including vasoconstriction, vasodilation, anti-apoptosis, angiogenesis, cell proliferation, cell defferentiation and ECM remodeling. (Modified from Nelson, 2003 and Sokolovsky, 1995)

Glaucoma and the roles of astrocytes in Optic Nerve Head (ONH)

Glaucoma is one of the leading causes of blindness throughout the world. There are over 70 million people suffering from this disease. Glaucoma is an optic neuropathy, characterized by cupping of the optic disc, progressive loss of retinal ganglion cells and slow degeneration of the optic nerve, resulting in blindness [85-87]. It is estimated that approximately 3 million Americans are suffering from primary open angle glaucoma, which is a common form of this disease and comprises about 90% of all glaucoma. There are lots of risk factors associated with glaucoma, including age, race, sex, hypertension, etc. Among these risk factors, increased intra ocular pressure (IOP) is significantly correlated with glaucoma, especially in primary open angle glaucoma.

The optic nerve head is one of the major pathological sites leading to glaucoma. It is the place where retinal ganglion cell axons exit the eye through an opening called the scleral canal. The optic nerve is composed of millions of nerve fibers that originate in the retinal ganglion cell layer and converge at the optic nerve head. The optic nerve head is divided into four regions based on the location: the surface nerve fiber layer, the prelaminar region, the lamina cribrosa and retrolaminar region. Changes in macromolecules in the optic nerve head of glaucoma not only result in ECM remodeling at this site, but also alter the responses of the tissues and cells to the external stimuli such as mechanic pressure, in glaucoma patients and in experimental animal models of glaucoma, including laser-induced monkey glaucoma and in Morrision's elevated-IOP rats [29, 88, 89]. In human primary open-angle glaucoma, Hernandez et al demonstrated that

there was an elevation of immunoreactivity of elastin and collagen VI detected in the lamina cribrosa as well as increased collagen IV detected around nerve bundle [90], suggesting ECM remodeling is an indication of glaucoma progression. Quigley et al showed that there was structural changes in elastin, including curling of elastin and disconnection from the other elements of the connective tissue matrix [91], but not changes in elastin fibril density in glaucomatous eyes [92]. Morrison et al also suggested that there was a deposition of several different collagens in optic nerve head and the increased staining of collagen IV was detected along the margins of beams in the lamina cribrosa in experimental glaucoma primates [93]. In monkeys with laser-induced glaucoma, some preteoglycan proteins were increased with elevated IOP [94], and reactivation and migration of astrocytes were observed as well [95].

There are several possible mechanisms to interpret the progressive enlargement of the optic disc: 1) the loss of ganglion cell axons (nerve fibers), but not astrocytes, is one of reasons to cause cupping [96]; 2) the enlargement of the scleral canal also makes the cupping worse [96]; 3) ECM remodeling at this site participates in the whole event [88, 89, 97, 98]. However, in response to mechanical pressure, the optic nerve was distorted by abnormal ECM remodeling[88, 89], and the transport of axons was also occluded [99, 100] at the optic nerve head. Astrocytes were also proposed to participate in ECM remodeling as well [89].

Astrocytes are the major glial cells in the optic nerve head. Astrocytes constitute approximately 50% of the total cell number within the CNS and provide not only the

structural support to neurons and maintenance of the extracellular milieu (including K^+, glutamate, etc.), but also secretion of neurotrophic factors, regulation of apoptosis, and even regulation of neurotransmission [89, 101]. There are two types of astrocytes in the optic nerve regions: Type Ia astrocytes expressing glial fibrillary acidic protein (GFAP) are located in glial columns and the cribriform plates, and Type Ib expressing both GFAP and neural cell adhesion molecule (NCAM) are the major cell type and located in whole optic nerve head [88, 102]. Generally, astrocytes are in a quiescent and quasi-differentiated state under normal conditions, and can be activated in response to exposure of mitogens, neurotrauma. Furthermore, astrocyte activation and proliferation have been demonstrated in several neuropathies, including ocular neuropathy and brain astrocyte tumor progression [29, 41, 103-107]. Astrogliosis is defined as an abnormal increase in the number of astrocytes due to the destruction of nearby neurons and is characterized by exhibiting proliferative and hypertrophic responses [108, 109]. Typically, astrogliosis is seen following neurotrauma, hypoxia/ischemia, and other pathologies and is manifested by a dramatic change in the expression of extracellular matrix profile, which in most cases results in a glial scar [89]. These cells, which are major glial cells in the optic nerve head, are essential for axon survival and provide structural support. As the astrocytes are activated, their cell bodies undergo hypertrophy and migrate into optic nerve bundles, and the pathological changes may induce axon loss [88, 110]. Since the axon loss is one of the characteristics of glaucoma, the optic nerve head is considered an important pathological change site. One of possible mechanisms is that elevated IOP induces ECM remodeling, leading to

pathological changes at the optic nerve head that causes physical compression on optic nerve axons. Such actions will block axoplasmic flow leading to ischemia, and also block anterograde and retrograde transports between axons and retinal ganglion cell bodies [88, 89, 111]. Regarding the regulation of ECM components in the brain and eyes, astrocytes are a major source of MMPs and the extracellular matrix components [89]. Reactive astrocytes, involved in astrogliosis, may be responsible for ECM remodeling in glaucoma. We have shown that increased IOP is strongly correlated with elevated endothelin-1 (ET-1) at the optic nerve with increases in ET_B receptors in astrocytes and marked elevation in GFAP [29]. Therefore, ET-1 may be involved in ECM remodeling of optic nerve head in glaucoma as a result of the astrogliosis and reactivation of astrocytes by ET-1.

Endothelin-1 (ET-1), ECM remodeling in optic nerve head in glaucoma:

Endothelins, a family of vasoactive peptides that include ET-1, are implicated in numerous physiological and pathological conditions, including hypertension, cardiac failure, brain and myocardial infarction, disseminated intravascular coagulation, Alzheimer's disease, and glaucoma [32, 41, 112]. ET-1, the predominant isoform of ET, is a potent mitogen in many cells including smooth muscle cells, fibroblasts, and astrocytes [33, 108, 113-116]. ET receptors, ET_A and ET_B, are also expressed in many types of cells in the central nervous system (CNS) with ET_B as the predominant receptor in the CNS [117]. The changes in ET-1 expression and/or regulation of ET receptors appear to play an important role in CNS astrogliosis [36, 57].

ET-1 is not only known as a potent vasoactive peptide, it is also involved in many physiological functions and pathological conditions. Abundant studies show a role of ET-1 in tumor homeostasis. In addition to promoting cell proliferation in tumor cells through activation of its receptors, ET-1 also inhibits apoptosis, shifts the balance of MMPs/TIMPs to induce extracellular matrix remodeling that leads to neovascularization in certain tumors, and increases metastasis of tumor cells as well [32, 35, 47]. In addition, the growing evidences showed that ET-1 induces the expression of many types of MMPs and TIMPs leading to increased degradation of collagens, laminin and fibronectin which are deposited in the extracellular space, and that ET-1 also induced ECM protein expression, including collagens, laminin and fibronectin in *in vitro* cell culture and *in vivo* animal models [118-122].

Interruption of the connection between retinal ganglion cells and the brain by compression or severing their axons causes the loss of ganglion cells and optic nerve. This may be due to blockade of anterograde and retrograde neurotrophin transport [88, 89, 111]. However, animals display the different MMP expression profile in ECM as part of remodeling of the optic nerve head in response to the different insults of the optic nerve. In laser-induced glaucoma in primates, there is significant increase in expression of MT1-MMP and MMP-1 in reactive astrocytes at optic nerve head due to elevation of IOP, whereas in primates with optic nerve transection, there is increased MT1-MMP, MMP-1, MMP-2, TIMP-1 and TIMP-2 expression by reactive astrocytes at the transection site [123]. Other investigators have shown that extensive ECM remodeling is correlated with RGC

apoptosis and axon loss, and that the increased MMP activity may enhance ECM degradation, including collagen degradation, to facilitate the migration of astrocytes into optic nerve bundles. Fini's group showed that RGC apoptosis may be significantly correlated with the degradation of laminin from the inner membrane and directly increased the activity of MMP-9 at the same layer[124]. Zhang also reported that following intravitreal injection of kainic acid in mice, upregulation of MMP-9 and activation of astrocytes were observed in the retina. The decrease in laminin immunoreactivity in the ganglion cell layer and significant loss of retinal ganglion cells were correlated with increased activity of MMP-9 [125]. Guo et al showed that elevated-IOP-induced RGC apoptosis was positively correlated with expression of MMP-9, TIMP-1 and collagen I, but negatively correlated with laminin at RGC layer [111]. In elevated-IOP rats, the extensive immunostaining of collagen IV, VI and laminin was detected at the optic nerve head by Morrison's group [126]. This increased ECM deposition is associated with the duration of increased IOP and increased level of IOP. Therefore, the key ECM molecules not only provide mechanical support for cells, but also are involved in cell apoptosis and axon loss at ONH.

It's reported that ET-1 levels were elevated in the vitreous humor and plasma in glaucoma patients [26, 27] and some glaucoma animal models, such as ET-1 levels were 4-fold higher in the aqueous humor than control in the dog with glaucoma, [28]; and in the Morrison model of elevated IOP in Brown Norway rats, there is an increase ET-1 levels in aqueous humor over controls [29] and in rabbits[30]. Our lab has shown that the increased

ET-1 levels in aqueous humor in the Morrison rat model of elevated IOP were correlated with the increased GFAP in astrocytes and ETB receptor immunoreactivity [29]. Morrison's group also demonstrated that there is a significant increase in mRNA levels of ET receptors, TIMP-1, MMP-3, ET-2, fibronectin and GFAP tested by RT-PCR in the elevated IOP in Brown Norway rats [127]. Furthermore, intravitreal injection or perfusion of ET-1 into eyes in many animal models such as primates, rabbits and rats, caused optic nerve head damage similar to that seen in glaucoma, including enlargement of disk cupping, axon loss, astrogliosis [128-131], as well as disruption of axonal transport between the cell body and axons [100, 132].

ET-1 is an important factor that contributes to the pathogenesis and progression of glaucoma [40, 41]. However, the mechanism involved in ET-1 regulation of ECM remodeling in optic nerve head as occurs through astrocytes is still unknown.

Hypothesis and Specific Aims:

Endothelin-1 (ET-1) is a vasoactive peptide and a potent mitogen for many cells including smooth muscle cells, fibroblasts, and astrocytes especially when ET-1 levels are elevated under pathophysiological conditions, including glaucoma. Previous studies show that PKC, MAPK and PI3K-Akt are involved in signaling induced by ET-1 through its receptors ET_AR and/or ET_BR. However, ET-1-mediated signaling involved in astrocyte proliferation and reactivation is not clear.

It is reported that astrocyte-mediated responses and changes in the extracellular

matrix (ECM) is involved at the optic nerve head in primary open angle glaucoma involves. The activities of ECM-remodeling enzymes, such as matrix metalloproteinases (MMPs) and tissue inhibitor of matrix metalloproteinases (TIMPs), play an important role and are regulated by MAPK and PKC pathways. ET-1 levels were elevated in vitreous humor and plasma both in glaucoma patients and in animal models of glaucoma. By altering the microenvironment of the optic nerve head through remodeling, these reactive astrocytes induced by ET-1 may cause axonal degeneration and progressive and irreversible pathological changes. Thus, the study of reactive astrocytes may provide approaches to modulate or to control the deleterious changes in the glaucomatous optic nerve head (ONH).

Hypothesis: **ET-1 induces an imbalance of the activity of MMPs and TIMPs through MAPK- and PKC-dependent pathways in optic nerve head astrocytes (ONA).**

Specific Aim 1: To determine whether ET-1 induced cell proliferation through MAPK, PKC and PI3K pathways in astrocytes. In order to complete this aim, primary optic nerve head astrocytes (ONA) and U373MG astrocytoma cells will be used in experiments. The function of MAPK, PKC and PI3K pathways in cell proliferation of astrocytes will be detected. Cell proliferation will be determined by MTT-formazan assay and ^{3}[H]-thymidine incorporation assay. Phosphorylation of ERK1/2, PKC, and PI3K will be monitored by Western Blot (WB) assay. PKC translocation assay and PKC kinase

assay will be employed to measure expression of PKC and PKC isoforms involved in ET-1-induced signal transduction. Inhibitors and dominant negatives of MAPK and PKC will be applied to block these pathways.

Specific Aim 2: To determine whether ET-1-mediated signaling is involved in ECM remodeling of human optic nerve head astrocytes. In order to complete this aim, ET-1's effects in activity and expression of MMPs and TIMPs, expression and matrix formation of substrates will be determined in primary ONA cells. Zymography assays will be applied to analyze the activities of MMP-2, 3 and 9. WB will be used to detect the expression of TIMPs at different time points. WB and immunofluorescent staining will be used to test substrate expression and deposition, including collagen IV, and fibronectin. Introduction of siRNA into cells will be used to knock down MMP-2 or TIMP-2 to determine the regulation of balance between MMPs and TIMPs.

Specific Aim 3: To determine whether ET-1 alters ECM remodeling at optic nerve head in rats with intravitreal injection of ET-1. To determine *in vivo* effects of ET-1 in eyes, ET-1 will be injected into the vitreous of one eye of Wistar rats and ET_B-deficient transgenic Wistar rats; the contralateral eye will serve as control. An additional set of animals will be treated with vehicle injection to one eye. Rats will be sacrificed at different time points. Immunostaining will be employed to detect MMPs, TIMPS, collagen type IV, type VI, fibronectin and Glial fibrillary acidic protein (GFAP) in optic

nerve head sections.

Significance:

In this study, we investigated the mechanisms by which ET-1 induces an imbalance in the activity of MMPs and TIMPs and how this imbalance contributes to the pathological changes at the ONH in glaucoma. Such studies provide insight into the mechanisms inducing glaucoma, but also indicate the strategies of new drug designs for glaucoma treatment.

Patients would not be diagnosed with glaucoma until they experience a loss of vision because there is no pain in glaucoma progression. However the death of retinal ganglion cells is irreversible at this stage. Therefore, understanding how to prevent the further apoptosis of retinal ganglion cells and the pathological changes at the trabecular meshwork, retina and the optic nerve head is crucial for glaucoma therapeutics. Understanding how ET-1 levels increase and ET-1 signaling involved in ECM changes will provide important information for early diagnosis and therapy. In the current study, we will determine if ET-1 induces an imbalance of MMPs/TIMPs through MAPK- and PKC-dependent pathways, resulting in ECM remodeling. Such studies could provide insight into the molecular regulation and signaling that leads to the pathological changes that occur at the optic nerve head. ET-1 activates astrocytes and the resultant astrogliosis, which contributes to the progressive loss of retinal ganglion cells and axons in glaucoma. This proposal will 1) establish a temporal regulation of ET-1 on MMPs/TIMPs, and

establish signaling mechanisms associated with ECM molecule expression; 2) determine if the ET-1's effects on the pathological changes at the optic nerve head occur through an imbalance of MMPs/TIMPs; and 3) demonstrate that the in vivo effects of ET-1 are correlated with ET-1-receptor mediated ECM remodeling and glaucomatous optic nerve damages.

The results from this study could suggest several strategies of new drug design for treating glaucoma: 1) Control ET-1 levels in ocular tissues: Elevated ET-1 levels in glaucoma patients indicate the possible involvement of ET-1 in glaucoma progression, therefore, the application of specific inhibitors of endothelin converting enzyme, the rate limiting step in ET synthesis, may facilitate the regulation of ET-1 levels in the eyes; 2) Development of ET_A and/or ET_B antagonists: Using antagonists to block ET-1's effects is a promising approach, for example, Bosentan, an antagonist of ET_A and ET_B receptors, has been used in the therapy of pulmonary hypertension; 3) Designing specific inhibitors of MMPs could also be a potential therapeutic targets for glaucoma: Administration of the inhibitor to control the activity of MMPs to maintain the balance at physiological levels would prevent any abnormal changes in ECM that may occur at the optic nerve head.

References:

1. Lee WJ, Shin CY, Yoo BK, et al. Induction of matrix metalloproteinase-9 (MMP-9) in lipopolysaccharide-stimulated primary astrocytes is mediated by extracellular signal-regulated protein kinase 1/2 (Erk1/2). *Glia* 2003;41:15-24.

2. Wstermarck J, Kahari V-M. Regulation of matrix metalloproteinase expression in tumor invasion. *FASEB J* 1999;13:781-792.

3. Stamenkovic I. Extracellular matrix remodelling: the role of matrix metalloproteinases. *J Pathology* 2003;200:448-464.

4. Chakraborti S, Mandal M, Das S, Mandal A, Chakraborti T. Regulation of matrix metalloproteinases: an overview. *Mol Cell Biochem* 2003;253:269-285.

5. Vu TH, Werb Z. Matrix metalloproteinases: effectors of development and normal physiology. *Genes Dev* 2000;14:2123-2133.

6. Shapiro SD. Matrix metalloproteinase degradation of extracellular matrix: biological consequences. *Curr Opin Cell Biol* 1998;10:602-608.

7. Hulmes DJS. Building Collagen Molecules, Fibrils, and Suprafibrillar Structures. *J Struct Biol*2002;137:2-10.

8. Ottani V, Raspanti M, Ruggeri A. Collagen structure and functional implications. *Micron* 2001;32:251-260.

9. Wierzbicka-Patynowski I, Schwarzbauer JE. The ins and outs of fibronectin matrix assembly. *J Cell Sci* 2003;116:3269-3276.

10. Pankov R, Yamada KM. Fibronectin at a glance. *J Cell Sci* 2002;115:3861-3863.

11. Hynes R. Fibronectin. *New York* 1990;Springer-Verlag.

12. Mosher D. Fibronectin. *New York* 1989;Academic Press.

13. Erik H.J. Danen KMY. Fibronectin, integrins, and growth control. *J Cell Physiol* 2001;189:1-13.

14. Mao Y, Schwarzbauer JE. Fibronectin fibrillogenesis, a cell-mediated matrix assembly process. *Matri Biol* 2005;24:389-399.

15. Farias E, Lu M, Li X, Schnapp LM. Integrin [alpha]8[beta]1-fibronectin interactions promote cell survival via PI3 kinase pathway. *Biochem Biophyl Res Communi* 2005;329:305-311.

16. Gardner J, Ghorpade A. Tissue inhibitor of metalloproteinase (TIMP)-1: The TIMPed balance of matrix metalloproteinases in the central nervous system. *J Neurosci Res* 2003;74:801-806.

17. Overall CM, Lopez-Otin C. Strategies for MMP inhibition in cancer: innovations for the post-trial era. *Nat Rev Can* 2002;2:657-672.

18. Baker AH, Edwards DR, Murphy G. Metalloproteinase inhibitors: biological actions and therapeutic opportunities. *J Cell Sci* 2002;115:3719-3727.

19. Dzwonek J, Rylski M, Kaczmarek L. Matrix metalloproteinases and their endogenous inhibitors in neuronal physiology of the adult brain. *FEBS Letters* 2004;567:129-135.

20. Yanagisawa M, Kurihara H, Kimura S, et al. A novel potent vasoconstrictor peptide produced by vascular endothelial cells. *Nature* 1988;332:411-415.

21. Inoue A, Yanagisawa M, Kimura S, et al. The Human Endothelin Family: Three Structurally and Pharmacologically Distinct Isopeptides Predicted by Three Separate Genes. *PNAS* 1989;86:2863-2867.

22. Yanagisawa H, Hammer RE, Richardson JA, et al. Disruption of ECE-1 and ECE-2 reveals a role for endothelin-converting enzyme-2 in murine cardiac development. *J Clin Invest* 2000;105:1373-1382.

23. Xu D, Emoto N, Giaid A, et al. ECE-1: A membrane-bound metalloprotease that catalyzes the proteolytic activation of big endothelin-1. *Cell* 1994;78:473-485.

24. Goraca A. New Views on the Role of Endothelin. *Endocri Reg* 2002;36:161-167.

25. Sokolovsky M. Endothelin receptor subtypes and their role in transmembrane signaling mechanisms. *Pharmacol Therapeu* 1995;68:435-471.

26. Noske, WHensen J, Wiederholt M. Endothelin-like immunoreactivity in aqueous humor of patients with primary open-angle glaucoma and cataract. *Graefes Arch Clin Exp Ophthalmol* 1997;235:551-552.

27. Tezel G, Kass M, Kolker A, Becker B, Wax M. Plasma and aqueous humor endothelin levels in primary open-angle glaucoma. *J Glaucoma* 1997;6:83-89.

28. Kallberg ME, Brooks DE, Garcia-Sanchez GA, Komaromy AM, Szabo NJ, Tian L. Endothelin 1 Levels in the Aqueous Humor of Dogs With Glaucoma. *J Glaucoma* 2002;11:105-109.

29. Prasanna G, Hulet C, Desai D, et al. Effect of elevated intraocular pressure on endothelin-1 in a rat model of glaucoma. *Pharmacol Res* 2005;51:41-50.

30. Oku H, Sugiyama T, Kojima S, Watanabe T, Azuma I. Experimental Optic Cup Enlargement Caused by Endothelin-1-Induced Chronic Optic Nerve Head Ischemia. *Sur Ophthalmol* 1999;44:S74-S84.

31. Narayan S, Prasanna G, Krishnamoorthy RR, Zhang X, Yorio T. Endothelin-1 Synthesis and Secretion in Human Retinal Pigment Epithelial Cells (ARPE-19): Differential Regulation by Cholinergics and TNF-{alpha}. *Invest Ophthalmol Vis Sci* 2003;44:4885-4894.

32. Grant K, Loizidou M, Taylor I. Endothelin-1: a multifunctional molecule in cancer. *Br J Cancer* 2003;88:163-166.

33. Nambi P, Clozel M, Feuerstein G. Endothelin and heart failure. *Heart Fail Rev* 2001;6:335-340.

34. Portik-Dobos V, Harris AK, Song W, et al. Endothelin antagonism prevents early EGFR transactivation but not increased matrix metalloproteinase activity in diabetes. *Am J Physiol Regul Integr Comp Physiol* 2006;290:R435-441.

35. Nelson J, Bagnato A, Battistini B, Nisen P. The endothelin axis: emerging role in cancer. *Nat rev: can* 2003;3:110-116.

36. Rogers S, Peters C, Pomonis J, Hagiwara H, Ghilardi J, Mantyh P. Endothelin B receptors are expressed by astrocytes and regulate astrocyte hypertrophy in the normal and injured CNS. *Glia* 2003;41:180-190.

37. Rosendorff C. Endothelin, vascular hypertrophy, and hypertension. *Cardiovascu Drugs Ther* 1997;10:795-802.

38. Naicker S, Bhoola KD. Endothelins: vasoactive modulators of renal function in health and disease. *Pharmacol Therapeut* 2001;90:61-88.

39. Kedzierski RM, Yanagisawa M. Endothelin System: The Double-Edged Sword in Health and Disease. *Ann Rev Pharmacol Toxicol* 2001;41:851-876.

40. Prasanna G, Narayan S, Krishnamoorthy RR, Yorio T. Eyeing endothelins: A cellular perspective. *Mol Cell Biochem* 2003;253:71 - 88.

41. Yorio T, Krishnamoorthy R, Prasanna G. Endothelin: is it a contributor to glaucoma pathophysiology? *J Glaucoma* 2002;11:259-270.

42. Felx M, Gutot M-C, Isler M, et al. Endothelin-1 (ET-1) promotes MMP-2 and MMP-9 induction involving the transcription factor NF-kB in human osteosarcoma. *Clin Sci* 2006;110:645–654.

43. Liu S, Premont RT, Kontos CD, Huang J, Rockey DC. Endothelin-1 Activates Endothelial Cell Nitric-oxide Synthase via Heterotrimeric G-protein {beta} {gamma} Subunit Signaling to Protein Kinase B/Akt. *J Biol Chem* 2003;278:49929-49935.

44. Sokolovsky M. Endothelin receptor heterogeneity, G-proteins, and signaling via cAMP and cGMP cascades. *Cell Mol Neurobiol* 1995;15:561-571.

45. Sugden PH, Clerk A. Endothelin Signalling in the Cardiac Myocyte and its Pathophysiological Relevance. *Curr Vascu Pharmacol* 2005;3:343-351.

46. Sugden P. An overview of endothelin signaling in the cardiac myocyte. *J Mol Cell Cardiol* 2003;35:871-886.

47. Bagnato A, Natali PG. Targeting endothelin axis in cancer. *Can Treat Res*

2004;119:293-314.

48. Arai H, Nakao K, Takaya K, et al. The human endothelin-B receptor gene. Structural organization and chromosomal assignment. *J Biol Chem* 1993;268:3463-3470.

49. Sakamoto A, Yanagisawa M, Sawamura T, et al. Distinct subdomains of human endothelin receptors determine their selectivity to endothelinA-selective antagonist and endothelinB- selective agonists. *J Biol Chem* 1993;268:8547-8553.

50. Hosoda K, Nakao K, Tamura N, et al. Organization, structure, chromosomal assignment, and expression of the gene encoding the human endothelin-A receptor. *J Biol Chem* 1992;267:18797-18804.

51. Arai H, Hori S, Aramori I, Ohkubo H, Nakanishi S. Cloning and expression of a cDNA encoding an endothelin receptor. *Nature* 1990;348:730-732.

52. D'Orleans-Juste P, Labonte J, Bkaily G, Choufani S, Plante M, Honore JC. Function of the endothelinB receptor in cardiovascular physiology and pathophysiology. *Pharmacol Therapeu* 2002;95:221-238.

53. Bockaert J, Pin JP. Molecular tinkering of G protein-coupled receptors: an evolutionary success. *The EMBO Journal* 1999;18:1723-1729.

54. Stork PJS, Schmitt JM. Crosstalk between cAMP and MAP kinase signaling in the regulation of cell proliferation. *Trends Cell Biol* 2002;12:258-266.

55. Kolch W. Meaningful relationships: the regulation of the Ras/Raf/MEK/ERK pathway by protein interactions. *Biochem J* 2000;351:289–305.

56. Robin P, Boulven I, Desmyter C, Harbon S, Leiber D. ET-1 stimulates ERK

signaling pathway through sequential activation of PKC and Src in rat myometrial cells. *Am J Physiol Cell Physiol* 2002;283:C251-260.

57. Peters CM, Rogers SD, Pomonis JD, et al. Endothelin receptor expression in the normal and injured spinal cord: potential involvement in injury-induced ischemia and gliosis. *Exp Neurol* 2003;180:1-13.

58. Shi-Wen X, Chen Y, Denton C, et al. Endothelin-1 promotes myofibroblast induction through the ETA receptor via a rac/PI3 kinase/Akt-dependent pathway and is essential for the enhanced contractile phenotype of fibrotic fibroblasts. *Mol Biol Cell* 2004.

59. Bisotto S, Fixman ED. Src-family tyrosine kinases, phosphoinositide 3-kinase and Gab1 regulate extracellular signal-regulated kinase 1 activation induced by the type A endothelin-1 G-protein-coupled receptor. *Biochem J* 2001;360:77-85.

60. Masaki T, Miwa S, Sawamura T, Ninomiya H, Okamoto Y. Subcellular mechanisms of endothelin action in vascular system. *Eur J Pharmacol* 1999;375:133-138.

61. Clerk A, Bogoyevitch M, Anderson M, Sugden P. Differential activation of protein kinase C isoforms by endothelin-1 and phenylephrine and subsequent stimulation of p42 and p44 mitogen- activated protein kinases in ventricular myocytes cultured from neonatal rat hearts. *J Biol Chem* 1994;269:32848-32857.

62. Robin P, Boulven I, Bole-Feysot C, Tanfin Z, Leiber D. Contribution of PKC-dependent and -independent processes in temporal ERK regulation by ET-1, PDGF, and

EGF in rat myometrial cells. *Am J Physiol Cell Physiol* 2004;286:C798-806.

63. McCudden C, Hains M, Kimple R, Siderovski D, Willard F. G-protein signaling: back to the future. *Cell Mol Life Sci* 2005;62:551-577.

64. Miyauchi T, Masaki T. Pathophysiology of Endothelin in the Cardiovascular System. *Ann Rev Physiol* 1999;61:391-415.

65. Arai K, Maruyama Y, Nishida M, et al. Differential Requirement of Galpha 12, Galpha 13, Galpha q, and Gbeta gamma for Endothelin-1-Induced c-Jun NH2-Terminal Kinase and Extracellular Signal-Regulated Kinase Activation. *Mol Pharmacol* 2003;63:478-488.

66. Kawanabe Y, Nauli SM. Involvement of extracellular Ca2+ influx through voltage-independent Ca2+ channels in endothelin-1 function. *Cell Signal* 2005;17:911-916.

67. Gohla A, Harhammer R, Schultz G. The G-protein G13 but Not G12 Mediates Signaling from Lysophosphatidic Acid Receptor via Epidermal Growth Factor Receptor to Rho. *J Biol Chem* 1998;273:4653-4659.

68. Lopez-Ilasaca M, Crespo P, Pellici PG, Gutkind JS, Wetzker R. Linkage of G Protein-Coupled Receptors to the MAPK Signaling Pathway Through PI 3-Kinase gamma. *Science* 1997;275:394-397.

69. Lewerenz J, Letz J, Methner A. Activation of stimulatory heterotrimeric G proteins increases glutathione and protects neuronal cells against oxidative stress. *J Neurochem* 2003;87:522-531.

70. Liu B, Wu D. The First Inner Loop of Endothelin Receptor Type B Is Necessary for Specific Coupling to Galpha 13. *J Biol Chem* 2003;278:2384-2387.

71. Saito Y, Berk BC. Transactivation: a Novel Signaling Pathway from Angiotensin II to Tyrosine Kinase Receptors. *J Mol Cell Cardiol* 2001;33:3-7.

72. Koyama Y, Yoshioka Y, Matsuda T, Baba A. Focal adhesion kinase is required for endothelin-induced cell cycle progression of cultured astrocytes. *Glia* 2003;43:185-189.

73. Koyama Y, Yoshioka Y, Hashimoto H, Matsuda T, Baba A. Endothelins increase tyrosine phosphorylation of astrocytic focal adhesion kinase and paxillin accompanied by their association with cytoskeletal components. *Neuroscience* 2000;101:219-227.

74. Hua H, Munk S, Whiteside CI. Endothelin-1 activates mesangial cell ERK1/2 via EGF-receptor transactivation and caveolin-1 interaction. *Am J Physiol Renal Physiol* 2003;284:F303-312.

75. Kawanabe Y, Masaki T, Hashimoto N. Involvement of epidermal growth factor receptor–protein tyrosine kinase transactivation in endothelin-1–induced vascular contraction. *J Neuroserg* 2004;100:1066-1071.

76. Kawanabe Y, Nozaki K, Hashimoto N, Masaki T. Involvement of extracellular Ca2+ influx and epidermal growth factor receptor tyrosine kinase transactivation in endothelin-1-induced arachidonic acid release. *Br J Pharmacol* 2003;139:1516-1522.

77. Imokawa G, Kobayasi T, Miyagishi M. Intracellular signaling mechanisms leading to synergistic effects of endothelin-1 and stem cell factor on proliferation of

cultured human melanocytes. Cross-talk via trans-activation of the tyrosine kinase c-kit receptor. *J Biol Chem* 2000;275:33321-33328.

78. Vacca F, Bagnato A, Catt KJ, Tecce R. Transactivation of the Epidermal Growth Factor Receptor in Endothelin-1-induced Mitogenic Signaling in Human Ovarian Carcinoma Cells. *Cancer Res* 2000;60:5310-5317.

79. Schinelli S, Zanassi P, Paolillo M, Wang H, Feliciello A, Gallo V. Stimulation of Endothelin B Receptors in Astrocytes Induces cAMP Response Element-Binding Protein Phosphorylation and c-fos Expression Via Multiple Mitogen-Activated Protein Kinase Signaling Pathways. *J Neurosci* 2001;21:8842-8853.

80. Shichiri M, Sedivy JM, Marumo F, Hirata Y. Endothelin-1 Is a Potent Survival Factor for c-Myc-Dependent Apoptosis. *Mol Endocrinol* 1998;12:172-180.

81. Chen S, Mukherjee S, Chakraborty C, Chakrabarti S. High glucose-induced, endothelin-dependent fibronectin synthesis is mediated via NF-kappa B and AP-1 10.1152/ajpcell.00192.2002. *Am J Physiol Cell Physiol* 2003;284:C263-272.

82. Iwai-Kanai E, Hasegawa K. Intracellular signaling pathways for norepinephrine- and endothelin-1-mediated regulation of myocardial cell apoptosis. *Mol Cell Biochem* 2004;259:163-168.

83. Chintalgattu V, Katwa LC. Role of Protein Kinase C{delta} in Endothelin-Induced Type I Collagen Expression in Cardiac Myofibroblasts Isolated from the Site of Myocardial Infarction. *J Pharmacol Exp Ther* 2004;311:691-699.

84. Hua H, Goldberg HJ, Fantus IG, Whiteside CI. High Glucose-Enhanced

Mesangial Cell Extracellular Signal-Regulated Protein Kinase Activation and {alpha}1(IV) Collagen Expression in Response to Endothelin-1: Role of Specific Protein Kinase C Isozymes. *Diabetes* 2001;50:2376-2383.

85. Quigley E, Quigley H, Pease M, Kerrigan L. Quantitative studies of elastin in the optic nerve heads of persons with primary open-angle glaucoma. *Ophthalmology* 1996;103:1680-1685.

86. Clark AF, Yorio T. Ophthalmic Drug Discovery. *Nat Rev Drug Discov* 2003;2:448 -459.

87. Quigley H. Number of people with glaucoma worldwide. *Br J Ophthalmol* 1996;80:389-393.

88. Hernandez M, Pena J. The optic nerve head in glaucomatous optic neuropathy. *Arch Ophthalmol* 1997;115:389-395.

89. Hernandez MR. The optic nerve head in glaucoma: role of astrocytes in tissue remodeling. *Prog Retin Eye Res* 2000;19:297-321.

90. Hernandez M, Andrzejewska W, Neufeld A. Changes in the extracellular matrix of the human optic nerve head in primary open-angle glaucoma. *Am J Ophthalmol* 1990;109:180-188.

91. Quigley H, Brown A, Dorman-Pease M. Alterations in elastin of the optic nerve head in human and experimental glaucoma. *Br J Ophthalmol* 1991;75:552-557.

92. Quigley H, Dorman-Pease M, Brown A. Quantitative study of collagen and elastin of the optic nerve head and sclera in human and experimental monkey glaucoma.

Curr Eye Res 1991;10:877-888.

93. Morrison J, Dorman-Pease M, Dunkelberger G, Quigley H. Optic nerve head extracellular matrix in primary optic atrophy and experimental glaucoma. *Arch Ophthalmol* 1990;108:1020-1024.

94. Fukuchi T, Sawaguchi S, Yue BJT, Iwata K, Hara H, Kaiya T. Sulfated Proteoglycans in the Lamina Cribrosa of Normal Monkey Eyes and Monkey Eyes with Laser-induced Glaucoma. *Exp Eye Res* 1994;58:231-244.

95. Hernandez M, Hanninen L, Hubbard W, Kaufman P, Weber A. Astrocyte responses in the lamina cribrosa in pressure dependent glaucoma in monkeys. *Invest Ophthalmol Vis Sci* 1995;36:S606.

96. Quigley H, Addicks E, Green W, Maumenee A. Optic nerve damage in human glaucoma. II. The site of injury and susceptibility to damage. *Arch Ophthalmol* 1981;99:635-649.

97. Fini ME, Cook JR, Mohan R. Proteolytic mechanisms in corneal ulceration and repair. *Arch Dermatol Res* 1998;290:Suppl:S12-23.

98. Sivak JM, Fini ME. MMPs in the eye: emerging roles for matrix metalloproteinases in ocular physiology. *Prog Retin Eye Res* 2002;21:1-14.

99. Stokely ME, Yorio T, King MA. Endothelin-1 modulates anterograde fast axonal transport in the central nervous system. *J Neurosci Res* 2005;79:598-607.

100. Stokely ME, Brady ST, Yorio T. Effects of Endothelin-1 on Components of Anterograde Axonal Transport in Optic Nerve. *Invest Ophthalmol Vis Sci* 2002;43:3223-

3230.

101. Morgan J. Optic nerve head structure in glaucoma: astrocytes as mediators of axonal damage. *Eye* 2000;14:437-444.

102. Varela H, Hernandez M. Astrocyte responses in human optic nerve head with primary open-angle glaucoma. *J Glaucoma* 1997;6:303-313.

103. Desai D, He S, Yorio T, Krishnamoorthy RR, Prasanna G. Hypoxia augments TNF-[alpha]-mediated endothelin-1 release and cell proliferation in human optic nerve head astrocytes. *Biochem Biophy Res Commun* 2004;318:642-648.

104. Naidoo V, Mahabeer R, Raidoo DM. Cellular Distribution of Endothelin-1 mRNA in Human Brain by In Situ RT-PCR. *Metab brain dis* 2001;16:207-218.

105. Takahashi K, Totsune K, Kitamuro T, Sone M, Murakami O, Shibahara S. Three vasoactive peptides, endothelin-1, adrenomedullin and urotensin-II, in human tumour cell lines of different origin: expression and effects on proliferation. *Clin Sci* 2002;103:35S–38S.

106. Egidy G, Eberl LP, Valdenaire O, et al. The Endothelin System in Human Glioblastoma. *Lab Investig* 2000;80:1681-1689.

107. Prasanna G, Hulet C, Desai D, et al. Effect of elevated intraocular pressure on endothelin-1 in a rat model of glaucoma. *Pharmacol Res* 2005;51:41-50

108. Prasanna G, Krishnamoorthy R, Clark AF, Wordinger RJ, Yorio T. Human Optic Nerve Head Astrocytes as a Target for Endothelin-1. *Invest Ophthalmol Vis Sci* 2002;43:2704-2713.

109. Hernandez M, Nieto ML, Sanchez Crespo M. Cytosolic phospholipase A2 and the distinct transcriptional programs of astrocytoma cells. *Trends Neurosci* 2000;23:259-264.

110. Quigley H, Hohman R, Addicks E, Massof R, Green W. Morphologic changes in the lamina cribrosa correlated with neural loss in open-angle glaucoma. *Am J Ophthal* 1983;95:673-691.

111. Guo L, Moss SE, Alexander RA, Ali RR, Fitzke FW, Cordeiro MF. Retinal Ganglion Cell Apoptosis in Glaucoma Is Related to Intraocular Pressure and IOP-Induced Effects on Extracellular Matrix. *Invest Ophthalmol Vis Sci* 2005;46:175-182.

112. Schinelli S. The brain endothelin system as potential target for brain-related pathologies. *Curr Drug Target CNS Neurol Disord* 2002;1:543-553.

113. Wedgwood S, Dettman RW, Black SM. ET-1 stimulates pulmonary arterial smooth muscle cell proliferation via induction of reactive oxygen species. *Am J Physiol Lung Cell Mol Physiol* 2001;281:L1058-1067.

114. Lazarini F, Strosberg AD, Couraud PO, Cazaubon SM. Coupling of ETB Endothelin Receptor to Mitogen-Activated Protein Kinase Stimulation and DNA Synthesis in Primary Cultures of Rat Astrocytes. *J Neurochem* 1996;66:459-465.

115. Wang Y, Rose P, Webb M, Dunn M. Endothelins stimulate mitogen activated protein kinase cascade through either ETA or ETB. *Am J Physiol* 1994;267:C1130-C1135.

116. Cazaubon S, Ramos-Morales F, Fischer S, Schweighoffer F, Strosberg A, Couraud P. Endothelin induces tyrosine phosphorylation and GRB2 association of Shc in

astrocytes. *J Biol Chem* 1994;269:24805-24809.

117. Morga E, Faber C, Heuschling P. Stimulation of Endothelin B Receptor Modulates the Inflammatory Activation of Rat Astrocytes. *J Neurochem* 2000;74:603-612.

118. Tian X, Tang G, Chen Y. The effects of endothelin-1 and selective endothelin receptor-type A antagonist on human renal interstitial fibroblasts in vitro. *Zhonghua Yi Xue Za Zhi* 2002;82:5-9.

119. Fraccarollo D, Bauersachs J, Kellner M, Galuppo P, Ertl G. Cardioprotection by long-term ETA receptor blockade and ACE inhibition in rats with congestive heart failure: mono- versus combination therapy. *Cardiovascu Res* 2002;54:85-94.

120. Fraccarollo D, Galuppo P, Bauersachs J, Ertl G. Collagen accumulation after myocardial infarction: effects of ETA receptor blockade and implications for early remodeling. *Cardiovascu Res* 2002;54:559-567.

121. Gomez-Garre D, Ruiz-Ortega M, Ortego M, et al. Effects and interactions of endothelin-1 and angiotensin II on matrix protein expression and synthesis and mesangial cell growth. *Hypertension* 1996;27:885-892.

122. Nakamura T, Ebihara I, Tomino Y, Koide H. Effect of a specific endothelin A receptor antagonist on murine lupus nephritis. *Kidney Int* 1995;47:481-489.

123. Agapova OA, Kaufman PL, Lucarelli MJ, Gabelt BAT, Hernandez MR. Differential expression of matrix metalloproteinases in monkey eyes with experimental glaucoma or optic nerve transection. *Brain Res* 2003;967:132-143.

124. Chintala SK, Zhang X, Austin JS, Fini ME. Deficiency in Matrix Metalloproteinase Gelatinase B (MMP-9) Protects against Retinal Ganglion Cell Death after Optic Nerve Ligation. *J Biol Chem* 2002;277:47461-47468.

125. Zhang X, Cheng M, Chintala SK. Kainic Acid-Mediated Upregulation of Matrix Metalloproteinase-9 Promotes Retinal Degeneration. *Invest Ophthalmol Vis Sci* 2004;45:2374-2383.

126. Johnson EC, Morrison JC, Farrell S, Deppmeier L, Moore C. G., McGinty M. R. The Effect of Chronically Elevated Intraocular Pressure on the Rat Optic Nerve Head Extracellular Matrix. *Exp Eye Res* 1996;62:663-674.

127. Ahmed F, Brown KM, Stephan DA, Morrison JC, Johnson EC, Tomarev SI. Microarray Analysis of Changes in mRNA Levels in the Rat Retina after Experimental Elevation of Intraocular Pressure. *Invest Ophthalmol Vis Sci* 2004;45:1247-1258.

128. Orgul S, Cioffi G, Bacon D, Van Buskirk E. An endothelin-1-induced model of chronic optic nerve ischemia in rhesus monkeys. *J Glaucoma* 1996;5:135-138.

129. Orgul S, Cioffi G, Wilson D, Bacon D, Van Buskirk E. An endothelin-1 induced model of optic nerve ischemia in the rabbit. *Invest Ophthalmol Vis Sci* 1996;37:1860-1869.

130. Chauhan BC, LeVatte TL, Jollimore CA, et al. Model of Endothelin-1-Induced Chronic Optic Neuropathy in Rat. *Invest Ophthalmol Vis Sci* 2004;45:144-152.

131. Cioffi G, Sullivan P. The effect of chronic ischemia on the primate optic nerve. *Eur J Ophthalmol* 1999;Suppl 1:S34-36.

132. Cioffi G, Orgul S, Onda E, Bacon D, Van Buskirk E. An in vivo model of chronic optic nerve ischemia: the dose-dependent effects of endothelin-1 on the optic nerve microvasculature. *Current Eye Research* 1995;14:1147-1153.

CHAPTER 2

Parallel signaling pathways in endothelin-1-induced proliferation of U373MG astrocytoma cells

Shaoqing He[1], Adnan Dibas[1], Thomas Yorio[1], Ganesh Prasanna[1, 2]

[1] Department of Pharmacology and Neuroscience, University of North Texas Health Science Center at Fort Worth, Fort Worth, TX 76107

[2] Current address: Research Pharmacology, Pfizer Global R& D, La Jolla, San Diego, CA 92121

Running title: MAPK, PKC and PI3K in Astrocyte Proliferation

Corresponding author:

Dr. Thomas Yorio, Department of Pharmacology and Neuroscience, University of North Texas Health Science Center at Fort Worth, Fort Worth, TX 76107

Tel: +1-817-735-0258; Fax: +1-817-735-0243; Email: yoriot@hsc.unt.edu

Grants: This work is supported by National Institute of Health Grants EY11979 (to T.Y.); a Texas Higher Education Coordination Board Advanced Technology Grant (to T.Y.); a UNTHSC Intramural Grant (to G.P.); an American Health Assistance Foundation Grants G200006P (to G.P.)

ABSTRACT

Endothelin-1 (ET-1) is a potent mitogen for many cells especially when its levels are elevated under pathological conditions as seen in tumor cell progression and astroglial activation in neuropathies. While ET-1 is known to cause astroglial proliferation, in the present study, multiple signaling pathways involved in ET-1-mediated astrocyte proliferation were characterized. Treatment with PD98059 and U0126 (MEK inhibitors) inhibited not only ET-1-induced cell proliferation but also ET-1-activated phosphorylation of ERK1/2 in U373MG astrocytoma cells. Whereas the non-selective PKC inhibitor chelerythrine attenuated ET-1-induced cell proliferation, it was unable to block ET-1-induced ERK phosphorylation. However, ET-1 did not activate conventional or novel PKCs and did not elevate intracellular calcium. In addition, U73122 (a selective phospholipase C inhibitor), FTI-277 (an H-Ras inhibitor), as well as protein tyrosine kinase inhibitors also did not abolish ET-1-induced ERK1/2 phosphorylation. ET-1 treatment increased the activity of total Ras but not H-Ras. The PI3 kinase pathway appeared to be involved in signal transduction induced by ET-1, but it did not appear to participate in crosstalk with the MAPK pathway. Activated ET receptors didn't propagate signals either through protein tyrosine kinases or transactivation of EGF receptor tyrosine kinases, which typically trigger Ras-Raf-MAPK pathways. The results suggest that ET-1 stimulates cell proliferation by the activation of MAPK-, PKC- and PI3K-dependent pathways that appear to function in a parallel manner. There is no apparent, direct "cross-talk" between these pathways in U373MG cells.

INTRODUCTION

Astrocyte activation and proliferation has been demonstrated in several neuropathies, including ocular neuropathy and brain astrocyte tumor progression(1-6). Astrogliosis is defined as an abnormal increase in the number of astrocytes due to the destruction of nearby neurons and is characterized by exhibiting proliferative and hypertrophic responses (7, 8). Typically, astrogliosis is seen following neurotrauma, hypoxia/ischemia, and other pathologies and is manifested by a dramatic change in the expression of extracellular matrix profile, which in most cases results in a glial scar (9).

Endothelins, a family of vasoactive peptides that include endothelin-1 (ET-1), are implicated in numerous physiological and pathological conditions, including hypertension, cardiac failure, brain and myocardial infarctions, disseminated intravascular coagulation, Alzheimer's disease, and glaucoma (1, 10, 11). ET-1, the predominant isoform of ET, is a potent mitogen in many cells including smooth muscle cells, fibroblasts, and astrocytes (7, 12-16). ET receptors, ET_A and ET_B, are also expressed in many types of cells in central nervous system (CNS) with ET_B as the predominant receptor in the CNS (17). The changes in ET-1 expression and/or regulation of ET receptors appear to play an important role in CNS astrogliosis (18, 19).

The mitogen activated protein kinase (MAPK) signaling pathway is an important pathway in governing cell proliferation, differentiation, and cell death (20, 21). In response to diverse stimuli, such as growth factors, stresses, etc., components of the MAPK become phosphorylated and activated, consequently triggering signaling cascades

ultimately resulting in gene transcription (21, 22). The p44 and p42 MAP kinase/extracellular signal-regulated protein kinase1/2 (ERK1/2) is an important member of the MAPK family that is involved in cell growth, proliferation and differentiation (21-23).

ET-1, through its ET_A and ET_B receptors, activates the MAPK pathway by phosphorylation of ERK1/2 in many types of cells, including smooth muscle cells, fibroblasts, and astrocytes (1, 19, 21, 24). These studies indicated that ET_A receptor-mediated mitogenic activity occurred predominantly through two pathways: protein kinase C (PKC)- and phosphoinositide 3-kinase (PI3K)- dependent pathways, both of which stimulate MAPK (25-27), whereas activation of ET_B receptor-mediated mitogenic activity appears to utilize PKC-independent pathways (21-24). PKC can also act upstream of the MAPK pathway via activation of Ras and Raf, to influence cell proliferation through classical Ras-Raf-MEK-ERK pathways identified through activation of growth factor receptors (23, 28, 29).

Previously, we have shown that ET-1 induces cell proliferation in human U373MG astrocytoma cells and in human optic nerve head astrocytes in culture (7). However, little is known about the ET-1-induced signaling pathways responsible for astrocyte cell proliferation and specifically in U373MG astrocytoma cells that are extremely invasive tumorigenic cells in the CNS. Presently, the mechanism by which ET-1 stimulates the proliferation of human U373MG astrocytoma cells is addressed and the hypothesis that MAPK and PKC pathways are both involved was tested. Our study

indicated that PKC, MAPK and PI3K pathways are directly involved in astrocyte cell proliferation induced by ET-1, and that the activation of ERK1/2 does not appear to involve a cross-talk between c/nPKC (conventional and novel) and PI3K pathways.

MATERIALS AND METHODS

Materials. Dulbecco's modified Eagle's medium (DMEM, catalog no. 11995-040), penicillin- streptomycin-glutamine was obtained from Gibco (Rockville, MD, USA). Fetal bovine serum (FBS) was obtained from Hyclone Labratoraries, Inc. (Logan, UT). PD98059, U0126, chelerythrine, RO-31-8425, genistein, AG82, herbimycin, LY294002, and FTI-277 were purchased from Calbiochem (La Jolla, CA, USA). Rabbit anti-ERK1/2 polyclonal antibody, rabbit anti-phospho-ERK1/2 (Thr202/Tyr 204) polyclonal antibody, rabbit anti-phospho-pan-PKC polyclonal antibody and rabbit anti-phospho-Akt (Ser 473) polyclonal antibody were purchased from Cell Signaling Technology (Beverly, MA); H-Ras plasmid cDNA and H-RasS17N dominant negative cDNA were obtained from Guthrie cDNA Resource Center (Sayre, PA); EZ-Detect-Ras activity Kit were from Pierce Biotechnology, Inc. (Rockford, IL); Fura-2/AM was purchased from Molecular Probes, Inc (Eugene, OR); phorbol 12-myristate 13-acetate (PMA), phorbol 12-monomyristate (PMM), and all other chemicals were purchased from Sigma (St Louis, MO, USA). Endothelin-1, BQ610, and BQ788 were obtained from Peninsula Laboratories (Belmont, CA).

Cell Cultures. U373MG cells (human astrocytoma glioblastoma) obtained from the American Type Culture Collection (ATCC, Manassas, VA) were maintained in DMEM containing 10% fetal bovine serum supplemented with 10u/ml penicillin, 100μg/ml streptomycin and 0.3 μg/ml glutamine under a humidified 5% CO_2 at 37 °C. For plasmid cDNA transfection, cells were cultured to 80% confluence and the media were changed

to serum-free DMEM without penicillin and streptomycin. For experiment with DNA transfection, in each 100mm-dish cell culture, 10μg plasmid cDNA was used for transfection with lipofectamine 2000 (Invitrogen Inc., CA, USA) according to the instruction of manufacturer. After 8 hours, cells were washed with serum-free DMEM and cultured for 24 hours before treatment.

Western Blot. U373MG cells were cultured in 100mm dishes to confluence; 24 hours later the media were changed to serum-free DMEM, cells were pretreated with different inhibitors/ET receptor antagonists for 30 minutes, then cells were stimulated with 100nM ET-1 for various times described herein. The reaction was stopped by adding ice-cold PBS. The cells were scraped and lysed in a lysis buffer (50mM Tris, pH8.0; 100mM NaCl; 1mM EGTA; 1 mM Na-Orthovanadate; 5μM $ZnCl_2$; 50mM NaF; 1mM PMSF; 10μg/ml aprotinin, leupeptin and soybean trypsin inhibitor; 1%(v/v) NP-40; 1%(v/v) triton X-100). Total cell lysate was applied to 10% SDS-PAGE and transferred to nitrocellulose membranes (Protran Bioscience, Keene, NH). The transferred membranes were blocked with 5% non-fat milk in TBS/T (Tris-buffered saline (TBS), 10 mM Tris-HCl, pH 8.0, 150 mM NaCl, and 0.5% Tween 20) for 1 hr and incubated with primary antibody for 1hr at room temperature or overnight at 4°C. A horseradish peroxidase conjugated anti-mouse or anti-rabbit IgG antibodies (Amersham Pharmacia Biotech, Piscataway, NJ) were used as secondary antibody and the enhanced chemiluminescence reagents (Amersham Pharmacia Biotech, Piscataway, NJ) were used for the blotting detection. X-ray films (Kodak, Rochester, NY) were exposed and scanned using an HP

scanner. Density of bands was determined by the software, Scion Image (Scion Corporation, Maryland, USA). Error bars shown in figures represent the standard deviation of mean from the triplicate of a representative experiment.

Cell Proliferation Assays. Formazan-MTT and [methyl-^{3}H]-thymidine incorporation assays were used in present paper. Formazan-MTT assay (Promega, Madison, WI, USA) was performed as previously described (2, 7). U373MG cells were seeded in 96 well-plate in DMEM containing 10% FBS at concentration of 1000 cells per well. On the second day, the media was changed to serum-free DMEM, U373MG cells were pretreated with drugs for 30 minutes, and then stimulated with or without 100 nM ET-1 for 24 hours. The media was aspirated, and 120 μl of a formazan mixed reagent (100 μl pre-warmed SF-DMEM and 20 μl formazan one solution reagent) was added per well. Cells were incubated at 37°C, 5% CO_2 and detected OD value at 490nm wavelength by the plate reader (Molecular Devices, SpectraMax 340pc, Sunnyvale, CA).

A [^{3}H]-thymidine incorporation assay was also performed as previously described (30). Briefly, cells were seeded at 1×10^5 cells per well in 24-well plates in quadruplicate wells. After 8 hours, the cells were placed in serum-free medium for 24 h. ET-1 was then added at final concentration 100nM for 16 h, followed by addition of [^{3}H]-thymidine (1 μCi/well, Amersham Biosciences(NJ, USA)) for 8 hours. Cells were incubated with ice-cold 5% TCA (trichloroacetic acid) for 30 minutes and later washed with ice-cold PBS. Cells were then washed once with PBS followed by incubation with 0.5 ml of lysis solution (0.5M NaOH/0.5% SDS). Lysis solution was transferred into a scintillation vial

containing scintillation cocktail and vials were counted in a beta counter. For inhibitor studies, cells were pretreated for 30 minutes followed by addition of ET-1 and [^{3}H]-thymidine as described above.

PKC Translocation Assay. To determine the translocation of PKC isoforms as a mean to demonstrate PKC activation, the membrane and the cytosol fractions were isolated from cell lysates using previously described procedures (31). U373MG astrocytoma cells treated with different drugs were harvested and sonicated 15 times with 1 second sonication and 1 second intervals in ice-cold Buffer A containing 10 mM HEPES (pH 7.4), 1 mM EDTA, 1 mM EGTA, 0.34 M sucrose, 10% glycerol, 10 μg/mL leupeptin, 10 μg/mL aprotinin, 1 mM benzamidine and 1 mM phenylmethylsulfonyl fluoride. Cell lysates were centrifuged at 16,000xg for 5 minutes, and then the supernatant was centrifuged at 100,000xg at 4°C for 45 minutes to separate membrane and cytosolic fractions. The supernatant was considered the cytosolic fraction. The pellet was resuspended with Buffer B, which is Buffer A with 1% Triton X-100 and placed on ice for 1 hour with several times of gentle mixing. The suspension was centrifuged at 16,000xg at 4°C for 10 minutes, the supernatant contained the solublized membrane fraction. Proteins in each fraction were analyzed by Western blot as described above.

PKC Kinase Assay. PKC activity was determined by measuring ^{32}P incorporation from [γ-^{32}P]ATP into a synthetic PKC substrate peptide, a fragment of glycogen synthase (GS) (Sigma, St Louis, MO, USA), according to the procedures previously described (31-33).

Cytosolic and membrane fractions of cells were isolated by procedures described in PKC Translocation Assay above. PKC activity was calculated as the difference between ^{32}P incorporated into the GS substrate peptide in the presence of $CaCl_2$-phosphatidylserine vs. EGTA. Results were expressed as picomoles of ^{32}P incorporated per milligram of protein per minute ($pmol.mg^{-1}.min^{-1}$).

Activated Ras activity assay. Activated Ras was detected by an affinity pull-down assay with GST-Raf-1 agarose (EZ-Ras-Detect kit) obtained from Pierce Co. and used according to the manufacturer's instructions. U373MG cells transfected with vector, H-Ras wildtype active cDNA or H-Ras dominant negative cDNA, were exposed to ET-1(100nM) for 5 min, or serum-starved untransfected U373MG cells exposed to ET-1(100nM) for 2 min to 30 min. Cells were washed with 1ml ice-cold PBS and lysed in 500 μl Lysis-Binding-Wash (LBW) buffer. 500 μg fresh cell lysate were incubated with 30 μg GST-Raf-1-RBD agarose in a spin column for 1 hr at 4 °C with gentle rotation. The agarose beads were washed 4 times with LBW buffer, and added 50 μl of sample buffer was added and boiled for 5 min. After a brief spin, supernatants were collected and applied to 12% SDS-PAGE. The proteins were transferred from gels to nitrocellulose membranes and probed with monoclonal anti-Ras (1:200, provided with kit). A horseradish peroxidase conjugated anti-mouse IgG antibody was used as secondary antibody and the ECL reagents were used for immunoblotting detection.

Calcium Imaging. Intracellular Ca^{++} ($[Ca^{2+}]_i$) release was determined by calcium imaging (by ratiometric technique using Fura-2 AM) as previously described (34). U373MG cells were seeded on the coverslip in 35mm dish and grown for 24 hours. On the following day, cells were washed with a modified Krebs-Ringer buffer solution (KRB, 115 mM NaCl, 2.5 mM $CaCl_2$, 1.2 mM $MgCl_2$, 24 mM $NaHCO_3$, 5 mM KCl, 5 mM glucose, and 25mM HEPES, pH 7.4) and incubated with 3 μM Fura-2/AM (Molecular Probes) for 30 minutes at 37°C. Fura-2 fluorescence from these cells was monitored at 37 °C by the ratio technique (excitation at 340 and 380 nm, emission at 500 nm) under a Nikon Diaphot microscope using Metafluor software (Universal Imaging, West Chester, PA). $[Ca^{2+}]_i$ was calculated according to the formula provided by Grynkiewicz et al. (35). Calibrations were performed *in vivo*, and conditions of high $[Ca^{2+}]_i$ were achieved by adding the Ca^{2+} ionophore 4-Bromo-A23187 (3 μM; Calbiochem, San Diego, CA), whereas conditions of low $[Ca^{2+}]_i$ were obtained by adding EGTA (5 μM). $[Ca^{2+}]_i$ for each treatment was measured in at least 8 different cells and in two coverslips.

RESULTS:

ET-1 induced cell proliferation of U373MG astrocytoma cells and phosphorylation of ERK1/2

Previous observations demonstrated that 100nM ET-1 treatment for 24 hours increased U373MG astrocytoma cell proliferation using both [^{3}H]-thymidine incorporation and formazan MTT assays (7). In the present series of experiments, the role of ERK1/2 in ET-1-induced cell proliferation was determined using a similar ET-1 dosing. The [^{3}H]-thymidine incorporation assay was employed to investigate ET-1-induced cell proliferation in the absence or presence of inhibitors of several signaling pathways (Fig 1A.). ET-1 induced 25-30% increase in cell proliferation (n=3) whereas 10 μM U0126 (an inhibitor of MEK1/2), 2 μM chelerythrine (an inhibitor of PKC) and 25 μM LY294002 (an inhibitor of PI3 kinase) completely blocked ET-1-induced cell proliferation, while 5 μM genistein (an inhibitor of protein tyrosine kinases) had no effect.

A formazan MTT assay was also employed to measure cell proliferation in the presence of inhibitors of signaling pathways. U373MG astrocytoma cells were seeded in 96-well plates and treated with 100nM U0126 (inhibitor of MEK1/2) and 5μM PD98059 (inhibitor of MEK1) with and without 100nM ET-1. Cell proliferation was stimulated by ET-1 in U373MG significantly ($p<0.05$) by 170% after 24 hours treatment, and this effect was completely blocked by U0126, even at a low concentration (100nM), whereas it was only partially blocked by 5μM PD98059 (Fig. 1B). Although the trend of inhibition of cell proliferation by drugs was similar in both assays, there were some differences shown

between them. The lower basal levels of cell proliferation in treatments with drugs than those in control were seen in the thymidine incorporation assay, whereas the basal levels in the drug-treated groups were almost same as those in control of the formazan-MTT assay. In the thymidine incorporation assay the cells were treated with drugs for 24 hours, whereas [^{3}H]-thymidine was added 8 hours before the cells were harvested. Therefore, the cell proliferation in the drug-treated group had been inhibited for 16 hours before [^{3}H]-thymidine was added. Thus, the lower uptake of thymidine into cells treated with drugs compared to the control. Such an effect can explain the lower basal levels detected in the thymidine incorporation assay.

Extracellular signaling regulated kinase (ERK1/2), the key element of the MAPK pathway, was phosphorylated by 100nM ET-1 in a time-dependent manner (Fig. 1C). The phosphorylation of ERK1/2 reached the highest level after 5-minute treatment with ET-1 and subsequently returned to basal level after 30 minutes. PD98059 at 25 μM partially blocked the phosphorylation induced by ET-1 as well as attenuated the basal level of ERK1/2 phosphorylation (Fig. 1D). Both basal and ET-1-induced phosphorylation of ERK1/2 was completely blocked by 10 μM U0126 (Fig. 1E).

ET-1-induced phosphorylation of ERK1/2 occurs through ET_B receptors

Although the ET_B receptor is predominantly expressed in U373MG cells (36), it was important to determine which receptor was responsible for ERK1/2 phosphorylation induced by ET-1. To address this question, selective ET-receptor antagonists BQ610 (ET_A antagonist) and BQ788 (ET_B antagonist) were used. These compounds were used at

2 μM and were administered to U373MG cells for 30 minutes before ET-1 treatment. BQ788 (IC_{50}=1.2nM) completely blocked the ERK1/2 phosphorylation induced by ET-1, whereas BQ610 (IC_{50}=20nM) had no effect (Fig. 2). This result is also consistent with the binding assay results in which the ET_B receptor antagonist BQ788 completely blocked [^{125}I]-ET-1 binding in U373MG astrocytoma cells, whereas the ET_A receptor antagonist BQ610 and FR139317 did not (36).

Involvement of PKC is necessary for proliferation of U373MG but not necessary for phosphorylation of ERK1/2 induced by ET-1

To test the role of PKCs in ET-1-induced cell proliferation of U373MG astrocytoma cells, 2 μM chelerythrine and 1 μM RO-31-8425, general inhibitors of PKCs, were employed. Blockade of PKC activity by chelerythrine and RO-31-8425 inhibited ET-1-induced proliferation of U373MG cells (Fig. 1A and 3A). Both MAPK-ERK and PKCs were found to be involved in the ET-1-induced cell proliferation of U373MG astrocytoma cells. However it is well known that PKC activation can result in MAPK-ERK activation, therefore the question was whether these pathways exerted their effects in a parallel pattern or whether there was a direct interaction or "cross-talk" between them? To address this question, the effects of PKC inhibitors on ERK1/2 phosphorylation were determined. Phorbol-12-myristate-13-acetate (PMA), the phorbol ester known to activate PKCs, was administered (1μM) in U373MG cells for 30 minutes and it induced a strong phosphorylation of ERK1/2 (Fig. 3B). However, the application

of either 2 μM chelerythrine or 1 μM RO-31-8425 did not abolish the ERK1/2 phosphorylation induced by ET-1 (Fig. 3B).

ET-1 did not activate conventional and/or novel (c/n)PKC isoforms

Our results have shown that PKCs are involved in the ET-1-induced cell proliferation of U373MG astrocytoma, but not in ET-1-induced ERK1/2 phosphorylation. To identify the isoforms of PKCs involved in cell proliferation, we measured the phosphorylation of PKC and translocation of PKC from cytosol to membranes both by Western blot and a PKC kinase assay. In the PKC kinase assay, ET-1 treatment for 5 minutes in U373MG cells did not activate the conventional and/or novel PKCs, whereas 1 μM PMA treatment increased the activities of PKCs, which resulted in PKC phosphorylation and translocation from cytosol to membrane (Fig. 4A and 4B). Furthermore, the results from the kinase assay also showed that blockade of MEK1/2 by U0126 did not affect the activation and translocation of PKCs. Therefore, MEK1/2 and ERK1/2 did not directly activate PKCs in U373MG astrocytoma. Phosphorylation of PKCs in cytosolic and membrane fractions was also determined by Western blot using anti-phospho-pan-PKC antibody, which can recognize phosphorylated PKC-α, βI, βII, δ, η, θ and ε (Fig. 4C). SDS-PAGE gels stained with coomassie blue were used as loading controls. ET treatment of U373MG cells from 1 to 10 minutes did not alter the pattern of phosphorylation and translocation of PKC-α, βI, βII, δ and ε either in cytosolic or membrane fractions (Fig. 4C). In positive controls, after a 30-minute treatment with 1 μM PMA, these phosphorylated isoforms of PKC, shown as 4 bands in the blot, were

translocated to membrane, whereas 1 μM PMM, which is an inactive analog of PMA, did not activate PKC. Because this anti-phospho-pan-PKC antibody can recognize both conventional PKCs (-α, βI, βII) and novel PKCs (-δ, η, θ and ε), it was concluded that ET-1 did not activate c/nPKCs.

ET-1 did not elevate the intracellular Ca^{++} $[Ca^{++}]_i$ mobilization and IP_3 generation

The current data indicated that ET-1 did not activate c/nPKC isoforms, but we still needed to investigate whether ET-1 treatment increases $[Ca^{2+}]_i$ levels, which could activate cPKCs. Fura-2 calcium imaging was used to monitor the concentration of $[Ca^{++}]_i$. After ET-1 was applied to U373MG cells, the ratio at 340nm/380nm did not change (Fig. 5A), whereas carbachol, an agonist of acetylcholine receptors, increased the 340/380 ratio slightly. Treatment with A23187, a calcium ionophore reagent, increased $[Ca^{++}]_i$ rapidly. To further confirm that IP_3-induced $[Ca^{2+}]_i$ and DAG signaling were not involved in ET-1-induced PKC activation and ERK1/2 activation, astrocytoma cells were treated with U73122 (a phospholipase C inhibitor). U73122 did not attenuate the ERK1/2 phosphorylation induced by ET-1 (Fig. 5B). The results suggested that ET-1 did not promote the calcium release in U373MG cells and that there was no cross-talk between PKC and ERK1/2 pathways. These findings were also consistent with the result that ET-1 did not activate c/nPKCs in U373MG cells and could activate atypical PKCs, since chelerythrine, a PKC inhibitor, blocked ET-1-induced cell proliferation.

Inhibition of H-Ras does not block ERK1/2 phosphorylation induced by ET-1

Ras, a member of the small GTPase family, is considered an upstream element involved in the activation of ERK1/2 in mammalian cell types (22, 37, 38), including COS cells (39), Jurkat T cells (40), and astrocytes (41). To identify the role of Ras in the signaling pathway induced by ET-1, pharmacological and molecular biological approaches were used. First, a GST pulldown assay was used to detect Ras activities after ET treatment at different time points. Only the active GTP-bound Ras is pulled down by the GST-Raf-1 Binding Domain (RBD) agarose. At 2 and 5 minutes post ET treatment, the active form of Ras increased and began to decline after 15 minutes of ET treatment (Fig. 6A). U373MG cells were also pretreated for 30 minutes with FTI-277 (10 μM), which is a selective inhibitor of H-Ras, a member of Ras family (42, 43), followed by an application of 100 nM ET-1 for 5 minutes. Surprisingly, ET-1-induced phosphorylation of ERK1/2 was not blocked by FTI-277 (Fig. 6B).

In another set of experiments both ERK1/2 phosphorylation and Ras activity were assessed following ET-1 treatment of U373MG cells transfected with wild type, active, and dominant negative H-Ras plasmid cDNAs. U373MG were transfected with active H-Ras and dominant negative H-RasS17N plasmid cDNA for 36 hours, and followed by an application of ET-1 for 5 min. Phosphorylation of ERK1/2 was greatly amplified by over expression of active wild type H-Ras, with and without ET-1. Treatment with ET-1 enhanced this phosphorylation (Fig. 6C). However, introduction of a dominant negative of H-Ras did not abolish the ET-1-induced phosphorylation of ERK1/2 as compared to controls, which were transfected with the pcDNA3 vector. Activity of Ras was also determined in U373MG transfected with H-Ras cDNA and H-Ras S17N dominant

negative cDNA. In U373MG transfected with active wild type Ras, the activity of Ras was increased significantly by over expression of H-Ras (Fig. 6D). This elevated activity, a reflection of H-Ras over expression, was blocked partially by application of FTI-277 (Fig. 6D). It is therefore likely that a Ras unlike H-Ras may be involved in ET-1-mediated ERK1/2 phosphorylation in U373MG astrocytoma cells.

ET-1 induced phosphorylation of ERK1/2 was not blocked by inhibition of either protein tyrosine kinase or transactivation of receptor tyrosine kinase

Some studies reported that activation of Ras-Raf-MAPK pathway by ET-1 occurs through the protein tyrosine kinases (PTK) such as FAK, c-Src, etc. (26, 44, 45). We also considered that PTKs might be part of the upstream elements and play an important role to activate a similar signaling induced by ET-1 in U373MG astrocytoma cells. Genistein (5 μM), an inhibitor of protein tyrosine kinases, did not block either ET-1-induced cell proliferation (Fig. 1A.) or ET-1-induced phosphorylation of ERK1/2 (Fig. 7A). To further identify potentially other PTKs involved in the ET-1-induced signaling, the inhibitors of intracellular tyrosine kinases, such as AG82 and herbimycin A, were used to attenuate the kinase activity of p125FAK (focal adhesion kinase), p60 c-Src as well as other protein tyrosine kinases. Neither the co-administration of AG82 (10 μM) and herbimycin A (1 μM) nor administration of AG82 alone decreased ET-1-induced phosphorylation of ERK1/2 (Fig. 7B). Although previous reports in other cell types demonstrated that the ET-1 triggered Ras-Raf-MAPK pathway occurs through protein tyrosine kinases such as FAK, c-Src, etc. Such a mechanism does not appear to be

involved in ET-1-induced triggering of the Ras-Raf-MAPK in U373MG astrocytoma cells.

However, it has also been reported that ET-1 through its ET receptors can transactivate the EGF receptor by which ERK1/2 is phosphorylated and activated through Ras-Raf-MAPK pathway. This was shown in rat mesangial cells (46), human vascular smooth muscle cells (47, 48), human melanocytes (49) and human ovarian carcinoma cells(50). Therefore AG1478, an inhibitor of the EGF receptor tyrosine kinase, was used to examine ET-1 effects on receptor tyrosine kinases. AG14781 (1μM) inhibited EGF-induced phosphorylation of ERK1/2 completely, but did not block ET-1-induced phosphorylation of ERK1/2 (Fig. 7C). Additionally, EGF (10 ng/ml) was used as a positive control and its effects on ERK1/2 were blocked by AG1478 (1 μM) (Fig 7C). EGF induced phosphorylation of ERK1/2 by activation of the EGF receptor tyrosine kinase was completely blocked by application AG1478, an inhibitor of the EGF receptor tyrosine kinase. However, AG1478 did not inhibit the effects of ET-1 on activation of MAPK or phosphorylation of ERK1/2. Therefore in U373MG astrocytoma cells, there is no transactivation of the EGF receptor tyrosine kinase by ET-1 receptors and consequently it does not play a role in ERK1/2 activation.

PI3K is involved in ET-1-induced cell proliferation in U373MG, but ET-1-induced phosphorylation of ERK1/2 is independent on PKC and PI3K

The PI3K-Akt pathway has been implicated in the signaling pathways leading to cell proliferation (51, 52). It was reported that the βγ subunit of activated G proteins of

GPCRs activates PI3K and subsequently leading to activated PKB/Akt (53-55). The role of the PI3K pathway in ET-1-induced U373MG astrocytomas cell proliferation is unknown, therefore the effect of the PI3K on ET-1-induced cell proliferation was examined using a formazan and [^{3}H]-thymidine incorporation assays. Inhibition of PI3 kinase by 25 μM LY294002 completely blocked the ET-1 mitogenic effects in U373MG cells (Fig 1A and 8A). Based on this finding, Akt activation was assessed. A 5-minute ET-1 treatment significantly promoted the phosphorylation of Akt as well as phosphorylation of ERK1/2. The ET-1-induced phosphorylation of Akt was blocked completely by LY294002, but not by chelerythrine, whereas the phosphorylation of ERK1/2 was not blocked by either of these two compounds (Fig. 8B). Phosphorylation of ERK1/2 by ET-1 appears to be PKC and PI3K-independent, albeit activation of PI3K and AKT occurs.

DISCUSSION

In the current study, several findings were made which were reflective of ET-1's mitogenic potential in U373MG astrocytoma cells. It was determined that three signaling pathways, including ERK1/2, PKC, and PI3 kinase, were activated by ET-1 within a short period of time (i.e. by 5 minutes). The combined consequence of activating these three pathways resulted in U373MG cell proliferation. It appeared that ERK1/2 activation was involved but independent of PKC and PI3 kinase activation by ET-1. It was also determined that the ET_B receptor was the dominant receptor involved in ERK1/2 phosphorylation and in increased cell proliferation. Although Ras appears to be a signaling pathway involved in activation of the ERK-MAPK pathway by ET-1, H-Ras was not, indicating that some other Ras members may be involved. It was also shown that some general protein tyrosine kinases, including c-Src, FAK, etc., are not involved in ET-1 stimulation in U373MG as has been reported in other cell types (23, 26, 44, 45, 56),. In addition, ERK1/2 phosphorylation was not transactivated by the EGF receptor by ET-1.

ET-1 induces cell proliferation in many types of cells via its ET_A and ET_B receptors, and although diverse signaling pathways coupled to ET-1 receptors have been identified, the precise mechanisms by which ET-1 stimulates cell proliferation in astrocytes remains unclear. Our present study has shown that ET-1 is a mitogen for U373MG astrocytoma cells similar to that seen in earlier studies in human optic nerve head astrocytes (hONA) (7), and that the cell proliferation of U373MG cells induced by ET-1 is MAPK-ERK-, PKC- and PI3K-dependent. Blockade of one of these three parallel pathways will inhibit the mitogenic effects of ET-1 in U373MG astrocytoma cells. This

may arise from activation of the key components (e.g. common and discrete transcription factors) in the proliferation response. These key components could be downstream kinases of these initial signaling pathways or selective transcriptional factors in which these signaling pathways converge. The phosphorylation of ERK1/2 is a key step in triggering downstream signalings and potential activation of transcriptional factors, such as c-Myc, Elk-1, c-Fos, etc. (41, 57). PKC and PI3 kinase are also involved in ET-1-mediated activation of transcription factors (58) (41, 59, 60). It has been suggested that some transcription factors, such Elk-1, c-Fos, AP-1, are controlled simultaneously by MAPK-ERK and PKC (41, 61, 62) , whereas p38 and JNK share different transcription factors. Some other downstream kinases, including Rsk, p70S6K, are also under control of these three pathways. We propose that blockade of any one of the upstream pathways will completely abolish the activation of downstream kinases or transcription factors dependent on these signals of activation.

Mitogenic effects have been shown to be a characteristic of ET's effects on tumor cells. There are several reports showing that ET-1 is a survival factor for many different blastomas including T98G glioblastoma (Takahashi et al., 2002). Naidoo *et. al.* (3) showed a significant distribution of ET-1 mRNA by *in situ* hybridization in human brain autopsy samples and astrocytic tumors, suggestive of ETs' role in tumor progression. In another report, four human glioblastoma cell lines were found to express all components of ET-1 including endothelin converting enzyme (ECE) and $ET_{A/B}$ receptors and that Bosentan (an $ET_{A/B}$ antagonist) induced apoptosis in these cell lines (5). Furthermore, in one cell line LNZ308, Bosentan inhibited FLICE/Caspase-8 inhibitory protein (FLIP)

promoting cell survival (5). In the same study, it was reported that ET-1 induced ERK1/2 phosphorylation but did not promote cell proliferation of LNZ308 glioblastoma cells (5). However in the present study on U373MG cells, ET-1 did activate ERK1/2 and this resulted in increased cell proliferation as well.

ET-1 has been shown to promote proteolytic activity in ovarian carcinomas typically via ET_A receptor activation causing an increase in both expression and activity of MMP-2, MMP-9, urokinase-type plasminogen activator, PAI-1, and PAI-2 (63). This finding suggests that multiple signaling cascades are necessary to activate various aspects of tumor progression including proliferation, migration, and invasion. Furthermore, ET-1-induced phosphorylation of ERK1/2 was inhibited by BQ788, a selective antagonist of the ET_B receptor, suggesting that ET-1-induced activation of the MAPK pathway occurred through activation of the ET_B receptor. In T98G glioblastomas, treatment with an ET_A antagonist caused significant cell death, whereas treatment with an ET_B antagonist had no such effect (4). The ET_B receptor is predominant in the central nervous system (17). In the normal rat spinal cord, there is ET_A immunoreactivity in the vascular system and afferent nerve fibers, whereas there is broad ET_B immunoreactivity in gray and white matter(19). In response to spinal cord injury the expression of ET_B was increased, resulting in hypertrophy of astrocytes. In the optic nerve crush model, there is increased expression of GFAP and ET_B, which is abolished by an application of the $ET_{A/B}$ inhibitor, bosentan (18). We previously reported that the ET_B receptor and GFAP expression are increased and co-localized at the optic nerve head in rats that had their intra-ocular pressure elevated, moreover the immunoreactivity of ET-1 was also elevated

at the same sites (6). The results from both cell culture and *in vivo* animal models suggest that ET-1 and the ET_B receptor may contribute an important role in astrocyte hypertrophy resulting in astrogliosis.

One interesting finding in the current study is that there was no ET-1-induced calcium mobilization identified in U373MG cells. This observation was further supported by our finding that inhibition of phospholipase C didn't abolish ET-1-induced phosphorylation of ERK1/2. These findings suggest that classical Ca^{2+}-linked ET_A-mediated signaling is lacking in U373MG cells. It is generally considered that the ET_A receptor is coupled to Gαq, which is associated with activation of phospholipase Cβ (PLCβ)(64, 65). In this cell line, U373MG astrocytoma, no ET_A receptor was detectable by ligand binding assay (36) and by RT-PCR(66), suggesting this lack of ET_A receptor responsiveness was our finding that only the ET_B receptor antagonist, BQ788, blocked ET-1-induced phosphorylation of ERK1/2 (Figure 2). Therefore, ET-1 may not induce the activation of PKC and calcium mobilization in this cell line due to the lack of IP_3 and DAG. Moreover, the application of the PLC inhibitor, U73122, didn't block ET-1-induced phosphorylation of ERK1/2 (Figure 5B). We also did neither see any calcium mobilization with ET-1 treatment in this cell type (Figure 5A), nor the activation of the conventional and novel PKC isoforms detected by PKC kinase assay and western blot. Our results confirm that there is no ET_A receptor-mediated calcium mobilization induced by ET-1 in this cell type. The are some reports that ET-1 activates Gαq coupling with ET_B receptor and mediates the variety of signaling pathways in different cells, including hepatocyte (67), vascular smooth muscle cells, C6 glioma cells and Chinese hamster

ovary cells with stable expressing endothelin$_B$ receptors (68-70), and even in astrocyte cell lines, including neuroblastoma cell line, B103 (B103 cells) (71). In contrast to what we found in U373MG astrocytoma cells, inhibition of PLCβ completely abolished ET-1-induced ERK1/2 phosphorylation in C6 glioma cells (70), further indicating that there could be no coupling between Gαq and ET_B receptor in U373MG astrocytoma cells. The studies from other G protein-coupled receptors suggest that there are the differential G protein coupling patterns observed in different tissue and cells. For instance, the metabotropic glutamate receptors (mGluRs) are fully identified GPCRs coupling with the different G proteins. Group I receptors are coupled to Gαq to activation phospholipase C, whereas group II and III mGluRs are coupled to $G\alpha_i$ to down-regulate cyclic AMP (cAMP) levels (72). 5-HT_{1A} receptors interacted predominantly with Gαi in the anterior raphe, whereas they were coupled to Gαo proteins in the hippocampus (73). The β3b-adrenoceptor couples to both Gαs and Gαi in CHO-K1 cells, whereas the β3a-adrenoceptor couples specifically to Gαs (74). It suggests that the differential coupling between G proteins and endothelin receptors may contribute to the variety of actions of ET-1 in different cells and tissues. Although the lack of Gαq-mediated intracellular Ca^{++} mobilization was observed in U373MG astrocytoma cells, the rapid activation of MAPK-ERK by ET-1 was still mediated by other protein tyrosine kinases in a Ca^{++}-independent manner.

PKC also plays an important role in ET-1 induced signaling, and the current study indicated that PKC was also involved in cell proliferation of U373MG. It has been suggested that PKC can activate upstream of the MAPK pathway at Ras or/and Raf to

influence cell proliferation through the classical Ras-Raf-MAPK pathway (23, 28, 29). Although our results showed that activation of PKCs by PMA could induce phosphorylation of ERK1/2, ET-1 did not activate c/nPKCs in U373MG cells. Moreover, ET-1 did not elevate intracellular calcium through activation of PLC. The results confirmed our finding that c/nPKCs are not involved in ET-1-signaling in U373MG cells. In addition, the detection of phosphorylated ERK1/2 after pretreatment of PKC inhibitors and activation of PKCs after pretreatment of with MEK1/2 inhibitors indicated that there was no "cross-talk" between these two pathways. Although c/nPKCs have been ruled out in the signaling cascades induced by ET-1, the involvement of atypical PKC isoforms (ζ/τ) (29, 75, 76) might still play a role in controlling cell proliferation of U373MG cells. This needs further investigation.

In U373MG astrocytoma cells, Ras was activated following ET-1 treatment. These findings are in agreement with reports of ET-1 effects on other cell types, such as cardiac myocytes (77) and myometrial cells (23). FTI-277, an inhibitor of farnesyltransferase (FTase), increases the non-farnesylated cytoplasmic H-Ras, which competes with active Ras and binds to Raf protein to inactivate Ras/Raf complexes (42, 43, 78, 79). Surprisingly, application of FTI-277 and introduction of the dominant negative cDNA of H-Ras into U373MG did not inhibit the phosphorylation of ERK1/2 induced by ET-1, whereas wildtype active H-Ras significantly stimulated the phosphorylation of ERK1/2 independent of ET-1. However in U373MG cells, H-Ras appears not to be involved in ET-1 induced signaling. Other forms of Ras, such as K-Ras, N-Ras, M-Ras could play an important role in this cascade (37, 80).

In summary, the current studies indicate that ET-1-induced cell proliferation in U373MG astrocytoma cells occurs through an apparent concurrent activation of MAPK-ERK, PKC and PI3K pathways. ET-1 activates the Ras-Raf-1-MAPK-ERK pathway without activation of protein tyrosine kinase. In U373MG astrocytoma cells, neither c/nPKCs nor PI3 kinase are involved in ET-1-induced ERK1/2 signaling. However, MAPK-ERK, PKC and PI3K pathways appear to exert their roles in parallel without a direct, apparent "cross-talk". They do however appear to activate key components (e.g. common and discrete transcription factors) in the proliferation response, because inhibition of any one parallel pathway blocks proliferation. This parallel signaling is not unlikely as the proliferation response is dependent on many cellular processes that may be activated simultaneously in tumor cell proliferation through complex signaling systems and important transcriptional events.

ACKNOWLEDGMENTS

This work was supported by National Institute of Health Grants EY11979 (to T.Y.); a Texas Higher Education Coordination Board Advanced Technology Grant (to T.Y.); a UNTHSC Intramural Grant (to G.P.); an American Health Assistance Foundation Grants G200006P (to G.P.). We wish to thank Dr. Raghu Krishnamoorthy for helpful comments of the manuscript.

REFERENCE

1. Yorio T, Krishnamoorthy R, Prasanna G. Endothelin: is it a contributor to glaucoma pathophysiology? J Glaucoma 11:259-270, 2002.

2. Desai D, He S, Yorio T, Krishnamoorthy RR, Prasanna G. Hypoxia augments TNF-[alpha]-mediated endothelin-1 release and cell proliferation in human optic nerve head astrocytes. Biochem Biophys Res Commun 318:642-648, 2004.

3. Naidoo V, Mahabeer R, Raidoo DM. Cellular Distribution of Endothelin-1 mRNA in Human Brain by In Situ RT-PCR. Metabo Brain Dis 16:207-218, 2001.

4. Takahashi K, Totsune K, Kitamuro T, Sone M, Murakami O, Shibahara S. Three vasoactive peptides, endothelin-1, adrenomedullin and urotensin-II, in human tumour cell lines of different origin: expression and effects on proliferation. Clin Sci 103:35S–38S, 2002.

5. Egidy G, Eberl LP, Valdenaire O, Irmler M, Majdi R, Diserens A-C, Fontana A, Janzer R-C, Pinet F, Juillerat-Jeanneret L. The Endothelin System in Human Glioblastoma. Lab Invest 80:1681-1689, 2000.

6. Prasanna G, Hulet C, Desai D, Krishnamoorthy RR, Narayan S, Brun A-M, Suburo AM, Yorio T. Effect of elevated intraocular pressure on endothelin-1 in a rat model of glaucoma. Pharmacol Res 51:41-50, 2005.

7. Prasanna G, Krishnamoorthy R, Clark AF, Wordinger RJ, Yorio T. Human Optic Nerve Head Astrocytes as a Target for Endothelin-1. Invest Ophthalmol Vis Sci 43:2704-2713, 2002.

8. Hernandez M, Nieto ML, Sanchez Crespo M. Cytosolic phospholipase A2 and the distinct transcriptional programs of astrocytoma cells. Trends Neurosci 23:259-264, 2000.

9. Hernandez MR. The optic nerve head in glaucoma: role of astrocytes in tissue remodeling. Prog Retin Eye Res 19:297-321, 2000.

10. Grant K, Loizidou M, Taylor I. Endothelin-1: a multifunctional molecule in cancer. Br J Cancer 88:163-166, 2003.

11. Schinelli S. The brain endothelin system as potential target for brain-related pathologies. Curr Drug Target CNS Neurol Disord 1:543-553, 2002.

12. Wedgwood S, Dettman RW, Black SM. ET-1 stimulates pulmonary arterial smooth muscle cell proliferation via induction of reactive oxygen species. Am J Physiol Lung Cell Mol Physiol 281:L1058-1067, 2001.

13. Nambi P, Clozel M, Feuerstein G. Endothelin and heart failure. Heart Fail Rev 6:335-340, 2001.

14. Lazarini F, Strosberg AD, Couraud PO, Cazaubon SM. Coupling of ETB Endothelin Receptor to Mitogen-Activated Protein Kinase Stimulation and DNA Synthesis in Primary Cultures of Rat Astrocytes. J Neurochem 66:459-465, 1996.

15. Wang Y, Rose P, Webb M, Dunn M. Endothelins stimulate mitogen activated protein kinase cascade through either ETA or ETB. Am J Physiol 267:C1130-C1135, 1994.

16. Cazaubon S, Ramos-Morales F, Fischer S, Schweighoffer F, Strosberg A, Couraud P. Endothelin induces tyrosine phosphorylation and GRB2 association of Shc in astrocytes. J Biol Chem 269:24805-24809, 1994.

17. Morga E, Faber C, Heuschling P. Stimulation of Endothelin B Receptor Modulates the Inflammatory Activation of Rat Astrocytes. J Neurochem 74:603-612, 2000.

18. Rogers S, Peters C, Pomonis J, Hagiwara H, Ghilardi J, Mantyh P. Endothelin B receptors are expressed by astrocytes and regulate astrocyte hypertrophy in the normal and injured CNS. Glia 41:180-190, 2003.

19. Peters CM, Rogers SD, Pomonis JD, Egnazyck GF, Keyser CP, Schmidt JA, Ghilardi JR, Maggio JE, Mantyh PW. Endothelin receptor expression in the normal and injured spinal cord: potential involvement in injury-induced ischemia and gliosis. Exp Neurol 180:1-13, 2003.

20. Stork PJS, Schmitt JM. Crosstalk between cAMP and MAP kinase signaling in the regulation of cell proliferation. Trends Cell Biol 12:258-266, 2002.

21. Sugden P. An overview of endothelin signaling in the cardiac myocyte. J Mol Cell Cardiol 35:871-886, 2003.

22. Kolch W. Meaningful relationships: the regulation of the Ras/Raf/MEK/ERK pathway by protein interactions. Biochem J 351:289–305, 2000.

23. Robin P, Boulven I, Desmyter C, Harbon S, Leiber D. ET-1 stimulates ERK signaling pathway through sequential activation of PKC and Src in rat myometrial cells. Am J Physiol Cell Physiol 283:C251-260, 2002.

24. Naicker S, Bhoola KD. Endothelins: vasoactive modulators of renal function in health and disease. Pharmacol Ther 90:61-88, 2001.

25. Shi-Wen X, Chen Y, Denton C, Eastwood M, Renzoni E, Bou-Gharios G, Pearson J, Dashwood M, DuBois R, Black C, Leask A, Abraham D. Endothelin-1 promotes myofibroblast induction through the ETA receptor via a rac/PI3 kinase/Akt-dependent pathway and is essential for the enhanced contractile phenotype of fibrotic fibroblasts. Mol Biol Cell, 2004.

26. Bisotto S, Fixman ED. Src-family tyrosine kinases, phosphoinositide 3-kinase and Gab1 regulate extracellular signal-regulated kinase 1 activation induced by the type A endothelin-1 G-protein-coupled receptor. Biochem J 360:77-85, 2001.

27. Masaki T, Miwa S, Sawamura T, Ninomiya H, Okamoto Y. Subcellular mechanisms of endothelin action in vascular system. Eur J Pharmacol 375:133-138, 1999.

28. Clerk A, Bogoyevitch M, Anderson M, Sugden P. Differential activation of protein kinase C isoforms by endothelin-1 and phenylephrine and subsequent stimulation of p42 and p44 mitogen- activated protein kinases in ventricular myocytes cultured from neonatal rat hearts. J Biol Chem 269:32848-32857, 1994.

29. Robin P, Boulven I, Bole-Feysot C, Tanfin Z, Leiber D. Contribution of PKC-dependent and -independent processes in temporal ERK regulation by ET-1, PDGF, and EGF in rat myometrial cells. Am J Physiol Cell Physiol 286:C798-806, 2004.

30. Coward P, Wada HG, Falk MS, Chan SDH, Meng F, Akil H, Conklin BR. Controlling signaling with a specifically designed Gi-coupled receptor. Proc Natl Acad Sci USA 95:352-357, 1998.

31. Xu J, Weng Y-I, Simoni A, Krugh BW, Liao Z, Weisman GA, Sun GY. Role of PKC and MAPK in cytosolic PLA2 phosphorylation and arachadonic acid release in primary murine astrocytes. J Neurochem 83:259-270, 2002.

32. Dibas A, Wood J, Mia A, Yorio T. The ATP-depleting reagent iodoacetamide induces the degradation of protein kinase C alpha (PKC alpha) in LLC-PK1 pig kidney cells. Life Sci 61:1697-1704, 1997.

33. Castro AF, Amorena C, Muller A, Ottaviano G, Tellez-Inon MT, Taquini AC. Extracellular ATP and bradykinin increase cGMP in vascular endothelial cells via activation of PKC. Am J Physiol Cell Physiol 275:C113-119, 1998.

34. Prasanna G, Dibas AI, Yorio T. Cholinergic and Adrenergic Modulation of the Ca2+ Response to Endothelin-1 in Human Ciliary Muscle Cells. Invest Ophthalmol Vis Sci 41:1142-1148, 2000.

35. Grynkiewicz G, Poenie M, Tsien R. A new generation of Ca2+ indicators with greatly improved fluorescence properties. J Biol Chem 260:3440-3450, 1985.

36. Wu-Wong J, Chiou W, Magnuson S, Opgenorth T. Endothelin receptor in human astrocytoma U373MG cells: binding, dissociation, receptor internalization. J Pharmacol Exp Ther 274:499-507, 1995.

37. Ehrhardt A, Ehrhardt GRA, Guo X, Schrader JW. Ras and relatives--job sharing and networking keep an old family together. Exp Hematol 30:1089-1106, 2002.

38. Chong H, Vikis HG, Guan K-L. Mechanisms of regulating the Raf kinase family. Cell Signal 15:463-469, 2003.

39. Yan J, Roy S, Apolloni A, Lane A, Hancock JF. Ras Isoforms Vary in Their Ability to Activate Raf-1 and Phosphoinositide 3-Kinase. J Biol Chem 273:24052-24056, 1998.

40. Zisoulis DG, Kansas GS. H-Ras and PI3K cooperate to induce FucT-VII expression in Jurkat T cells. J Biol Chem 279:39495-39504, 2004.

41. Schinelli S, Zanassi P, Paolillo M, Wang H, Feliciello A, Gallo V. Stimulation of Endothelin B Receptors in Astrocytes Induces cAMP Response Element-Binding Protein Phosphorylation and c-fos Expression Via Multiple Mitogen-Activated Protein Kinase Signaling Pathways. J Neurosci 21:8842-8853, 2001.

42. Lerner EC, Qian Y, Blaskovich MA, Fossum RD, Vogt A, Sun J, Cox AD, Der CJ, Hamilton AD, Sebti SM. Ras CAAX Peptidomimetic FTI-277 Selectively Blocks Oncogenic Ras Signaling by Inducing Cytoplasmic Accumulation of Inactive Ras-Raf Complexes. J Biol Chem 270:26802-26806, 1995.

43. Upadhyay D, Correa-Meyer E, Sznajder JI, Kamp DW. FGF-10 prevents mechanical stretch-induced alveolar epithelial cell DNA damage via MAPK activation. Am J Physiol Lung Cell Mol Physiol 284:L350-359, 2003.

44. Koyama Y, Yoshioka Y, Matsuda T, Baba A. Focal adhesion kinase is required for endothelin-induced cell cycle progression of cultured astrocytes. Glia 43:185-189, 2003.

45. Koyama Y, Yoshioka Y, Hashimoto H, Matsuda T, Baba A. Endothelins increase tyrosine phosphorylation of astrocytic focal adhesion kinase and paxillin accompanied by their association with cytoskeletal components. Neuroscience 101:219-227, 2000.

46. Hua H, Munk S, Whiteside CI. Endothelin-1 activates mesangial cell ERK1/2 via EGF-receptor transactivation and caveolin-1 interaction. Am J Physiol Renal Physiol 284:F303-312, 2003.

47. Kawanabe Y, Masaki T, Hashimoto N. Involvement of epidermal growth factor receptor–protein tyrosine kinase transactivation in endothelin-1–induced vascular contraction. J Neurosurg 100:1066-1071, 2004.

48. Kawanabe Y, Nozaki K, Hashimoto N, Masaki T. Involvement of extracellular Ca2+ influx and epidermal growth factor receptor tyrosine kinase transactivation in endothelin-1-induced arachidonic acid release. Br J Pharmacol 139:1516-1522, 2003.

49. Imokawa G, Kobayasi T, Miyagishi M. Intracellular signaling mechanisms leading to synergistic effects of endothelin-1 and stem cell factor on proliferation of cultured human melanocytes. Cross-talk via trans-activation of the tyrosine kinase c-kit receptor. J Biol Chem 275:33321-33328, 2000.

50. Vacca F, Bagnato A, Catt KJ, Tecce R. Transactivation of the Epidermal Growth Factor Receptor in Endothelin-1-induced Mitogenic Signaling in Human Ovarian Carcinoma Cells. Cancer Res 60:5310-5317, 2000.

51. Matsui T, Nagoshi T, Rosenzweig A. Akt and PI 3-Kinase Signaling in Cardiomyocyte Hypertrophy and Survival. Cell Cycle 2:220-223, 2003.

52. Chang F, Lee J, Navolanic P, Steelman L, Shelton J, Blalock W, Franklin R, McCubrey J. Involvement of PI3K/Akt pathway in cell cycle progression, apoptosis, and neoplastic transformation: a target for cancer chemotherapy. Leukemia 17:590-603, 2003.

53. Lopez-Ilasaca M, Crespo P, Pellici PG, Gutkind JS, Wetzker R. Linkage of G Protein-Coupled Receptors to the MAPK Signaling Pathway Through PI 3-Kinase gamma. Science 275:394-397, 1997.

54. Liu S, Premont RT, Kontos CD, Huang J, Rockey DC. Endothelin-1 Activates Endothelial Cell Nitric-oxide Synthase via Heterotrimeric G-protein {beta} {gamma} Subunit Signaling to Protein Kinase B/Akt. J Biol Chem 278:49929-49935, 2003.

55. Lewerenz J, Letz J, Methner A. Activation of stimulatory heterotrimeric G proteins increases glutathione and protects neuronal cells against oxidative stress. J Neurochem 87:522-531, 2003.

56. Miyamoto Y, Yamauchi J, Itoh H. Src Kinase Regulates the Activation of a Novel FGD-1-related Cdc42 Guanine Nucleotide Exchange Factor in the Signaling Pathway from the Endothelin A Receptor to JNK. J Biol Chem 278:29890-29900, 2003.

57. Shichiri M, Sedivy JM, Marumo F, Hirata Y. Endothelin-1 Is a Potent Survival Factor for c-Myc-Dependent Apoptosis. Mol Endocrinol 12:172-180, 1998.

58. Chen S, Mukherjee S, Chakraborty C, Chakrabarti S. High glucose-induced, endothelin-dependent fibronectin synthesis is mediated via NF-kappa B and AP-1. Am J Physiol Cell Physiol 284:C263-272, 2003.

59. Iwai-Kanai E, Hasegawa K. Intracellular signaling pathways for norepinephrine- and endothelin-1-mediated regulation of myocardial cell apoptosis. Mol Cell Biochem 259:163-168, 2004.

60. Chintalgattu V, Katwa LC. Role of Protein Kinase C{delta} in Endothelin-Induced Type I Collagen Expression in Cardiac Myofibroblasts Isolated from the Site of Myocardial Infarction. J Pharmacol Exp Ther 311:691-699, 2004.

61. Sugden PH, Clerk A. Endothelin Signalling in the Cardiac Myocyte and its Pathophysiological Relevance. Curr Vasc Pharmacol 3:343-351, 2005.

62. Hua H, Goldberg HJ, Fantus IG, Whiteside CI. High Glucose-Enhanced Mesangial Cell Extracellular Signal-Regulated Protein Kinase Activation and {alpha}1(IV) Collagen Expression in Response to Endothelin-1: Role of Specific Protein Kinase C Isozymes. Diabetes 50:2376-2383, 2001.

63. Rosano L, Salani D, Castro VD, Spinella F, Natali PG, Bagnato A. Endothelin-1 promotes proteolytic activity of ovarian carcinoma. Clin Sci 103:306S–309S, 2002.

64. Prasanna G, Narayan S, Krishnamoorthy RR, Yorio T. Eyeing endothelins: A cellular perspective. Mol Cell Biochem 253:71 - 88, 2003.

65. Adamsa JW, Brown JH. G-proteins in growth and apoptosis: lessons from the heart. Oncegene 20:1626-1634, 2001.

66. Paolillo M, Barbieri A, Zanassi P, Schinelli S. Expression of endothelins and their receptors in glioblastoma cell lines. J Neurooncol 79:1-7, 2006.

67. Jouneaux C, Mallat A, Serradeil-Le Gal C, Goldsmith P, Hanoune J, Lotersztajn S. Coupling of endothelin B receptors to the calcium pump and phospholipase C via Gs and Gq in rat liver. J Biol Chem 269:1845-1851, 1994.

68. Kawanabe Y, Hashimoto N, Masaki T. Characterization of G proteins involved in activation of nonselective cation channels by endothelinB receptor. Br J Pharmacol 136:1015-1022, 2002.

69. Kawanabe Y, Nauli SM. Involvement of extracellular Ca2+ influx through voltage-independent Ca2+ channels in endothelin-1 function. Cell Signal 17:911-916, 2005.

70. Cramer H, Schmenger K, Heinrich K, Horstmeyer A, Boning H, Breit A, Piiper A, Lundstrom K, Muller-Esterl W, Schroeder C. Coupling of endothelin receptors to the ERK/MAP kinase pathway. Roles of palmitoylation and G(alpha)q. Eur J Biochem 268:5449-5459, 2001.

71. Kawanabe Y, Hashimoto N, Masaki T. B103 neuroblastoma cells predominantly express endothelin ETB receptor; effects of extracellular Ca2+ influx on endothelin-1-induced mitogenesis. Eur J Pharmacol 425:173-179, 2001.

72. Wroblewska B, Wegorzewska IN, Bzdega T, Olszewski RT, Neale JH. Differential negative coupling of type 3 metabotropic glutamate receptor to cyclic GMP levels in neurons and astrocytes. J Neurochem 96:1071-1077, 2006.

73. la Cour CM, El Mestikawy S, Hanoun N, Hamon M, Lanfumey L. Regional Differences in the Coupling of 5-Hydroxytryptamine-1A Receptors to G Proteins in the Rat Brain. Mol Pharmacol 70:1013-1021, 2006.

74. Sato M, Hutchinson DS, Bengtsson T, Floren A, Langel U, Horinouchi T, Evans BA, Summers RJ. Functional Domains of the Mouse {beta}3-Adrenoceptor Associated with Differential G Protein Coupling. J Pharmacol Exp Ther 315:1354-1361, 2005.

75. Monick MM, Carter AB, Flaherty DM, Peterson MW, Hunninghake GW. Protein Kinase C {zeta} Plays a Central Role in Activation of the p42/44 Mitogen-Activated Protein Kinase by Endotoxin in Alveolar Macrophages. J Immunol 165:4632-4639, 2000.

76. Liberto GD, Dallot E, Parco IE-L, Cabrol D, Ferre F, Breuiller-Fouche M. A critical role for PKC{zeta} in endothelin-1-induced uterine contractions at the end of pregnancy. Am J Physiol Cell Physiol 285:C599-607, 2003.

77. Bogoyevitch M, Glennon P, Andersson M, Clerk A, Lazou A, Marshall C, Parker P, Sugden P. Endothelin-1 and fibroblast growth factors stimulate the mitogen- activated protein kinase signaling cascade in cardiac myocytes. The potential role of the cascade in the integration of two signaling pathways leading to myocyte hypertrophy. J Biol Chem 269:1110-1119, 1994.

78. Battaglia A, Pak K, Brors D, Bodmer D, Frangos JA, Ryan AF. Involvement of ras activation in toxic hair cell damage of the mammalian cochlea. Neuroscience 122:1025-1035, 2003.

79. Bolick S, Landowski T, Boulware D, Oshiro M, Ohkanda J, Hamilton A, Sebti S, Dalton W. The farnesyl transferase inhibitor, FTI-277, inhibits growth and induces apoptosis in drug-resistant myeloma tumor cells. Leukemia 17:451-457, 2003.

80. Ellis CA, Clark G. The importance of being K-Ras. Cell Signal 12:425-434, 2000.

FIGURE LEGENDS

Figure 1. Cell proliferation of U373MG was blocked by inhibition of phosphorylation of ERK1/2 induced by ET-1.

A. Cell proliferation of U373MG was determined using a [^{3}H]-thymidine incorporation assay 24 hrs after U373MG cells were pretreated with 10 μM U0126 (a MEK1/2 inhibitor), 2 μM chelerythrine (CHE, a PKC inhibitor), 25 μM LY294002 (LY, a PI3 kinase inhibitor), and 5 μM genistein (GE, a protein tyrosine kinase inhibitor) 30 min before treated with 100 nM ET-1. * $p<0.05$ vs. ET-1 treatment alone; Oneway ANOVA/SNK test. **B.** Cell proliferation of U373MG was determined by Formazan MTT assay 24 hrs after U373MG cells were pretreated with 100nM U0126 (a MEK1/2 inhibitor) and 5 μM PD98059 (a MEK 1 inhibitor) 30 min before treated with100 nM ET-1. * $p<0.05$ vs. ET-1 treatment alone; Oneway ANOVA/SNK test. **C.** Western blot is employed to detect the phosphorylation of ERK1/2 induced by ET-1 over several time points after U373MG cells were treated with 100 nM ET-1 from 2 min to 30 min. **D.** and **E.** Western blot indicates phosphorylation of ERK1/2 induced by ET-1 after cells were pretreated with PD98059 (25 μM) and U0126 (10 μM) for 30min followed by application 100nM ET-1 for 5min. The data shown are from a representative from 3 individual experiments. * $p<0.05$ ET-1 treatment vs. relative control; Oneway ANOVA/SNK test (for **C. D.** and **E.**).

Figure 2. ET-1-induced phosphorylation of ERK1/2 occurred through ET_B receptors.

Western blot shows phosphorylation of ERK1/2 induced by ET-1 after U373MG astrocytoma cells were pretreated with BQ610 (2 μM) and BQ788 (2 μM) for 30 min followed by an application 100nM ET-1 for 5min. The data shown are from a representative from 3 individual experiments. * $p<0.05$ ET-1 treatment vs. relative control; Oneway ANOVA/SNK test.

Figure 3. Involvement of PKC is necessary for proliferation of U373MG, however, phosphorylation of ERK1/2 induced by ET-1 is PKC-independent.

A. Cell proliferation of U373MG was determined by Formazan MTT assay 24 hrs after U373MG cells were treated with 2 μM chelerythrine (CHE, a PKC inhibitor). * $p<0.05$ vs. ET-1; Oneway ANOVA/SNK test. **B.** U373MG cells were pretreated with 1 μM PMA, 2 μM chelerythrine and 1 μM RO-31-8425 (RO) followed application of ET-1 for 5 min. Western blot was employed to detect the phosphorylation of ERK1/2 in total cell lysate. The data shown are from a representative from 3 individual experiments. * $p<0.05$ ET-1 treatment vs. relative control; Oneway ANOVA/SNK test.

Figure 4. ET-1 did not activate conventional and novel (c/n) PKC isoforms in U373MG.

A. B. Activities of c/n PKC were determined by kinase assay that used a PKC substrate phosphorylated by cytosolic and membrane fraction in the presence of Ca^{++} and DAG. * $p<0.05$ PMA treatment vs. relative control; Oneway ANOVA/SNK test. **C.** Phosphorylation and translocation of c/n PKC isoforms were detected by Western blot for

cytosolic and membrane fractions isolated from U373MG which was pretreated with 1 μM PMA (positive control), 1 μM PMM (negative control) and DMSO (vehicle, labeled as "V") for 30 min followed by an application of 100 nM ET-1 for 1min to 10 min. The data shown are from a representative from 3 individual experiments.

Figure 5. Intracellular Ca^{++} was not changed after U373MG was treated with 100nM ET-1 and blockade of IP3 generation did not block the phosphorylation of ERK1/2 induced by ET-1.

A. Concentration of intracellular Ca^{++} in U373MG cells was monitored by Fura-2 Calcium imaging. U373MG cells cultured on coverslips were treated with 100 nM ET-1, 100 μM carbachol, AG23187 and EGTA after preincubation with Fura-2 for 30 min. (n=8) **B.** U373MG cells were pretreated with 2 μM U-73122, followed by an application of ET-1 for 5 min. Western blot was employed to detect the phosphorylation of ERK1/2 in total cell lysate.

* $p<0.05$ ET-1 treatment vs. relative control; Oneway ANOVA/SNK test.

Figure 6. Inhibition of H-Ras does not block the phosphorylation of ERK1/2 induced by ET-1 even though ET-1 activates Ras.

A. GST-pulldown assay was used to detect Ras activity after cells were treated with 100 nM ET-1 for different time points. **B.** Phosphorylation of ERK1/2 induced by ET-1 was determined by Western blot after cells were pretreated with FTI-277 (FTI, 10 μM), an inhibitor of Ras, for 30 min followed by an application of 100 nM ET-1 for 5 min. **C.**

Western blot was employed to detect phosphorylation of ERK1/2 induced by ET-1 after U373MG cells were transfected with 10 μg vector, wildtype H-Ras (WT) and dominant negative H-Ras (DN) cDNA for 24 hrs followed by an application of 100 nM ET-1 for 5 min. **D.** GST-pulldown assay was used to detect Ras activity after U373MG cells were transfected with 10 μg vector, wildtype H-Ras and dominant negative H-Ras cDNA for 24 hrs followed by an application of 100 nM ET-1 for 5 min. The data shown are from a representative from 2 individual experiments. * $p<0.05$ ET-1 treatment vs. relative control; Oneway ANOVA/SNK test.

Figure 7. Inhibition of protein tyrosine kinases did not block the phosphorylation of ERK1/2 induced by ET-1. Also ET-1 did not transactivate EGF receptor tyrosine kinase.

A. U373MG cells were pretreated with 5 μM genistein (GENI), an inhibitor of protein tyrosine kinase, followed by an application of ET-1 for 5 min. Western blot was employed to detect the phosphorylation of ERK1/2 in total cell lysate. **B.** 10 μM AG82 (AG) and/or 1 μM herbimycin A (HER) were used to pretreat U373MG for 30 min followed a 5 min ET-1 treatment. **C.** Genistein and 1 μM AG1478 (an inhibitor of EGF receptor tyrosine kinase) were used to pretreat U373MG for 30 min followed a 5 min ET-1 or EGF (10 ng/ml) treatment. The data shown are form a representative from 3 individual experiments. * $p<0.05$ ET-1 treatment vs. relative control; Oneway ANOVA/SNK test.

Figure 8. Inhibition of PI3 kinase by LY294002 abolished cell proliferation of U373MG stimulated by ET-1, and ERK1/2 phosphorylation induced by ET-1 is PKC- and PI3 Kinase-independent.

A. Cell proliferation of U373MG was determined by Formazan MTT assay 24 hrs after U373MG cells were treated with 25 μM LY294002 (LY). * $p<0.05$ vs. ET-1; Oneway ANOVA/SNK test. **B.** U373MG cells were pretreated with 2 μM chelerythrine (CHE) and 25 μM LY294002 followed by an application of ET-1 for 5 min. Western blot was employed to detect the phosphorylation of ERK1/2 and Akt in total cell lysate. The data shown are from a representative from 3 individual experiments. * $p<0.05$ ET-1 treatment vs. relative control; Oneway ANOVA/SNK test.

Figure 9. Possible signaling pathways involved in ET-1-induced U373MG astrocytoma cell proliferation.ERK-MAPK, PKC and PI3-kinase pathways are involved in ET-1-induced cell proliferation in U373MG astrocytoma. Blockade of one of these three pathways will completely abolish the cell proliferation induced by ET-1. No direct crosstalks among these pathways are found in this cell type. Some of well-identified protein tyrosine kinases including c-Src, FAK, are not involved in this event, and transactivation of EGF receptor by ET-1 through $ET_{A/B}$ receptors is not found in this cell line.

Figure 1.

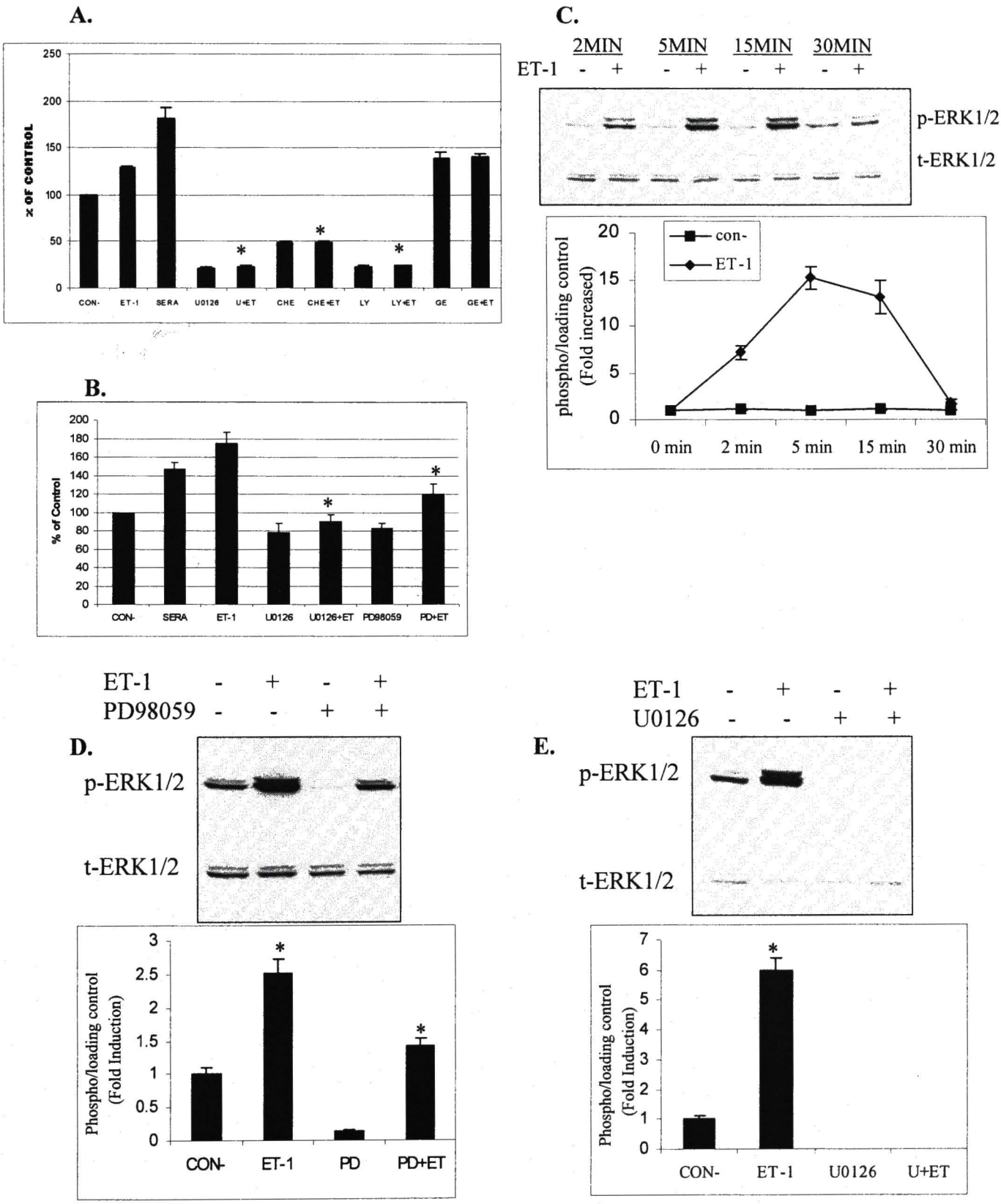
A.
% OF CONTROL
250
200
150
100
50
0
CON-
ET-1
SERA
U0126
U+ET
CHE
CHE+ET
LY
LY+ET
GE
GE+ET
B.
% of Control
200
180
160
140
120
100
80
60
40
20
0
CON-
SERA
ET-1
U0126
U0126+ET
PD98059
PD+ET
C.
2MIN
5MIN
15MIN
30MIN
ET-1 - + - + - + - +
p-ERK1/2
t-ERK1/2
phospho/loading control
(Fold increased)
20
15
10
5
0
con-
ET-1
0 min
2 min
5 min
15 min
30 min
ET-1 - + - +
PD98059 - - + +
D.
p-ERK1/2
t-ERK1/2
Phospho/loading control
(Fold Induction)
3
2.5
2
1.5
1
0.5
0
CON-
ET-1
PD
PD+ET
ET-1 - + - +
U0126 - - + +
E.
p-ERK1/2
t-ERK1/2
Phospho/loading control
(Fold Induction)
7
6
5
4
3
2
1
0
CON-
ET-1
U0126
U+ET

Figure 2.

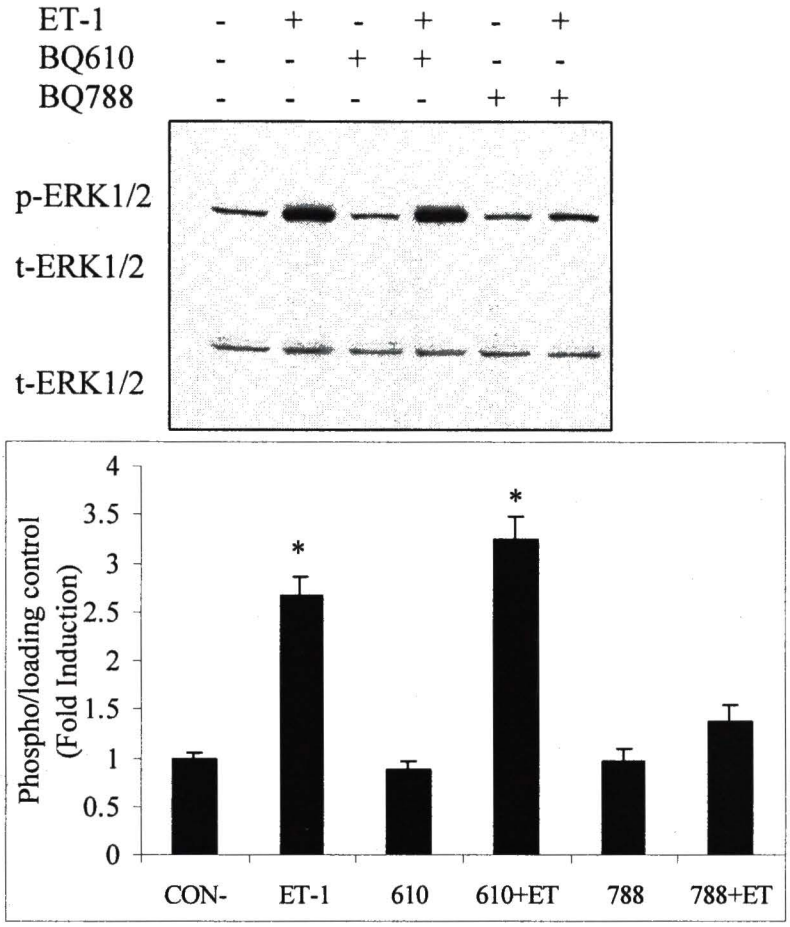
ET-1 - + - + - +
BQ610 - - + + - -
BQ788 - - - - + +
p-ERK1/2
t-ERK1/2
t-ERK1/2
Phospho/loading control (Fold Induction)
4
3.5
3
2.5
2
1.5
1
0.5
0
*
*
CON-
ET-1
610
610+ET
788
788+ET

Figure 3.

A.

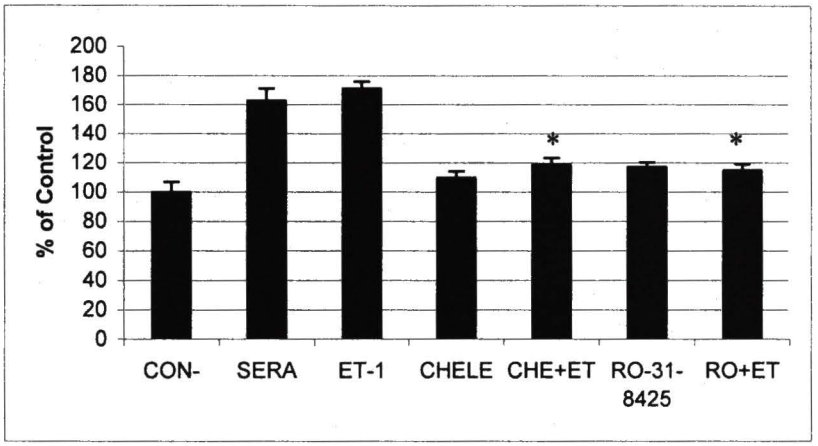
% of Control
200
180
160
140
120
100
80
60
40
20
0
CON-
SERA
ET-1
CHELE
CHE+ET
RO-31-8425
RO+ET
*
*

B.

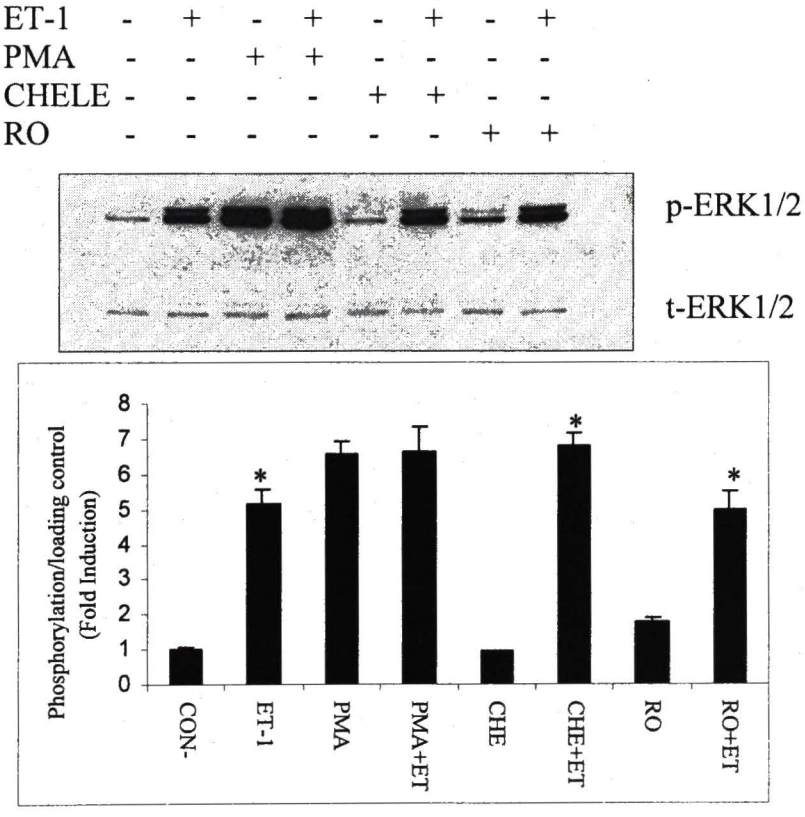
ET-1 - + - + - + - +
PMA - - + + - - - -
CHELE - - - - + + - -
RO - - - - - - + +
p-ERK1/2
t-ERK1/2
Phosphorylation/loading control (Fold Induction)
8
7
6
5
4
3
2
1
0
CON-
ET-1
PMA
PMA+ET
CHE
CHE+ET
RO
RO+ET
*
*
*

Figure 4.

A.

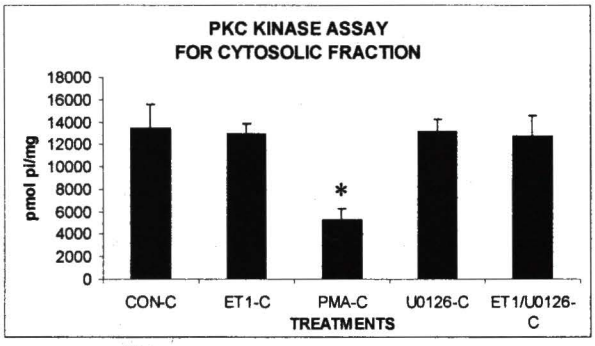

B.

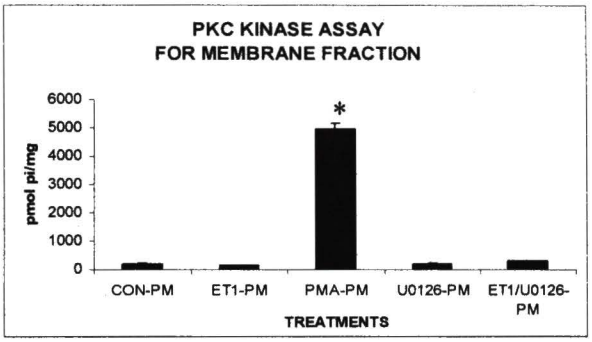

C.

ET-1	-	-	-	1	5	10	MIN
PMA	+	-	-	-	-	-	
PMM	-	+	-	-	-	-	

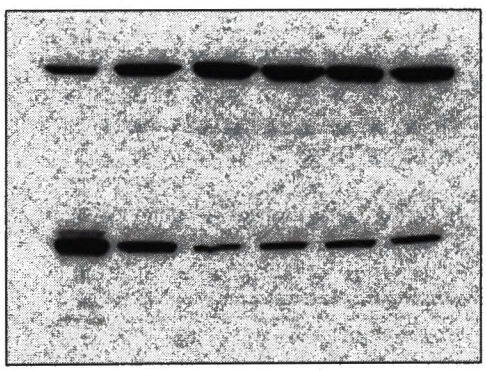

p-Pan-PKC (Cytosolic fractions)

p-Pan-PKC (Membrane fractions)

Figure 5.

A.

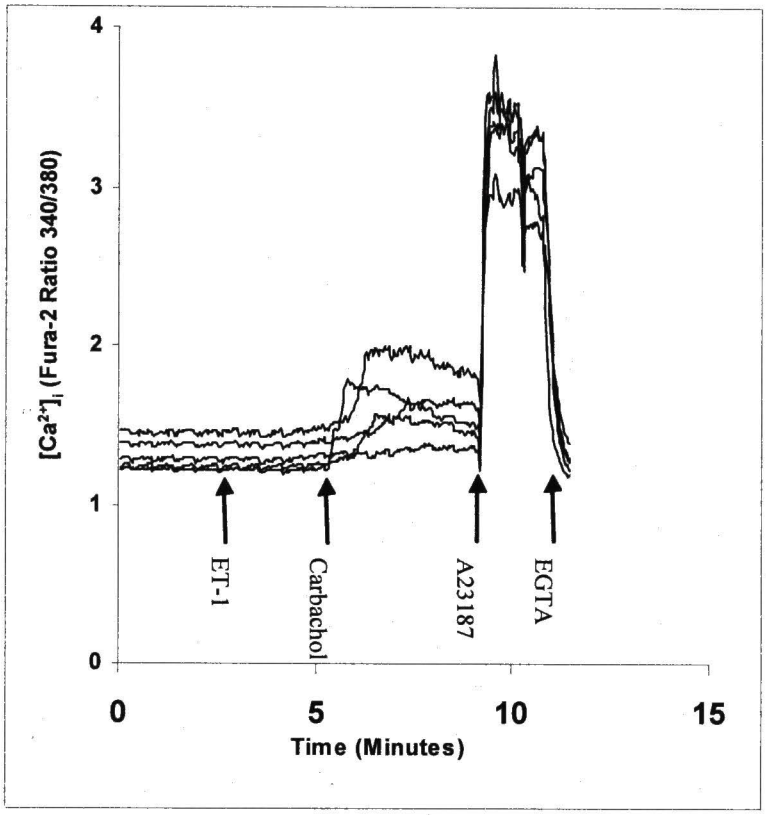
[Ca2+]i (Fura-2 Ratio 340/380)
4
3
2
1
0
ET-1
Carbachol
A23187
EGTA
0
5
10
15
Time (Minutes)

B.

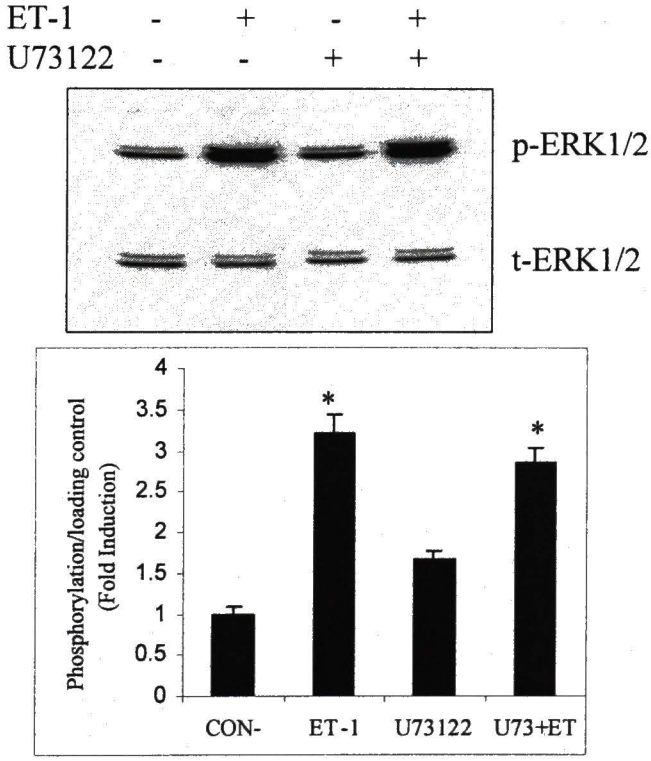
ET-1 - + - +
U73122 - - + +
p-ERK1/2
t-ERK1/2
Phosphorylation/loading control (Fold Induction)
4
3.5
3
2.5
2
1.5
1
0.5
0
*
*
CON-
ET-1
U73122
U73+ET

Figure 6.

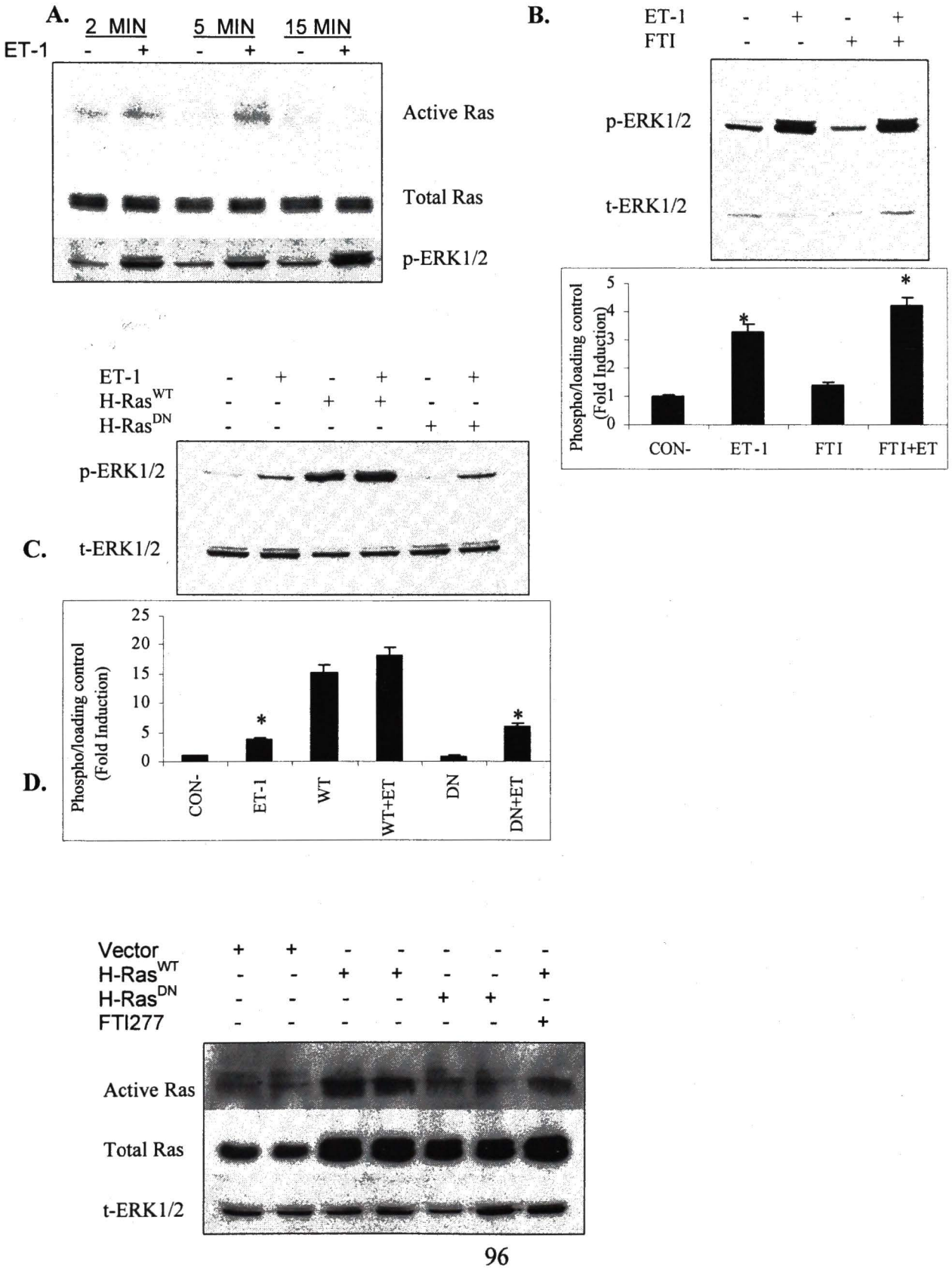
A.
2 MIN
5 MIN
15 MIN
ET-1
Active Ras
Total Ras
p-ERK1/2
B.
ET-1
FTI
p-ERK1/2
t-ERK1/2
Phospho/loading control (Fold Induction)
CON-
ET-1
FTI
FTI+ET
C.
H-Ras^WT
H-Ras^DN
p-ERK1/2
t-ERK1/2
D.
Phospho/loading control (Fold Induction)
CON-
ET-1
WT
WT+ET
DN
DN+ET
Vector
H-Ras^WT
H-Ras^DN
FTI277
Active Ras
Total Ras
t-ERK1/2

Figure 7.

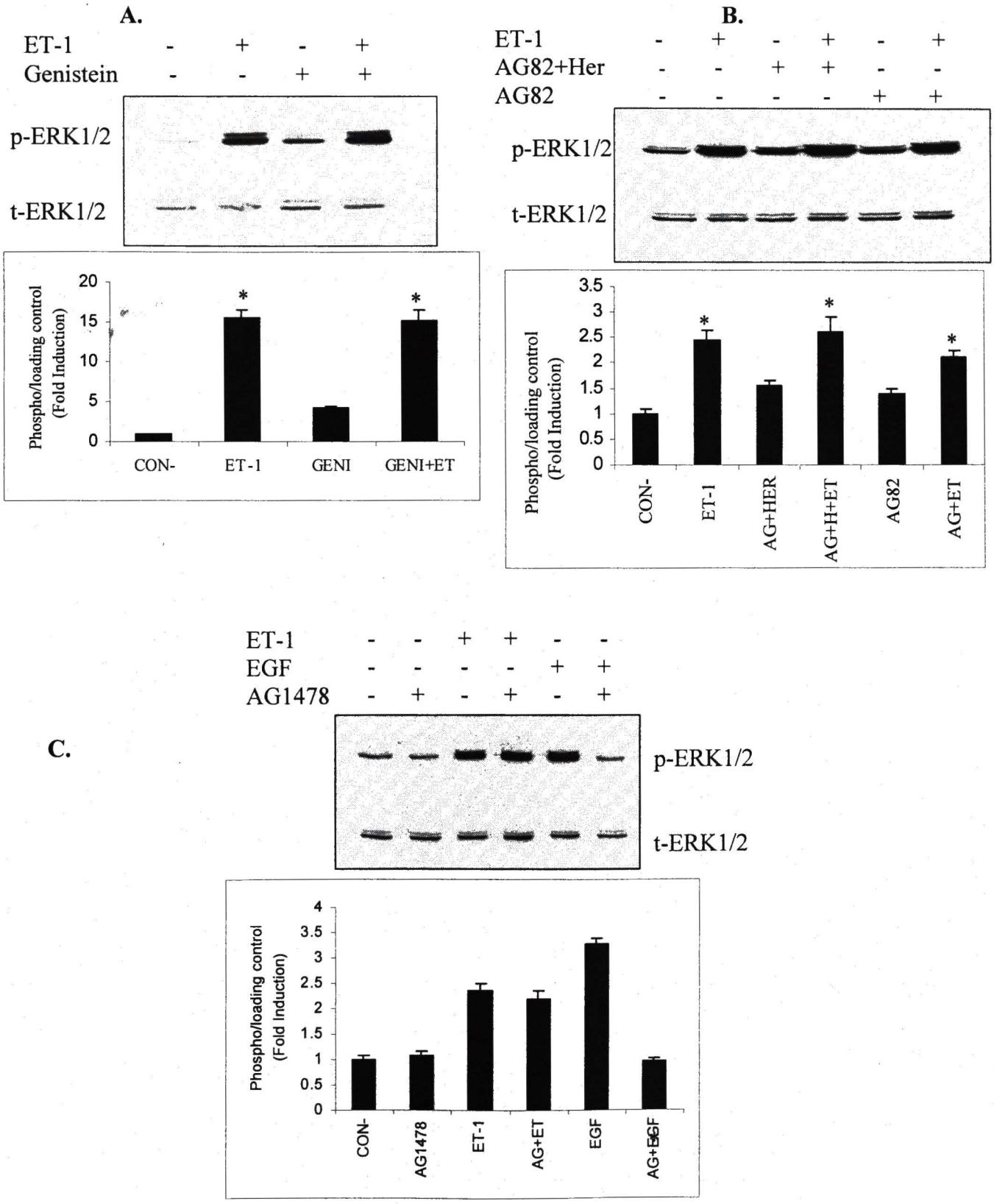
A.
ET-1 - + - +
Genistein - - + +
p-ERK1/2
t-ERK1/2
Phospho/loading control (Fold Induction)
20
15
10
5
0
*
*
CON-
ET-1
GENI
GENI+ET
B.
ET-1 - + - + - +
AG82+Her - - + + - -
AG82 - - - - + +
p-ERK1/2
t-ERK1/2
Phospho/loading control (Fold Induction)
3.5
3
2.5
2
1.5
1
0.5
0
*
*
*
CON-
ET-1
AG+HER
AG+H+ET
AG82
AG+ET
C.
ET-1 - - + + - -
EGF - - - - + +
AG1478 - + - + - +
p-ERK1/2
t-ERK1/2
Phospho/loading control (Fold Induction)
4
3.5
3
2.5
2
1.5
1
0.5
0
CON-
AG1478
ET-1
AG+ET
EGF
AG+EGF

Figure 8.

A

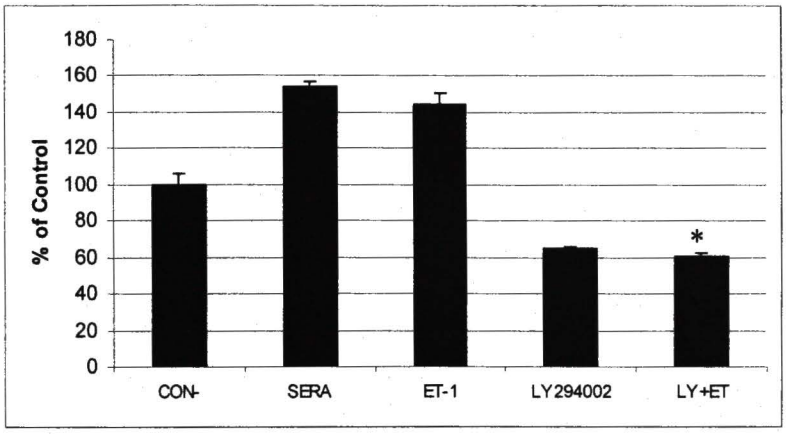
180
160
140
120
100
80
60
40
20
0
% of Control
*
CON-
SERA
ET-1
LY294002
LY+ET

B.

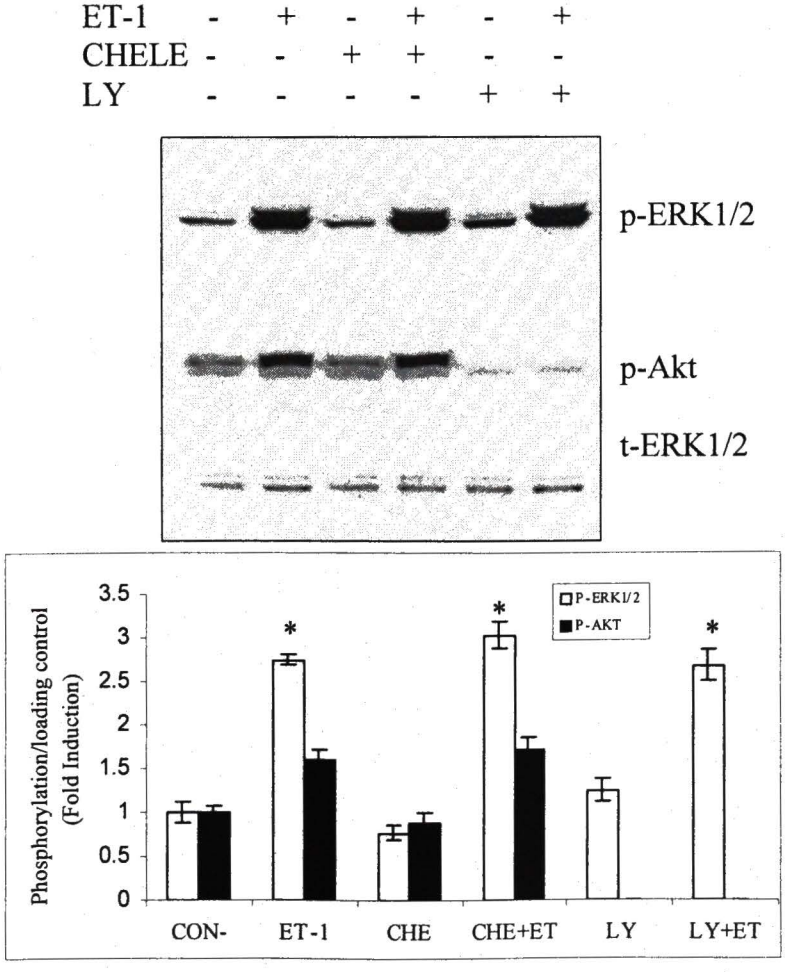
ET-1 - + - + - +
CHELE - - + + - -
LY - - - - + +
p-ERK1/2
p-Akt
t-ERK1/2
Phosphorylation/loading control (Fold Induction)
3.5
3
2.5
2
1.5
1
0.5
0
P-ERK1/2
P-AKT
*
*
*
CON-
ET-1
CHE
CHE+ET
LY
LY+ET

Figure 9.

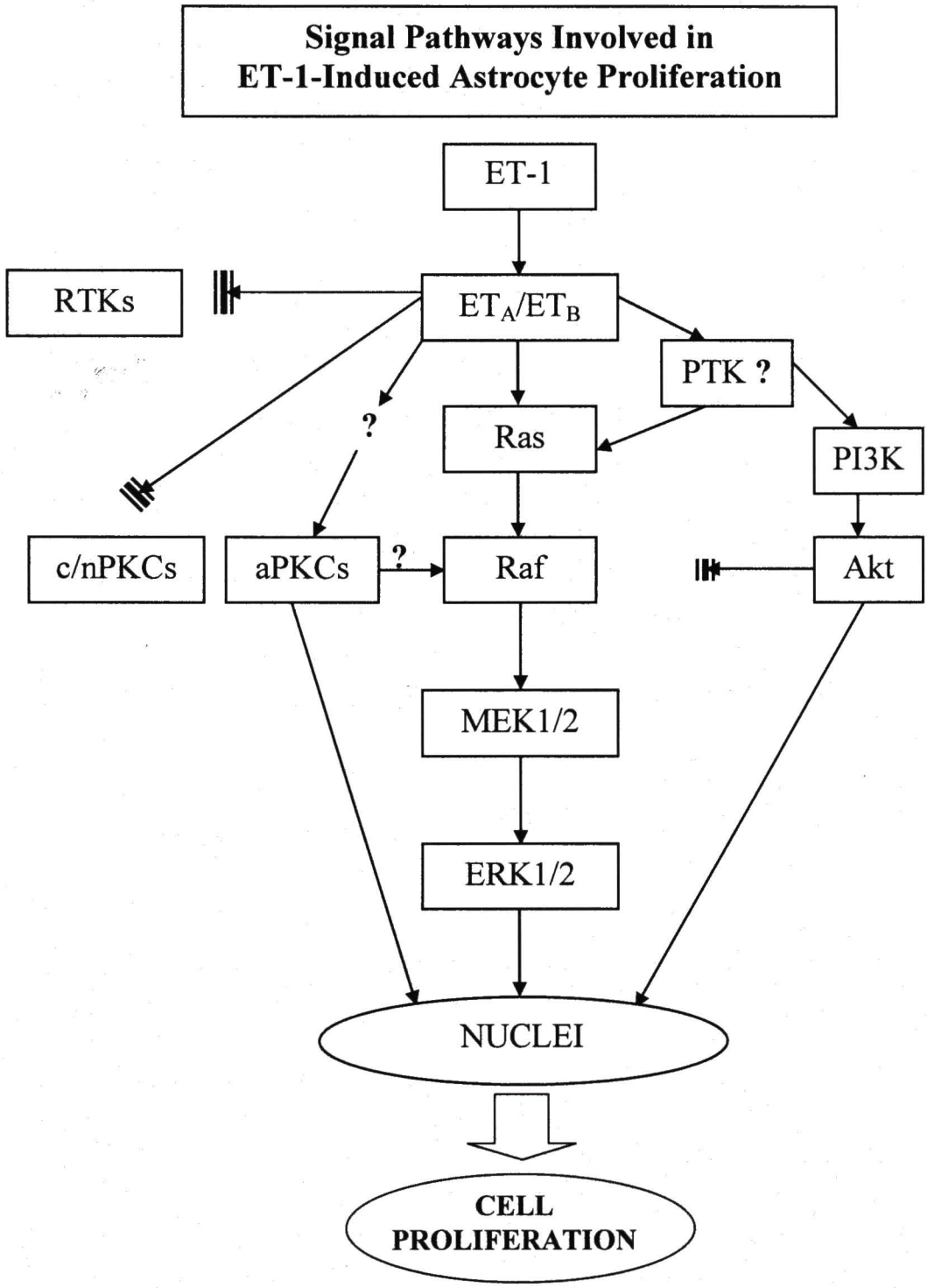
Signal Pathways Involved in
ET-1-Induced Astrocyte Proliferation
ET-1
RTKs
ET_A/ET_B
PTK ?
?
Ras
PI3K
c/nPKCs
aPKCs
?
Raf
Akt
MEK1/2
ERK1/2
NUCLEI
CELL
PROLIFERATION

CHAPTER 3

Endothelin-1-mediated Signaling in the Expression of Matrix Metalloproteinases (MMPs) and Tissue Inhibitors of Metalloproteinases (TIMPs) in Astrocytes

Shaoqing He[1], Ganesh Prasanna[1, 2], Thomas Yorio[1]*

[1] Department of Pharmacology and Neuroscience, University of North Texas Health Science Center at Fort Worth, Fort Worth, TX 76107

[2] Current address: Research Pharmacology, Pfizer Global R& D, La Jolla, San Diego, CA 92121

***Corresponding author:**

Dr. Thomas Yorio, Department of Pharmacology and Neuroscience, University of North Texas Health Science Center at Fort Worth, 3500 Camp Bowie BLVD, Fort Worth, TX 76107

Tel: +1-817-735-0258; Fax: +1-817-735-0243; Email: yoriot@hsc.unt.edu

Grants: **This work is supported by National Institute of Health Grants EY11979 (to T.Y.); a Texas Higher Education Coordination Board Advanced Technology Grant (to T.Y.)**

Abstract:

Purpose: Endothelin-1 (ET-1) levels are increased in aqueous and vitreous humor in glaucoma patients and animal models of glaucoma. Whether the elevated ET-1 induces extracellular matrix(ECM) remodeling in the optic nerve head is still unknown. In the present study, the regulation of MMPs/TIMPs and ECM remodeling in ET-1-activated human optic nerve head astrocytes(hONAs) was determined.

Methods: Primary hONAs were exposed to ET-1 for 1 and 4 days. Incubation media were subjected to zymography and western blot to detect activity and expression of MMPs and TIMPs. Fibronectin(FN) was monitored by western blot and immunofluorescent staining.

Results: ET-1 increased the activity of MMP-2 and the expression of TIMP-1 and 2 in hONAs. The expression of TIMP-1 and 2 induced by ET-1 was abolished by application of inhibitors of MAPK or PKC, leading to enhanced activity of MMP-2. Knock-down of MMP-2, using siRNA, not only decreased the activity of MMP-2 but also decreased the expression of TIMP-1 and 2. ET-1 increased the soluble FN expression as well as FN matrix formation. However, the accumulation sFN didn't enhance FN matrix formation. Unlike ET-1's effects on MMP-2, blockade of MAPK and PKC did not alter the expression and deposition pattern of FN in hONAs.

Conclusions: ET-1 increased the expression and activity of MMP-2 and TIMP-1, 2. The ERK-MAPK and PKC pathways are involved in the regulation of MMP-2 and TIMP-1, 2 expression. ET-1's effects on MMPs/TIMPs may be important not only in regulating the expression of MMPs and TIMPs but also in influencing ECM remodeling.

Introduction:

Glaucoma is an optic neuropathy, characterized by cupping of the optic disc, progressive loss of retinal ganglion cells and slow degeneration of the optic nerve, ultimately resulting in blindness [1, 2]. The optic nerve head is the major pathological site in glaucoma. It is reported that extensive remodeling of the extracellular matrix (ECM) occurs in the optic nerve head in glaucoma patients and in animal models of glaucoma[3, 4].

Numerous proteolytic enzymes participate in ECM degradation and remodeling, however one class that appears to play a pivotal role is the matrix metalloproteinases (MMPs)[5]. MMPs are a large family of zinc-dependent enzymes that degrade the constituents of the extracellular matrix (ECM). The activity of MMPs is tightly controlled by their tissue inhibitors of matrix metalloproteinases (TIMPs) [6]. The balance of MMPs and TIMPs is necessary for normal physiological and pathological conditions including embryonic development and growth as well as tissue remodeling and repair [7].

It is reported that differential MMP and TIMPs expression profiles were found as part of remodeling of the optic nerve head in response to different damage/insults to the optic nerve. For example, in laser-induced glaucoma in primates, there was an significant increase in expression of MT1-MMP (membrane type) and MMP-1 in reactive astrocytes at the optic nerve head due to elevation of intra ocular pressure (IOP), whereas in a parallel experiment in primates with optic nerve transection, there was increased expression of MT1-MMP, MMP-1, MMP-2, TIMP-1 and TIMP-2 in reactive astrocytes at the transection site [8]. Other investigators showed that extensive ECM remodeling was correlated with RGC apoptosis and axon loss, and that the increased MMP activity might

enhance ECM degradation, including collagen degradation, to facilitate the migration of astrocytes into optic nerve bundles[9-11]. Therefore, key ECM molecules not only provide mechanical support for cells, but also are involved in cell apoptosis and axon loss at the optic nerve head (ONH). Reactive astrocytes involved in astrogliosis may be responsible for ECM remodeling in glaucoma, and recently, endothelin-1 (ET-1) has been implicated as a potential factor in reactivation of astrocytes, which leads to astrogliosis [12-14].

ET-1 is not only known as a potent vasoactive peptide, but also involved in ECM remodeling by shifting the balance of MMPs/TIMPs [15-17]. In addition, growing evidence from other tissues suggests that ET-1 induces the expression of many types of MMPs and TIMPs as well as ECM protein expression, including collagens, laminin and fibronectin in cell culture and animal models [18, 19]. It has been shown that ET-1 levels are elevated not only in the aqueous humor and plasma of glaucoma patients [20, 21] but also in glaucoma animal models, including dogs [22], rats [23], and rabbits [24]. Our lab has shown that the increased ET-1 levels in aqueous humor in rats with elevated IOP are correlated with the increased GFAP expression in astrocytes and increased ET_B receptor immunoreactivity [23]. Ahmed et al. also demonstrated that there was a significant increase in retinal mRNA levels of ET receptors, TIMP-1, MMP-3, ET-2, fibronectin and GFAP tested by RT-PCR in the elevated IOP in Brown Norway rats [25]. Furthermore, intravitreal injection or perfusion of ET-1 into eyes in many animal models such as primates, rabbits and rats, produced the optic nerve head damage similar to that seen in glaucoma, including optic disk cupping, axon loss, astrogliosis [26, 27]. Therefore, ET-1 may be involved in ECM remodeling of the optic nerve head in glaucoma as a result of the

astrogliosis and reactivation of astrocytes by ET-1, however, a detailed study of ET-1 effects on optic nerve ECM, activity of MMPs and TIMPs has not been delineated.

In the current study, we investigated ET-1-induced activity of MMPs and expression of TIMPs in primary human optic nerve astrocytes (hONAs). In addition, we also determined if ET-1-induced differential activation of MMPs/TIMPs occurred through mitogen-activated protein kinase (MAPK)- and protein kinase C (PKC)-dependent pathways. This imbalance of MMPs/TIMPs could contribute to the ECM remodeling and the pathological changes seen at the optic nerve head (ONH) in glaucoma.

Materials and Methods

Materials.

Dulbecco's modified Eagle's medium (DMEM, catalog no. 11995-040), and penicillin- streptomycin-glutamine were obtained from Gibco (Rockville, MD, USA). Fetal bovine serum (FBS) was obtained from Hyclone Labratoraries, Inc. (Logan, UT). PD98059, U0126, chelerythrine, and RO-31-8425 were purchased from Calbiochem (La Jolla, CA, USA). Rabbit anti-ERK1/2 polyclonal antibody, Rabbit anti-phospho-ERK1/2 (Thr202/Tyr 204) polyclonal antibody, rabbit anti-phospho-pan-PKC polyclonal antibody and rabbit anti-phospho-PKC zeta polyclonal antibody were purchased from Cell Signaling Technology (Beverly, MA); Antibody against TIMP-1 (monoclonal, from mouse) from Chemicon Inc.; Antibody against TIMP-2 (polyclonal, from rabbit) from Santa Cruz Bio Tech. Endothelin-1 was obtained from Peninsula Laboratories (Belmont, CA). All other chemicals were purchased from Sigma (St Louis, MO, USA).

Cell Cultures and cell transfection.

Primary human optic nerve head astrocytes from normal donors (hONA cells, kindly given by Dr. Abbot F. Clark (Alcon Labs, Fort Worth, TX)) were maintained in DMEM containing 10% fetal bovine serum supplemented with 10u/ml penicillin, 100μg/ml streptomycin and 0.3 μg/ml glutamine under a humidified 5% CO_2 at 37 °C.

Western Blot:

hONA cells were cultured in 100mm dishes to confluence; 24 hours later media was changed to serum-free DMEM and cells were pretreated with different inhibitors for 30 minutes. Cells were then stimulated with 100nM ET-1 for various times described herein. The reaction was stopped by adding ice-cold PBS. The cells were scraped and placed in lysis buffer. Total cell lysate or concentrated supernatant of cell culture was applied to 10% SDS-PAGE with equal amount of total proteins and transferred to nitrocellulose membranes (Protran Bioscience, Keene, NH). The transferred membranes were blocked with 5% non-fat milk in TBS/T (Tris-buffered saline) for 1 hour and incubated with primary antibody for 1 hour at room temperature or overnight at 4°C. A horseradish peroxidase conjugated anti-mouse or anti-rabbit IgG antibodies (Amersham Pharmacia Biotech, Piscataway, NJ) were used as secondary antibody and the enhanced chemiluminescence reagents (Amersham Pharmacia Biotech, Piscataway, NJ) was used for the blotting detection. X-ray films (Kodak, Rochester, NY) was exposed and scanned using a HP scanner.

Gelatin and Casein Zymography:

In general, MMP-2 and 9 are analyzed on gelatin (Sigma, MO, USA) containing gels (7.5% polyacrylamide gel containing 2 mg/ml gelatin), and MMP-3 on β-casein (Sigma, MO, USA) containing gels (7.5% polyacrylamide gel containing 2mg/ml β-casein). Incubation medium samples for analysis by zymography were concentrated using Microcon YM-10 membranes and adjusted to equal volume. Thirty-five microliters concentrated media was applied to 7.5% SDS-PAGE containing 2 mg/ml gelatin or

casein. After electrophoresis, SDS was removed from the gel by washing 3 hours in 2.5% Triton X-100 solution (50 mM Tris (pH 7.6), 1 μM $ZnCl_2$, 5 μM $CaCl_2$) followed by washing for 16 hour in 1% Triton X-100 solution at 37 °C. After incubation, the gel was stained with a solution of 0.25% Coomassie blue R250, 40% methanol and 10% acetic acid for 1 hour at room temperature and destained with 40% methanol, 10% acetic acid until the white bands became clear. Positive media (C1) containing MMP-2, 9, 3 and TIMP-1, 2 was purchased from Triplepoints Biotech (OR, USA) and used in zymography.

Immunocytofluorescent Staining:

Cells were fixed in 4% paraformaldehyde in PBS for 30 minutes at room temperature followed by permeabilization with 0.1% Triton X-100 for 15 minutes. Cells were rinsed in PBS and incubated twice in 200 mM glycine, 15 minutes per incubation. Each coverslip was carefully inverted (cell-side facing solution) onto 200 μL of blocking solution containing 5% BSA+5% normal goat serum in PBS for 30 minutes. The coverslips were then incubated with mouse anti-fibronectin at room temperature for 2 hours. Coverslips were rinsed and allowed to incubate with Alexa 488–conjugated donkey anti-rabbit (2 μg/mL) for 1 hour in the dark at room temperature. Nuclei were stained with DAPI (300 nM; Molecular Probes) for 10 minutes. Coverslips were mounted on glass slides in antifade medium (FluorSave; Calbiochem, La Jolla, CA) and allowed to dry for 20 minutes in the dark. Cells were then viewed and images taken with Zeiss LSM 410 confocal microscope.

siRNA and Transfection of siRNA

We used vector-based siRNA techniques to suppress MMP-2 and TIMP-2 expression. The vector was pGeneClip™ U1 Hairpin hMGFP Vector from Promega Inc.(Madison, USA) The design of siRNAs was based on the assistance provided by Promega Inc. The sequences are provided below.

MMP-2

5'-TCTCGAAGATGCAGAAGTTCTTTAAGTTCTCTAAAGAACTTCTGCATCTTCCT -3'

5'-CTGCAGGAAGATGCAGAAGTTCTTTAGAGAACTTAAAGAACTTCTGCATCTTC -3'

TIMP-2:

5'-TCTCGACTCTGGAAACGACATTTAAGTTCTCTAAATGTCGTTTCCAGAGTCCT -3'

5'-CTGCAGGACTCTGGAAACGACATTTAGAGAACTTAAATGTCGTTTCCAGAGTC -3'

The fragment was inserted into the vector and identified by enzyme digestion and sequencing. The scrambled siRNA was also constructed as a control for our experiments.

For plasmid cDNA transfection, cells were freshly seeded to 80% confluence one day before transfection and serum-free media was used without penicillin and streptomycin. For each well in a 6-well plate, 4 μg plasmid cDNA was used for transfection with 10 μl lipofectamine 2000™ reagents (Invitrogen Inc., CA, USA) according to the manufacturer's instructions. Eight hours after transfection, cells were washed with serum-free DMEM and were subjected to a second transfection. For the second transfection in hONA cells, 4 μg plasmid cDNA was used for transfection with 4

μl lipofectamine 2000 reagents. After 8 hours, cells were washed with serum-free DMEM and incubated for another 24 hours before treatment.

Statistical Analysis

The density of bands in western blot and zymography was analyzed by NIH Image J software. For immunocytostaining, five regions (top-left, top-right, center, bottom-left and bottom-right) in each image was quantitated using NIH ImageJ software. Data obtained by ImageJ were represented as Mean +/- SD (standard deviation of mean). Data were analyzed using one-way analysis of variance (ANOVA) for multiple comparisons. Statistical significance was accepted when $p<0.05$.

Results:

ET-1 increased the active form of MMP-2, and expression of TIMP-1 and TIMP-2

Since primary hONAs' growth is slow in cell culture based on our previous experience [13], we selected 24-96 hours of ET-1 treatment for time course experiments. The concentrated media were collected from the hONA cell culture and gelatin and casein zymography was performed. When hONAs were treated with ET-1, there was an increased level of total MMP-2 activity when hONA cells were treated by ET-1 during the longer treatment of 48-96 hours, however maximal levels of the active form of MMP-2 was increased to a greater extent than total MMP-2 (Fig 1A). Similarly an upregulation of TIMP-1 and 2 was found with ET-1 treatment from 72 to 96 hours. MMP-3 levels were very low in our experiments, but it was also upregulated with the longer treatment time (data not shown). The expression of TIMP-2 was not detectable at the first day of ET-1 treatment using western blot. Therefore for hONAs, a 4-day (96 hours) treatment was used for further experiments with ET-1, unless otherwise noted. The results suggested that ET-1 increased not only the total activity of MMP-2 but also the conversion of active MMP-2 from the latent form.

ET-1 effects on the expression of MMPs and TIMPs were tested at different concentrations from 1 nM to 1000nM (Fig 1B). The results showed that ET-1 concentration from 100 nM to 1000 nM induced the highest level of expression of MMP-2, TIMP-1/2, and the highest level of active MMP-2. It is consistent with our previous reports [13].

ET-1 induced the phosphorylation of ERK1/2 and PKC βI/βII and δ in hONAs, but not PKC α, ε and ζ

Since ET-1 was shown to increase activity of MMP-2 and expression of TIMP-1 and -2 in hONAs, the signaling pathways activated by ET-1 including phosphorylation of ERK1/2 and activation of PKC isoforms were identified. A significant increase in phosphorylated ERK1/2 was detected in hONAs treated with 100 nM ET-1 for 5 minutes (Fig 2A). ET-1-induced phosphorylation of ERK1/2 as well as basal phosphorylation level of ERK1/2, was completely abolished by the application of U0126 (an inhibitor of MEK1/2 which are the upstream kinases of ERK1/2), whereas it was not affected by application of chelerythrine (a general inhibitor of PKC isoforms) (Fig 2B). To further assess PKC activation by ET-1, isolated membrane fractions of hONA cells were probed with antibodies against several phosphorylated isoforms of PKCs. There was an increase in phosphorylation of PKC βI/βII and δ in hONAs treated with ET-1 for 5 and 30 minutes, whereas no such phosphorylation was seen in PKC α, ε and ζ (Fig 2B). Pretreatment with chelerythrine decreased the basal phosphorylated level of PKC isoforms in hONAs.

Blockade of MAPK-ERK or PKC increased the activity of MMP-2 and decreased the expression of TIMP-1 and 2

When hONAs were pretreated with U0126 (10 μM) and PD 98059 (25 μM) (inhibitors of MEK1/2), the activity of MMP-2, especially the active form of MMP-2, was even further enhanced than that seen with ET-1 alone (Fig 3A). However, the

expression of TIMP-1 and TIMP-2 was decreased when inhibitors were applied (Fig 3A). The application of U0126 in hONAs inhibited the basal expression of TIMP-1 and TIMP-2. The very low level of MMP-3 was seen in casein zymography, and there was also an increased activity of MMP-3 in inhibitor-treated groups (data not shown).

As we had seen above, there was also increased activity of total MMP-2 detected with blockade of PKC signaling by chelerythrine (2 μM) or RO-31-8425 (1 μM) (PKC inhibitors), whereas the active MMP-2 was increased much more than total MMP-2 (Fig 3B). In addition, chelerythrine decreased the expression of TIMP-1 and TIMP-2 (Fig 3B).

The increased activity of MMP-2 and MMP-3 may be caused by the decreased expression of TIMP-1 and TIMP-2 that are endogenous inhibitors of MMP-2 and MMP-3. Therefore, it is likely that the balance of MMPs and TIMPs had been altered.

Knock-down of MMP-2 decreased the expression of TIMP-1 and TIMP-2

To evaluate the regulation of expression of MMPs and TIMPs and the relationship of the sensitive balance in MMPs and TIMPs to substrate degradation, siRNA was used to knock down MMP-2 and TIMP-2. There was a decrease in MMP-2 activity found in treatments with either MMP-2 siRNA or TIMP-2 siRNA. The decreased expression of TIMP-1 and 2 was also observed in hONAs transfected with MMP-2 siRNA (Fig 4). These results were in agreement with the preliminary experiments in U373MG astrocytoma cells, which were transfected siRNA constructs and used to test siRNA design and knock-down efficiency. The higher knock-down level of MMP-2 and TIMP-2 that was observed in U373MG cells was likely due to the higher transfection efficiency in

this cell line. Similarly, the decreased TIMP-1 and 2 was found in treatment with MMP-2 siRNA in U373MG cells (data not shown). The introduction of TIMP-2 siRNA lowered the activity of MMP-2 in hONA cells. It is suggested that alteration in the expression of either MMPs or TIMPs appears to affect each other, leading to the balance of MMPs and TIMPs reaching a new ratio.

ET-1 increases the soluble fibronectin in cell culture of hONAs

Typically, two forms of fibronectin (FN) are present where the newly synthesized dimer of fibronectin is soluble, and the polymerized fibronectin forming an fibrillar matrix network is insoluble [28, 29]. In the current study, both forms of fibronectin were investigated following ET-1 treatment. The soluble fibronectin (sFN) was monitored by western blot in culture media of hONAs and insoluble network fibronectin by immunocytostaining. The culture incubation media were collected at day 1 to day 4 and concentrated by YM-10 filters following ET-1 treatment in hONAs with or without pretreatment of U0126 (10 μM) or chelerythrine (2 μM) for 30 minutes. In dose-dependent experiments, the highest expression of sFN was observed in treatments with 100 nM and 1000 nM of ET-1 after 4-day treatment of hONAs (Fig 5A). The result was consistent with ET-1's effects on MMP-2 and TIMP-1/2 expression, which reached the highest levels with 100 nM ET-1 treatment after 4-day treatment (Fig. 1). In a time course experiment, sFN accumulated with increasing time with ET-1 treatment and reached the highest level on day 4 (Fig. 5B).

In order to investigate the effects of MAPK-ERK and PKC on sFN expression, hONAs were pretreated with either U0126 (10 μM) or chelerythrine (2 μM). The

application of inhibitors did not attenuate ET-1-induced sFN expression and the basal level of sFN (Fig 5C), suggesting that the expression of FN was not under the control of MAPK-ERK and PKC pathways. Furthermore, in hONAs, the ET-1-induced sFN secretion was reduced following treatments with siRNA for MMP-2 but not with siRNA for TIMP-2 (Fig 5D).

ET-1 increased the insoluble fibronectin participated to form matrix network in hONA

The experiments above showed that there was a significant increase of soluble fibronectin in hONAs treated with ET-1, therefore we wanted to further investigate ET-1's effects on insoluble fibronectin that forms a matrix network with other matrix proteins. ET-1-treated hONAs with or without U0126 (10 μM) and chelerythrine (2 μM) were used to probe fibronectin by immunofluorescent staining. The immunoreactivity of fibronectin was assessed in hONAs treated with ET-1 for 1 and 4 days (Fig 6A). The immunoreactivity seen in the 4-day ET-1 treatment was similar to that of the 4-day ET-1 treatment. There was a significant increase in sFN in the 4-day ET-1 treatment, but it seemed that not all of the increased sFN seen after 4 days of ET-1 treatment participated in the formation of the insoluble FN network formation.

In order to investigate the regulatory effects of MAPK and PKC pathways on insoluble FN deposition, the same immunostaining of FN was performed in hONA cells in the presence of U0126 and chelerythrine (Fig 6B). The application of either U0126 or chelerythrine did not attenuate ET-1-induced FN deposition in matrix network and this

was in agreement with the results shown in Figure 6C, in that the application of both inhibitors did not attenuate ET-1-induced sFN expression.

Discussion:

In the regulation of ECM components in the brain and eyes, astrocytes are a major source of MMPs and provide extracellular matrix components [30]. Reactive astrocytes involved in astrogliosis may be responsible for ECM remodeling in glaucoma[3]. In the present study, we have shown that ET-1 not only up-regulated the activity of active MMP-2 and the expression of TIMP-1 and 2 in hONAs, but also increased the deposition of fibronectin (FN) and formation of an ECM network in a hONA cell culture model. ET-1-mediated regulation of ECM remodeling in hONA cells appears to be involved in two signaling pathways, ERK-1/2 and PKC, since the blockade of these pathways increased the activity of MMP-2 but inhibited the expression of TIMP-1 and 2. Therefore, the balance of MMP/TIMP was shifted towards increased MMP production and activity (Fig 7).

ET-1 has been considered an important factor that contributes to the formation and progression of glaucoma [31, 32]. However, the mechanism involved in ET-1 regulation of ECM remodeling in the optic nerve head as may occur through astrocytes is still not fully determined. Our results showed that ET-1 upregulated the activity of the active form of MMP-2 and 3 as well as the expression of TIMP-1 and 2 in either dose- or time-dependent manner, suggesting that these cells reached a new balance of MMPs/TIMPs in response to stimuli. In addition, the rapid increase of MMP-2 and 3 was observed as early as 24 hours after ET-1 treatment in hONAs whereas upregulated TIMP-1 and 2 was detected only between 72 to 96 hours, indicating that the upregulation of MMPs was the early and immediate response to ET-1 followed by the late increased TIMP-1 and 2 to

counteract MMPs and thereby reaching a new balance. Another target in this study was MMP-9, which was considered a regulatory enzyme as compared to MMP-2. Monitoring the changes in MMP-9 could give us more information of ET-1's effects in ECM remodeling, but the basal level of MMP-9 in hONAs was too low to be investigated in the current study. In an elevated IOP model of glaucoma in rats, there were increased levels of ET-1[23], ET_B receptor[25] and upregulation of MMP-9, TIMP-1 and collagen I [10] in retina and collagen IV, VI at ONH [11], whereas there was a downregulation of laminin at the RGC layer[10]. In addition, apoptosis of RGCs was significantly correlated with the upregulation of MMP-9 and reduced laminin staining in rats following the intravitreal injection of the cytotoxic agent, kainic acid. The death of RGCs was rescued by application of a MMP inhibitor, GM6001 [33]. Such observations suggest that ECM remodeling may contribute to the deleterious pathological changes in the retina and optic nerve head. It is important to distinguish that while MMP-9 may be relevant to RGC apoptosis, activation of astrocytes may be dependent on MMP-2 and TIMP 1/2 activation. It is presently unknown whether ET-1-induced RGC apoptosis also involves upregulation of MMP-9.

Moreover, one unexpected finding in this study was that the increased activity of MMP-2 and 3 and the attenuated expression of TIMP-1 and 2 were observed in media collected from hONAs, in which MAPK-ERK and PKC pathways were blocked by application of several different inhibitors. This is the first report stating that the blockade of MAPK or PKC pathways induced the increased activity of MMP-2 and 3 in hONAs. Several reports have shown that these two pathways control the expression and activity of

MMPs. Blocking one or both of them decreases the level of MMPs [34-36]. For instance, PMA-induced MMP-9 was inhibited by curcumin through MAPK and PKC pathways in human astroglioma cells [34], and the expression and activity of MMP-2 and 9 induced by IL-1 were regulated by differential PKC isoforms via JNK or ERK1/2 MAPK pathways in cardiac fibroblasts [37]. However, the significantly attenuated levels of TIMP-1 and 2 observed in hONAs pretreated with inhibitors of ERK and PKC pathways indicate that such decreased endogenous inhibitors of MMPs may cause an imbalance between MMPs and TIMPs since TIMPs bind tightly with MMPs to inhibit the enzymatic activity at 1:1 molar ratio. Consequently, the activity of MMPs was increased in hONAs as shown in our results.

In this study, ET-1 increased the soluble fibronectin (sFN) in the incubation media of cell cultures in a time-dependent pattern, whereas matrix-formed FN was maximally increased at day 1 and maintained or slightly decreased on day 4 in hONAs (Fig 5B and 6A). It suggests that cells may utilize certain amount of fibronectin network in order to maintain their physiological state and avoid forming the excess network that may prevent cells from migrating when necessary (i.e. development, injury or neurotrauma). There are two possible explanations: 1) Cells need to balance their extracellular matrix (ECM) in that they not only need ECM formation for mechanical support and signal transduction, but also they must control the amount FN matrix and limit the extent of the matrix for physiological functions including cell migration. Evidence exists for ET-1 induced cell migration in many types of cells including human ovarian carcinoma cell lines [38] and neural stem cells [39]. Therefore, matrix formation could

be regulated to a certain extent to facilitate cell migration. In the current study, hONA migration in response to ET-1 was not assessed but is the subject of ongoing studies. 2) Although excess sFN was secreted by hONAs, it was unable to form an insoluble matrix perhaps due to increased MMP-2 production. Therefore substrate synthesis and degradation is another balance in this system. Furthermore, FN is necessary to bind with its receptor, integrin, to induce or mediate signal transduction. Preventing FN binding with integrin by application of an antibody against FN inhibited outgrowth of neurites in dorsal root ganglion neurons[40]. The defective scaffold formation and a failure of normal vascular development in the retina were also observed in mice null for orphan nuclear receptor-tailless due to an impaired FN matrix formation[41]. It suggests that FN mediates a wide variety of cellular interactions with the ECM and plays important roles in cell adhesion, migration, growth and differentiation [42]. In addition to being an important constituent of ECM and structural support, FN exerts its diverse biological functions by binding and interacting with integrins, heparin, collagen/gelatin, elastin and fibrin. These interactions are also important for communication between cells [28]. Thus altering the balance of sFN to FN matrix could impact these cells significantly leading to communication dysregulation.

In summary, ET-1 increased the activity of MMP-2 and the expression of TIMP-1, 2 as well as the expression of soluble FN and FN matrix formation in hONA cells. In addition, the ERK-MAPK and PKC pathways appear to be involved in the regulation of MMP-2 activity and TIMP-1, 2 expression, but not in ET-1-mediated FN expression. A balance of MMPs/TIMPs may be important not only to regulate the expression of MMPs

and TIMPs but also to influence ECM remodeling. Our current data show that ET-1 shifted the balance of MMP activity and substrates in a temporal fashion, and that this may subsequently lead to ECM remodeling in activated hONA cells. Astrogliosis is seen following neurotrauma, hypoxia/ischemia, and other pathologies and is manifested by a dramatic change in the expression of extracellular matrix (ECM) profile, which in most cases results in a glial scar [30]. Migration of the activated astroglia into optic nerve bundles may induce axon loss [3, 43]. Since the axon loss is one of the characteristics of glaucoma, the optic nerve head is considered to be an important site for glaucomatous pathological changes. The putative effect of elevated IOP is thought to induce pathological changes at the optic nerve head that causes physical compression on optic nerve axons. Such actions would lead to ischemia to the optic nerve and also block axoplasmic flow, specifically anterograde and retrograde transport between axons and retinal ganglion cell bodies [3, 30]. ET-1 has been shown to affect axonal transport in the optic nerve[44]. Therefore, the current study provides additional insight into ECM remodeling, another critical component of the endothelin-glial-axon interactions that may be important for genesis of glaucoma as well as in other neuropathies.

Acknowledgments

This work was supported by a National Institute of Health Grant EY11979 (to T.Y.) and a Texas Higher Education Coordination Board Advanced Technology Grant (to T.Y.). We wish to thank Dr. Abbot F. Clark for kindly providing primary human optic nerve head astrocytes in this study.

References:

1. Quigley E, Quigley H, Pease M, Kerrigan L. Quantitative studies of elastin in the optic nerve heads of persons with primary open-angle glaucoma. *Ophthalmology* 1996;103:1680-1685.

2. Clark AF, Yorio T. Ophthalmic Drug Discovery. *Nat Rev Drug Discov* 2003;2:448 -459.

3. Hernandez M, Pena J. The optic nerve head in glaucomatous optic neuropathy. *Arch Ophthalmol* 1997;115:389-395.

4. Morrison J, Dorman-Pease M, Dunkelberger G, Quigley H. Optic nerve head extracellular matrix in primary optic atrophy and experimental glaucoma. *Arch Ophthalmol* 1990;108:1020-1024.

5. Stamenkovic I. Extracellular matrix remodelling: the role of matrix metalloproteinases. *J Pathol* 2003;200:448-464.

6. Gardner J, Ghorpade A. Tissue inhibitor of metalloproteinase (TIMP)-1: The TIMPed balance of matrix metalloproteinases in the central nervous system. *J Neurosci Res* 2003;74:801-806.

7. Shapiro SD. Matrix metalloproteinase degradation of extracellular matrix: biological consequences. *Curr Opin Cell Biol* 1998;10:602-608.

8. Agapova OA, Kaufman PL, Lucarelli MJ, Gabelt BAT, Hernandez MR. Differential expression of matrix metalloproteinases in monkey eyes with experimental glaucoma or optic nerve transection. *Brain Res* 2003;967:132-143.

9. Chintala SK, Zhang X, Austin JS, Fini ME. Deficiency in Matrix Metalloproteinase Gelatinase B (MMP-9) Protects against Retinal Ganglion Cell Death after Optic Nerve Ligation. *J Biol Chem* 2002;277:47461-47468.

10. Guo L, Moss SE, Alexander RA, Ali RR, Fitzke FW, Cordeiro MF. Retinal Ganglion Cell Apoptosis in Glaucoma Is Related to Intraocular Pressure and IOP-Induced Effects on Extracellular Matrix. *Invest Ophthalmol Vis Sci* 2005;46:175-182.

11. Johnson EC, Morrison JC, Farrell S, Deppmeier L, Moore C. G., McGinty M. R. The Effect of Chronically Elevated Intraocular Pressure on the Rat Optic Nerve Head Extracellular Matrix. *Exp Eye Res* 1996;62:663-674.

12. Schinelli S. The brain endothelin system as potential target for brain-related pathologies. *Curr Drug Target CNS Neurol Disord* 2002;1:543-553.

13. Prasanna G, Krishnamoorthy R, Clark AF, Wordinger RJ, Yorio T. Human Optic Nerve Head Astrocytes as a Target for Endothelin-1. *Invest Ophthalmol Vis Sci* 2002;43:2704-2713.

14. Rogers S, Peters C, Pomonis J, Hagiwara H, Ghilardi J, Mantyh P. Endothelin B receptors are expressed by astrocytes and regulate astrocyte hypertrophy in the normal and injured CNS. *Glia* 2003;41:180-190.

15. Nelson J, Bagnato A, Battistini B, Nisen P. The endothelin axis: emerging role in cancer. *Nat Rev: Cancer* 2003;3:110-116.

16. Grant K, Loizidou M, Taylor I. Endothelin-1: a multifunctional molecule in cancer. *Br J Cancer* 2003;88:163-166.

17. Bagnato A, Natali PG. Targeting endothelin axis in cancer. *Cancer Treat Res* 2004;119:293-314.

18. Fraccarollo D, Galuppo P, Bauersachs J, Ertl G. Collagen accumulation after myocardial infarction: effects of ETA receptor blockade and implications for early remodeling. *Cardiovascu Res* 2002;54:559-567.

19. Gomez-Garre D, Ruiz-Ortega M, Ortego M, et al. Effects and interactions of endothelin-1 and angiotensin II on matrix protein expression and synthesis and mesangial cell growth. *Hypertension* 1996;27:885-892.

20. Noske, WHensen J, Wiederholt M. Endothelin-like immunoreactivity in aqueous humor of patients with primary open-angle glaucoma and cataract. *Graefes Arch Clin Exp Ophthalmol* 1997;235:551-552.

21. Tezel G, Kass M, Kolker A, Becker B, Wax M. Plasma and aqueous humor endothelin levels in primary open-angle glaucoma. *J Glaucoma* 1997;6:83-89.

22. Kallberg ME, Brooks DE, Garcia-Sanchez GA, Komaromy AM, Szabo NJ, Tian L. Endothelin 1 Levels in the Aqueous Humor of Dogs With Glaucoma. *J Glaucoma* 2002;11:105-109.

23. Prasanna G, Hulet C, Desai D, et al. Effect of elevated intraocular pressure on endothelin-1 in a rat model of glaucoma. *Pharmacol Res* 2005;51:41-50.

24. Oku H, Sugiyama T, Kojima S, Watanabe T, Azuma I. Experimental Optic Cup Enlargement Caused by Endothelin-1-Induced Chronic Optic Nerve Head Ischemia. *Surv Ophthalmol* 1999;44:S74-S84.

25. Ahmed F, Brown KM, Stephan DA, Morrison JC, Johnson EC, Tomarev SI. Microarray Analysis of Changes in mRNA Levels in the Rat Retina after Experimental Elevation of Intraocular Pressure. *Invest Ophthalmol Vis Sci* 2004;45:1247-1258.

26. Chauhan BC, LeVatte TL, Jollimore CA, et al. Model of Endothelin-1-Induced Chronic Optic Neuropathy in Rat. *Invest Ophthalmol Vis Sci* 2004;45:144-152.

27. Cioffi G, Sullivan P. The effect of chronic ischemia on the primate optic nerve. *Eur J Ophthalmol* 1999;Suppl 1:S34-36.

28. Pankov R, Yamada KM. Fibronectin at a glance. *J Cell Sci* 2002;115:3861-3863.

29. Armstrong PB, Armstrong MT. Intercellular invasion and the organizational stability of tissues: a role for fibronectin. *Biochim Biophys Acta* 2000;1470:O9-O20.

30. Hernandez MR. The optic nerve head in glaucoma: role of astrocytes in tissue remodeling. *Prog Retin Eye Res* 2000;19:297-321.

31. Yorio T, Krishnamoorthy R, Prasanna G. Endothelin: is it a contributor to glaucoma pathophysiology? *J Glaucoma* 2002;11:259-270.

32. Prasanna G, Narayan S, Krishnamoorthy RR, Yorio T. Eyeing endothelins: A cellular perspective. *Mol Cell Biochem* 2003;253:71 - 88.

33. Zhang X, Cheng M, Chintala SK. Kainic Acid-Mediated Upregulation of Matrix Metalloproteinase-9 Promotes Retinal Degeneration. *Invest Ophthalmol Vis Sci* 2004;45:2374-2383.

34. Woo M-S, Jung S-H, Kim S-Y, et al. Curcumin suppresses phorbol ester-induced matrix metalloproteinase-9 expression by inhibiting the PKC to MAPK signaling

pathways in human astroglioma cells. *Biochem Biophys Res Commun* 2005;335:1017-1025.

35. Lee WJ, Shin CY, Yoo BK, et al. Induction of matrix metalloproteinase-9 (MMP-9) in lipopolysaccharide-stimulated primary astrocytes is mediated by extracellular signal-regulated protein kinase 1/2 (Erk1/2). *Glia* 2003;41:15-24.

36. Alexander JP, Acott TS. Involvement of the Erk-MAP Kinase Pathway in TNF{alpha} Regulation of Trabecular Matrix Metalloproteinases and TIMPs. *Invest Ophthalmol Vis Sci* 2003;44:164-169.

37. Xie Z, Singh M, Singh K. Differential Regulation of Matrix Metalloproteinase-2 and -9 Expression and Activity in Adult Rat Cardiac Fibroblasts in Response to Interleukin-1{beta}. *J Biol Chem* 2004;279:39513-39519.

38. Rosano L, Spinella F, Di Castro V, et al. Endothelin-1 Is Required During Epithelial to Mesenchymal Transition in Ovarian Cancer Progression. *Exp Biol Med* 2006;231:1128-1131.

39. Kruger GM, Mosher JT, Tsai Y-H, et al. Temporally Distinct Requirements for Endothelin Receptor B in the Generation and Migration of Gut Neural Crest Stem Cells. *Neuron* 2003;40:917-929.

40. Tom VJ, Doller CM, Malouf AT, Silver J. Astrocyte-Associated Fibronectin Is Critical for Axonal Regeneration in Adult White Matter. *J Neurosci* 2004;24:9282-9290.

41. Uemura A, Kusuhara S, Wiegand SJ, Yu RT, Nishikawa S-I. Tlx acts as a proangiogenic switch by regulating extracellular assembly of fibronectin matrices in retinal astrocytes. *J Clin Invest* 2006;116:369-377.

42. Wierzbicka-Patynowski I, Schwarzbauer JE. The ins and outs of fibronectin matrix assembly. *J Cell Sci* 2003;116:3269-3276.

43. Quigley H, Hohman R, Addicks E, Massof R, Green W. Morphologic changes in the lamina cribrosa correlated with neural loss in open-angle glaucoma. *Am J Ophthalmol* 1983;95:673-691.

44. Martha E. Stokely TY, Michael A. King,. Endothelin-1 modulates anterograde fast axonal transport in the central nervous system. *J Neurosci Res* 2005;79:598-607.

Figure legends

Figure 1. ET-1 increased the active form of MMP-2, TIMP-1 and TIMP-2

A. Time course studies: Gelatin zymography was used to detect the activity and expression of MMP-2 in incubation media collected from different time points after 100nM ET-1 treatment; western blot was use to detect the expression of TIMP-1 and 2 in incubation media collected from different time points after 100nM ET-1 treatment. 1μM PMA treatment was used as positive control. There was greater activity of MMP-2 and expression of TIMP-1 and 2 with a longer treatment with ET-1. **B.** Dose-response studies: Gelatin zymography was used to detect the activity of MMP-2 in incubation media collected from hONA cells treated with different concentration of ET-1 for 4 days; western blot was used to detect the activity of TIMP-1 and -2 in incubation media collected from hONA cells treated with different concentration of ET-1 for 4 days. The highest activity of MMP-2 and expression of TIMP-1 and 2 were observed in the treatment with 100nM ET-1. MMP-3 was not detectable in western blot. * $p<0.05$, ET-1 treatment vs. corresponding control, one-way ANOVA. The data are from a representative of 3 individual experiments with consistent results.

Figure 2. ET-1 induced the phosphorylation of ERK1/2, PKCβI/βII/δ, but not PKCε/α/ζ in hONAs.

A. Western Blot (WB) showed phosphorylation of ERK1/2 induced by 5-min ET-1(100nM) treatment in hONA cells after cells were pretreated with U0126 (10 μM), chelerythrine (2 μM, chele) or DMSO (vehicle) for 30 mins. ET-1 induced the rapid

phosphorylation of ERK1/2, which was abolished by U0126 but not chelerythrine. **B.** The phosphorylated isoforms of PKC were detected by western blot in hONA cells, which were treated with ET-1 (100 nM) for 5 and 30 min. One set was pretreated with chelerythrine (2 μM) for 30 mins before ET-1 treatment. Phosphorylation of PKCβI/βII/δ was induced by ET-1 in hONAs. * $p<0.05$, ET-1 treatment vs. corresponding control, one-way ANOVA. # $p<0.05$, inhibitor treatments vs. vehicle control, one-way ANOVA. The data are from a representative of 2 individual experiments with consistent results.

Figure 3. Blockade of MAPK-ERK and PKC increased the activity of MMP-2, 3 and decreased the expression of TIMP-1 and 2.

A. Gelatin zymography was used to detect the activity of MMP2, 9 in incubation media collected from hONA cells, which were pretreated with 25 μM PD98059 and 10 μM U0126 (both are MAPK-ERK inhibitors) for 30 min followed with or without a 100nM ET-1 treatment for 4 days. Western blot was used to detect the expression of TIMP-1 and 2 in incubation media collected from hONA cells. Application of inhibitors of MAPK reduced the expression of TIMP-1 and 2, but increased the activity of MMP-2. **B.** Gelatin zymography was used to detect the activity of MMP2, 9 in incubation media collected from hONA cells, which were pretreated with 2 μM chelerythrine (CHE) and 1 μM RO-31-8425 (RO) for 30 min followed with or without a 100nM ET-1 treatment for 4 days. Western blot was used to detect the expression of TIMP-1 and 2 in incubation media collected from hONA cells. Application of inhibitors of PKC reduced the expression of

TIMP-1 and 2, but increased the activity of MMP-2. * $p<0.05$, ET-1 treatment vs. corresponding control, one-way ANOVA. # $p<0.05$, inhibitor treatments vs. vehicle control, one-way ANOVA. The data are from a representative of 3-4 individual experiments with consistent results.

Figure 4. The activity MMPs and the expression TIMPs were decreased in hONAs transfected with siRNA of MMP-2.

Gelatin zymography was used to detect the activity of MMP-2 and western blot to detect expression of TIMPs in incubation media collected from hONA cells, which were transfected with siRNA of MMP-2 48 hours before treatment with 100nM ET-1. The incubation media were collected 24 hours after cells were treated with ET-1. Knock-down of MMP-2 using siRNA not only decreased the activity of MMP-2 but also decreased the expression of TIMP-1 and 2 (SCR: scramble siRNA). * $p<0.05$, ET-1 treatment vs. corresponding control, one-way ANOVA. The data are from a representative of 2 individual experiments with consistent results.

Figure 5. ET-1 increases the soluble fibronectin in cell culture of hONAs

Western blot was used to detect the soluble FN (sFN) in concentrated media collected from hONA cell culture. **A.** hONAs were treated with ET-1 from 1 nM to 1000 nM for 4 days. Expression of sFN was increased in treatment of ET-1 from 10nM to 1000 nM. **B.** hONAs were treated with 100 nM ET-1 for different time points from 1 day to 4 days. Expression of sFN was accumulated with the longer treatment time of ET-1. **C.** hONA

cells were pretreated with 10 μM U0126 or 2 μM chelerythrine (CHE) for 30min followed ET-1 treatment for 24 hours. Inhibition of MAPK or PKC pathways didn't reduce the expression of sFN. **D.** hONAs were transected with siRNA two times for 48 hours followed ET-1 treatment for 24 hours. Knock-down of MMP-2 decreased the expression of sFN (SCR: scramble siRNA). * $p<0.05$, ET-1 treatment vs. corresponding control, one-way ANOVA. The data are from a representative of 2-3 individual experiments with consistent results.

Figure 6. ET-1 increased the deposition of fibronectin in hONA cells.

A. Immunofluorescent (IF) staining was used to detect the deposition of fibronectin in hONA cells, which were treated with 100 nM ET-1 treatment for 1 to 4 days (Green: fibronectin; Blue: DAPI). Treatment of ET-1 increased the FN matrix, which did not accumulate like sFN. **B.** IF showed the deposition of fibronectin in hONA cells, which were pretreated with 10 μM U0126 or 2 μM chelerythrine (CHELE) for 30 min followed 100nM ET-1 treatment for 24 hrs (Green: fibronectin; Blue: DAPI). Application of inhibitors of MAPK or PKC did not affect the deposition of FN matrix. * $p<0.05$, ET-1 treatment vs. corresponding control, one-way ANOVA. The data are from a representative of 3 individual experiments with consistent results.

Figure 7. ET-1 increased the deposition of fibronectin in hONA cells.

ET-1 activated the rapid phosphorylation of ERK1/2 and PKC βI/βII/δ, which play important roles in cell proliferation and reactivation of hONAs. ET-1 not only up-

regulated the activity of MMP-2 and the expression of TIMP-1 and 2 in hONAs, but also increased the deposition of fibronectin (FN) and formation of an ECM network in a hONA cell culture model with a time-dependent manner. PKC and MAPK pathways are not involved in the expression and deposition of FN. However, they are involved in ET-1-mediated regulation of ECM remodeling in hONA cells, since the blockade of ERK-1/2 or PKC inhibited the expression of TIMP-1 and 2, resulting in an increase level of the activity of MMP-2. Therefore, the balance of MMP/TIMP was shifted towards increased MMP activity.

Figure 1

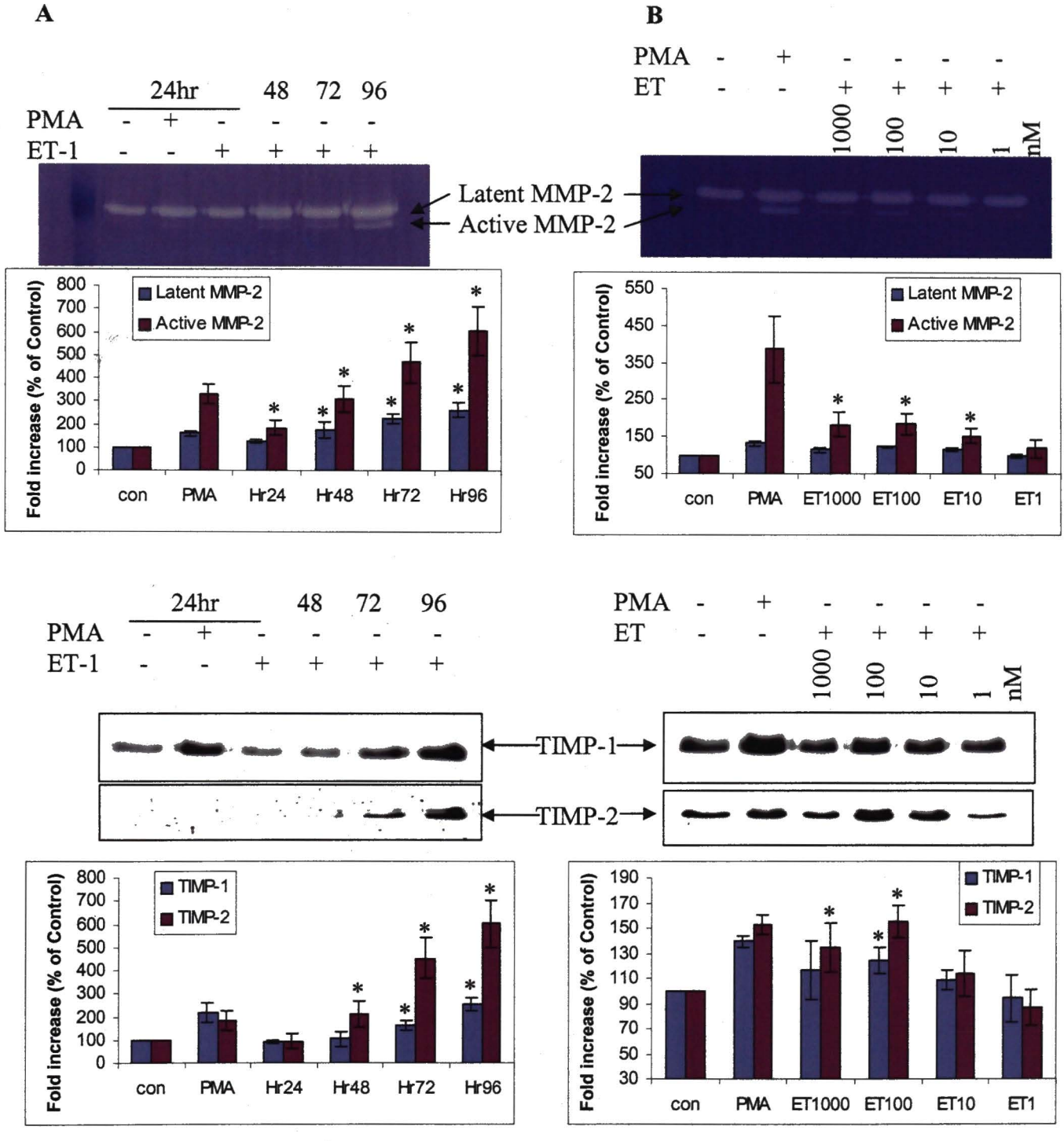
A
24hr
48
72
96
PMA - + - - - -
ET-1 - - + + + +
Latent MMP-2
Active MMP-2
Fold increase (% of Control)
Latent MMP-2
Active MMP-2
con
PMA
Hr24
Hr48
Hr72
Hr96
B
PMA - + - - - -
ET - - + + + +
1000
100
10
1
nM
Fold increase (% of Control)
Latent MMP-2
Active MMP-2
con
PMA
ET1000
ET100
ET10
ET1
24hr
48
72
96
PMA - + - - - -
ET-1 - - + + + +
TIMP-1
TIMP-2
Fold increase (% of Control)
TIMP-1
TIMP-2
con
PMA
Hr24
Hr48
Hr72
Hr96
PMA - + - - - -
ET - - + + + +
1000
100
10
1
nM
Fold increase (% of Control)
TIMP-1
TIMP-2
con
PMA
ET1000
ET100
ET10
ET1

Figure 2

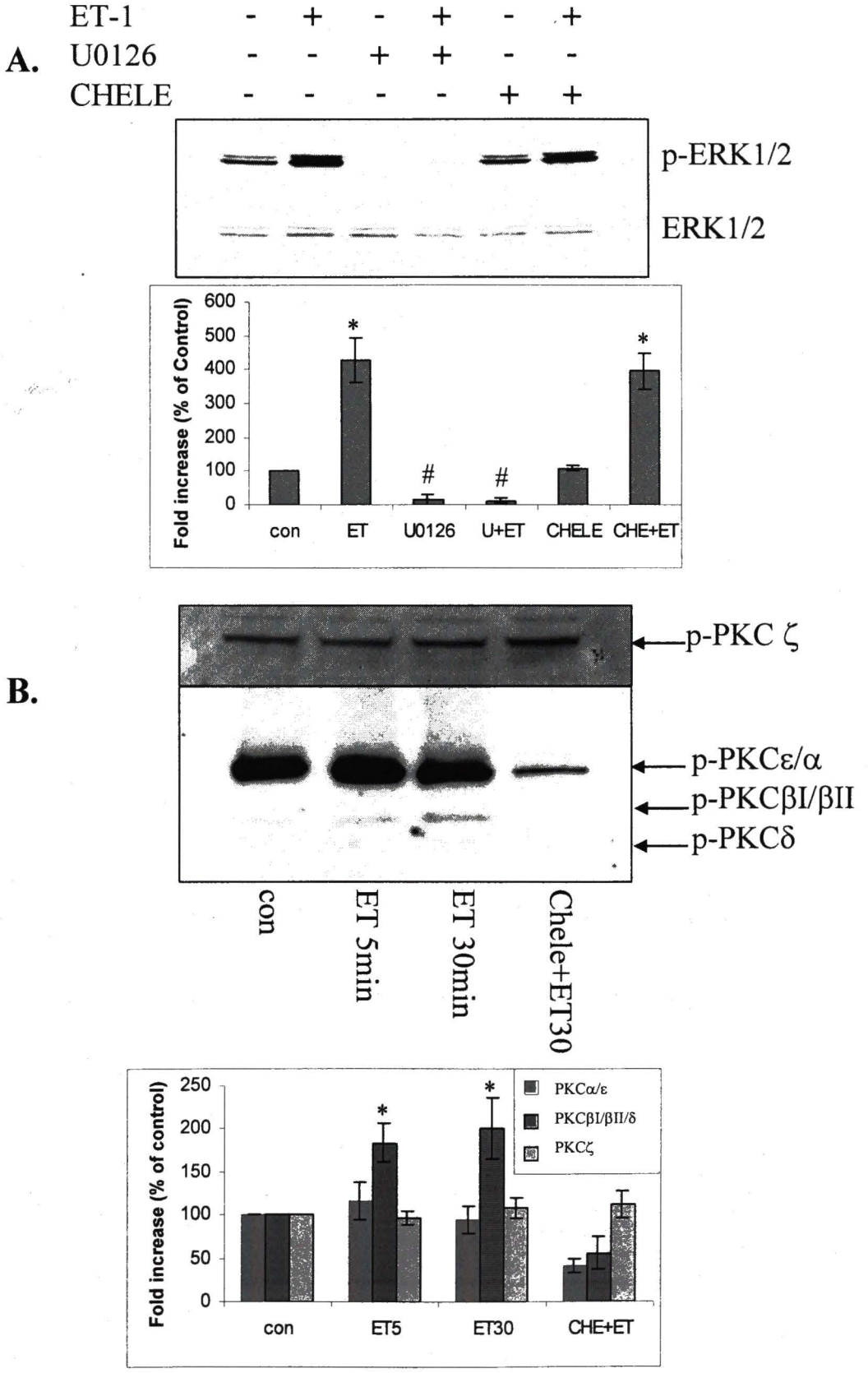
A.
ET-1 - + - + - +
U0126 - - + + - -
CHELE - - - - + +
p-ERK1/2
ERK1/2
Fold increase (% of Control)
600
500
400
300
200
100
0
*
#
con
ET
U0126
U+ET
CHELE
CHE+ET
B.
p-PKC ζ
p-PKCε/α
p-PKCβI/βII
p-PKCδ
con
ET 5min
ET 30min
Chele+ET30
Fold increase (% of control)
250
200
150
100
50
0
PKCα/ε
PKCβI/βII/δ
PKCζ
con
ET5
ET30
CHE+ET

Figure 3

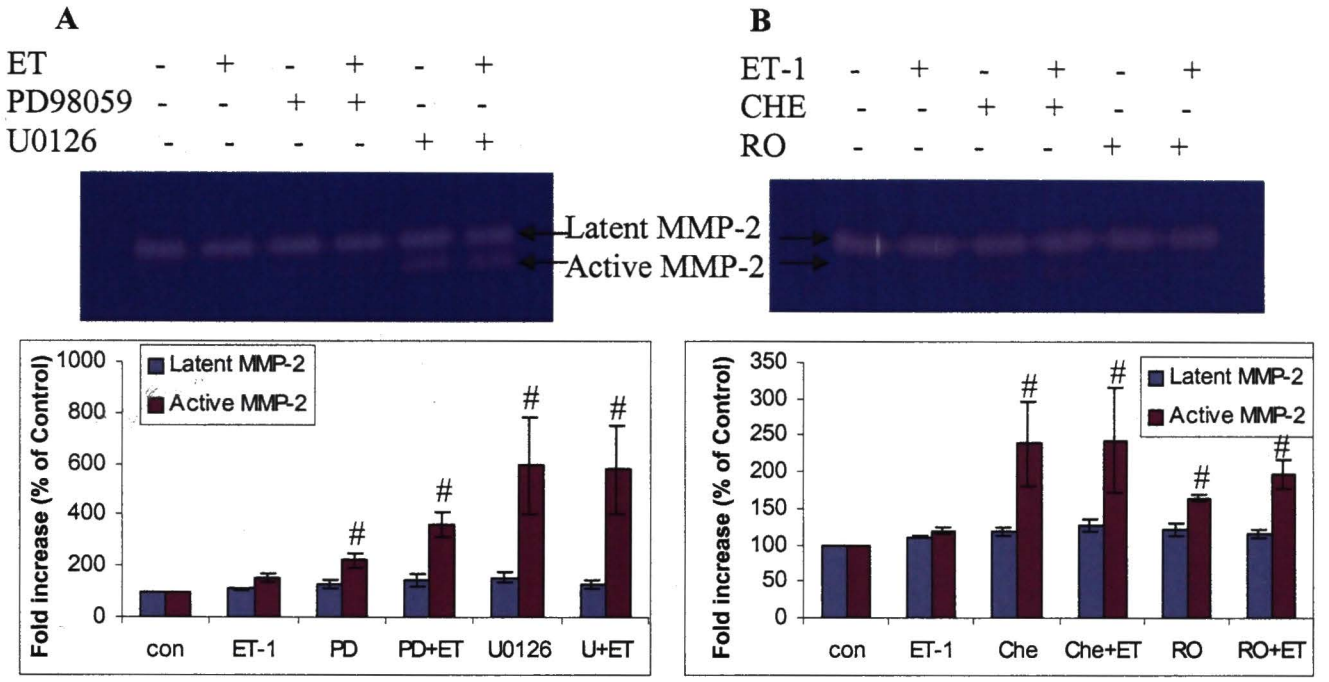
A
ET - + - + - +
PD98059 - - + + - -
U0126 - - - - + +
Latent MMP-2
Active MMP-2
Fold increase (% of Control)
Latent MMP-2
Active MMP-2
con
ET-1
PD
PD+ET
U0126
U+ET
B
ET-1 - + - + - +
CHE - - + + - -
RO - - - - + +
Fold increase (% of Control)
Latent MMP-2
Active MMP-2
con
ET-1
Che
Che+ET
RO
RO+ET

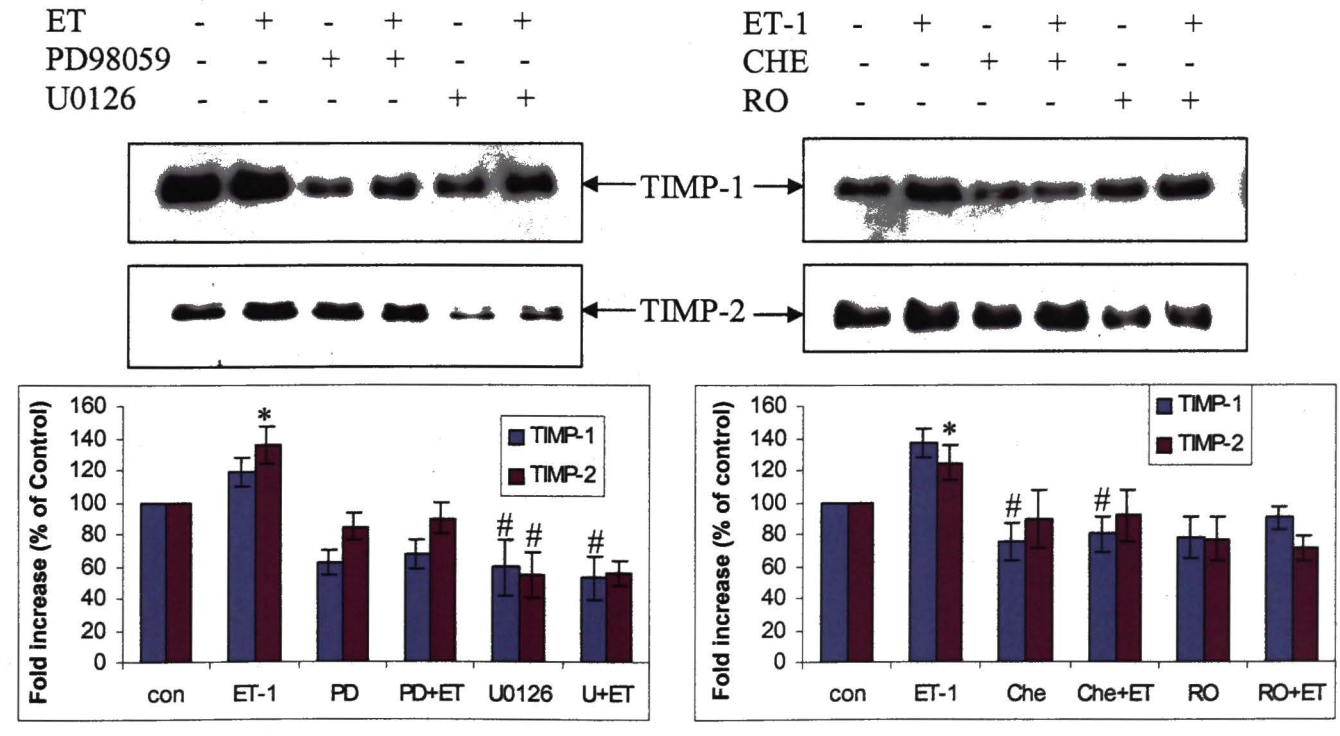
ET - + - + - +
PD98059 - - + + - -
U0126 - - - - + +
TIMP-1
TIMP-2
Fold increase (% of Control)
TIMP-1
TIMP-2
con
ET-1
PD
PD+ET
U0126
U+ET
ET-1 - + - + - +
CHE - - + + - -
RO - - - - + +
Fold increase (% of control)
TIMP-1
TIMP-2
con
ET-1
Che
Che+ET
RO
RO+ET

Figure 4

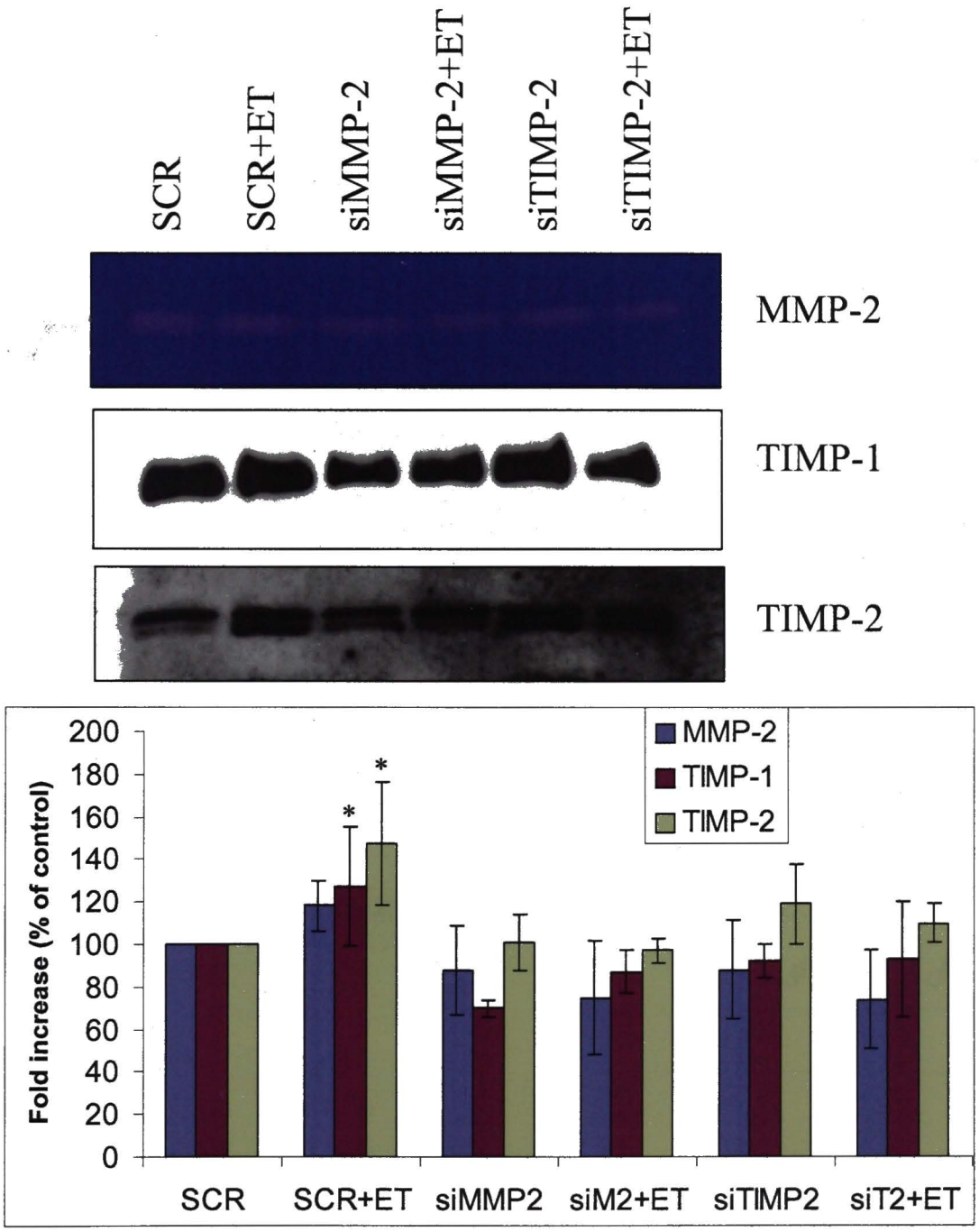
SCR
SCR+ET
siMMP-2
siMMP-2+ET
siTIMP-2
siTIMP-2+ET
MMP-2
TIMP-1
TIMP-2
Fold increase (% of control)
200
180
160
140
120
100
80
60
40
20
0
MMP-2
TIMP-1
TIMP-2
*
*
SCR
SCR+ET
siMMP2
siM2+ET
siTIMP2
siT2+ET

Figure 5

A.

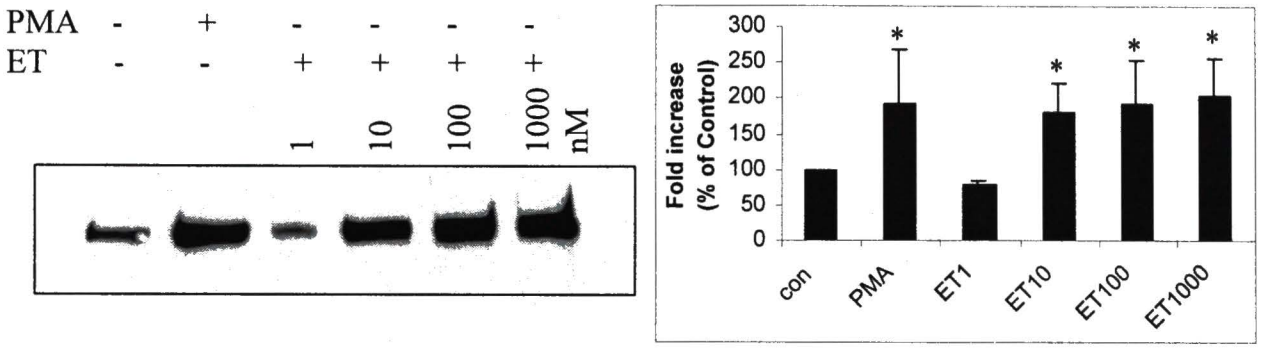

B.

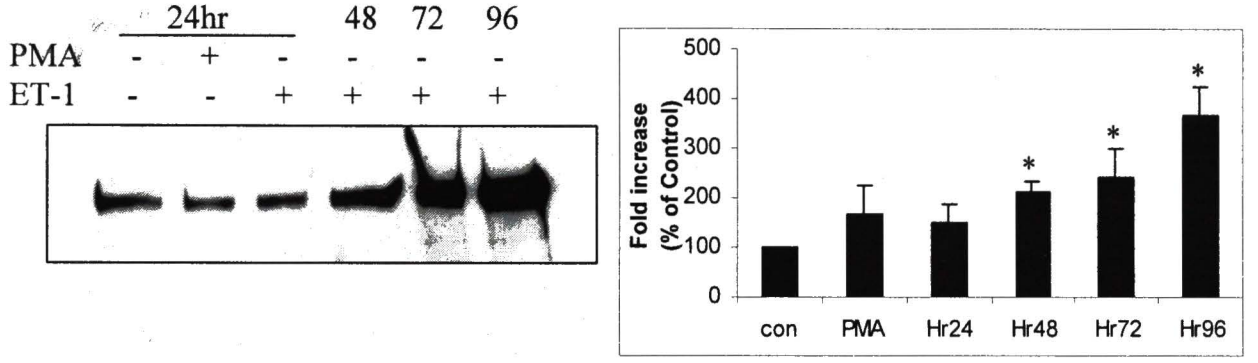

C.

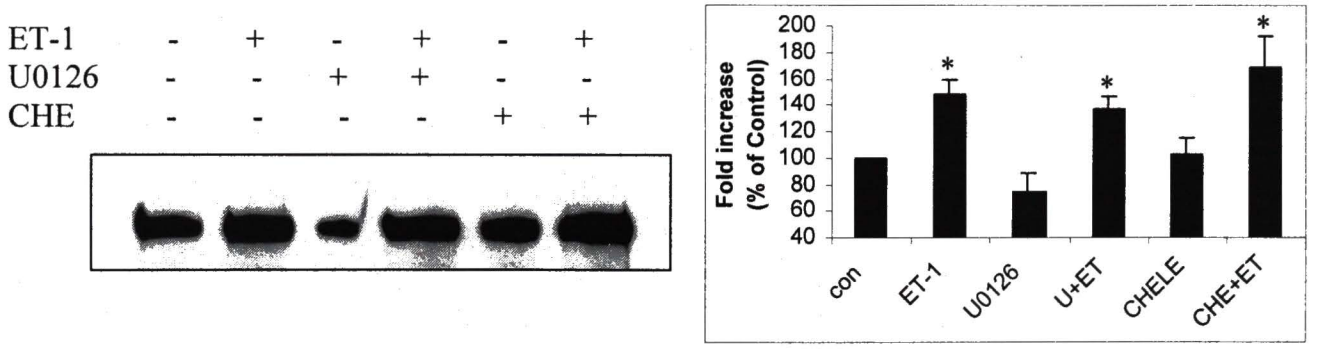

D.

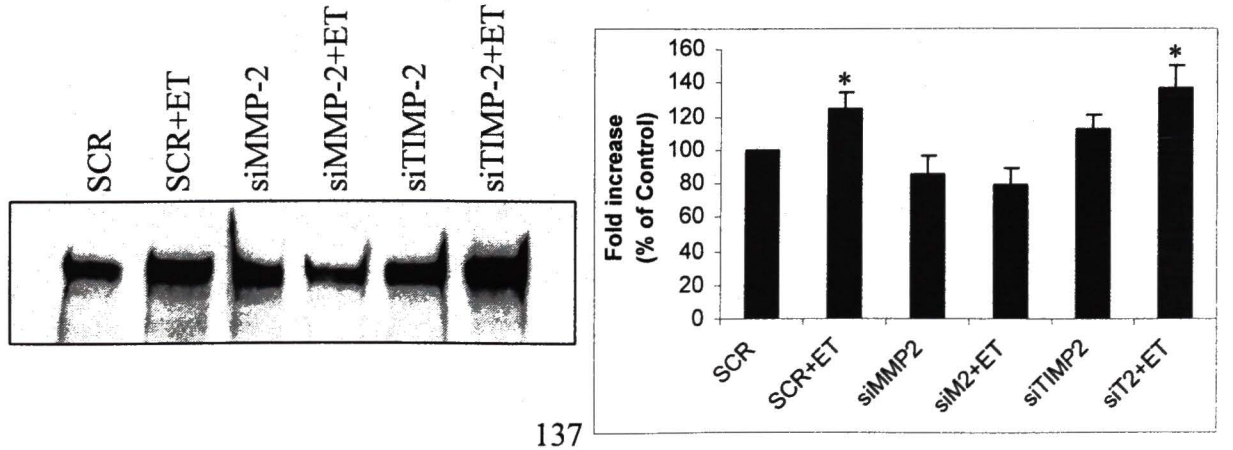

Figure 6

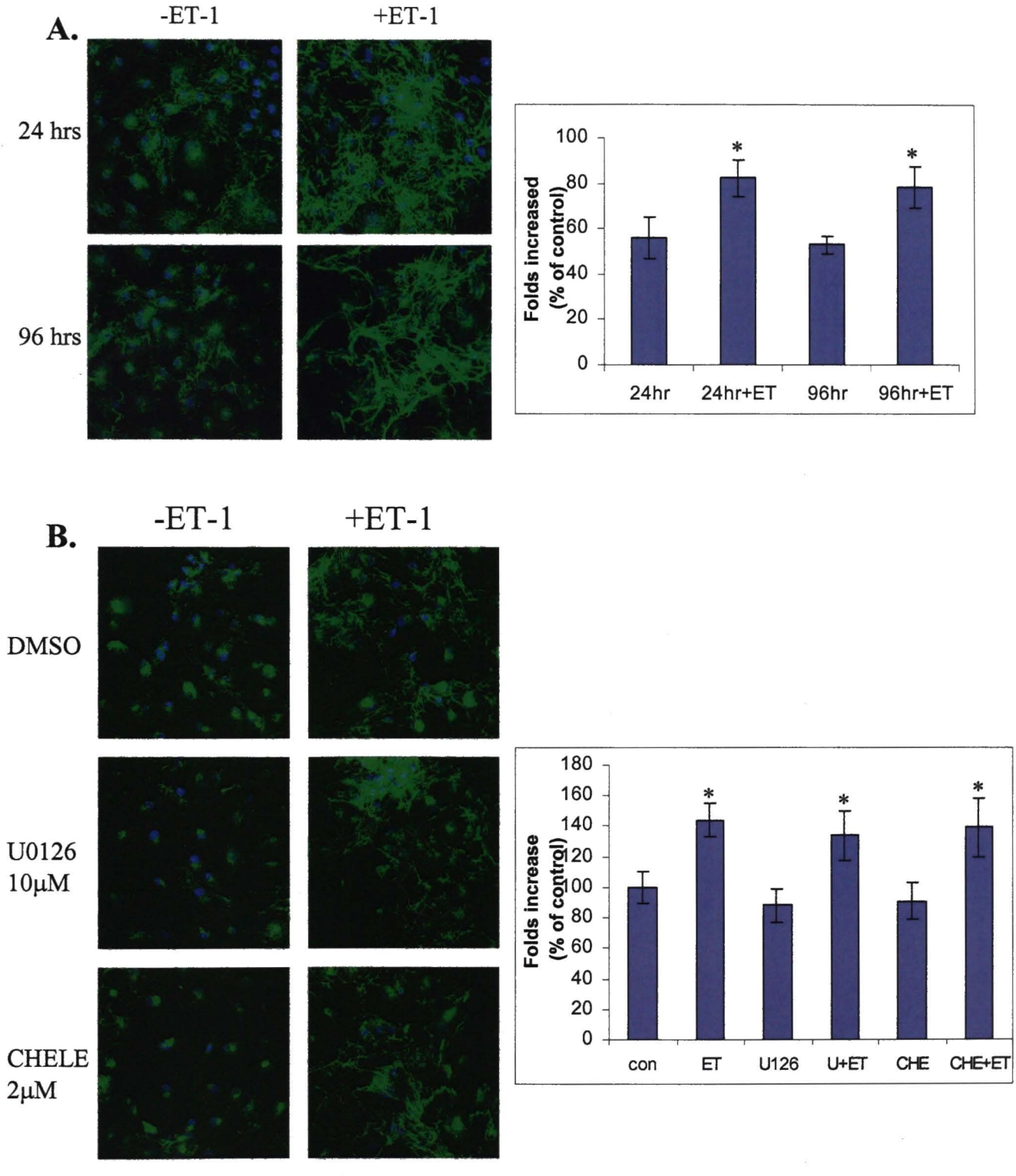
A.
-ET-1
+ET-1
24 hrs
96 hrs
Folds increased (% of control)
100
80
60
40
20
0
*
*
24hr
24hr+ET
96hr
96hr+ET
B.
-ET-1
+ET-1
DMSO
U0126 10μM
CHELE 2μM
Folds increase (% of control)
180
160
140
120
100
80
60
40
20
0
*
*
*
con
ET
U126
U+ET
CHE
CHE+ET

Figure 7

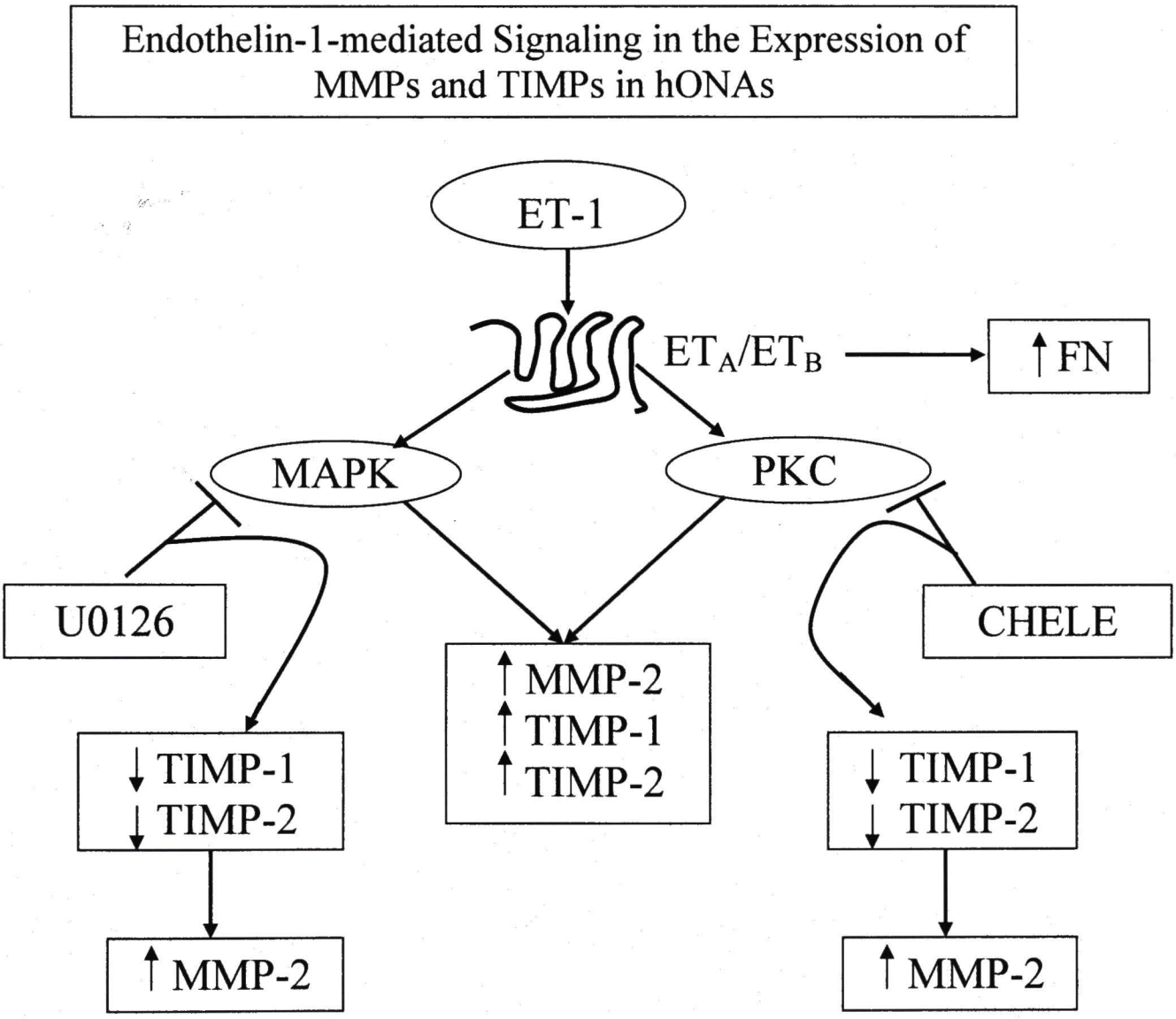
Endothelin-1-mediated Signaling in the Expression of MMPs and TIMPs in hONAs
ET-1
ET_A/ET_B
↑FN
MAPK
PKC
U0126
CHELE
↑MMP-2
↑TIMP-1
↑TIMP-2
↓TIMP-1
↓TIMP-2
↓TIMP-1
↓TIMP-2
↑MMP-2
↑MMP-2

CHAPTER 4

Intravitreal Injection of ET-1 Induces Extracellular Matrix Remodeling (ECM) at the Optic Nerve Head in Rats

Shaoqing He, Raghu Krishnamoorthy, Vidhya Rao, Adnan Dibas, Christina Johnson, Thomas Yorio*

Department of Pharmacology and Neuroscience, University of North Texas Health Science Center at Fort Worth, Fort Worth, TX 76107

***Corresponding author:**

Dr. Thomas Yorio, Department of Pharmacology and Neuroscience, University of North Texas Health Science Center at Fort Worth, 3500 Camp Bowie BLVD, Fort Worth, TX 76107

Tel: +1-817-735-0258; Fax: +1-817-735-0243; Email: yoriot@hsc.unt.edu

Grants: **This work is supported by National Institute of Health Grants EY11979 and a Texas Higher Education Coordination Board Advanced Technology Grant (to T.Y.)**

Abstract

Purpose: To determine ECM remodeling at the optic nerve head in a model of endothelin (ET-1)-mediated optic neuropathy in rats.

Method: 2 nmol ET-1 was injected into the vitreous of wildtype wistar and ET_B deficient rats. The expression of matrix metalloproteinases (MMPs), tissue inhibitors of metalloproteinase-2 (TIMP-2) and glial fibrillar acidic protein (GFAP) and the accumulation of ECM molecules, including collagen IV, collagenVI, fibronectin (FN), were determined by immunofluorescent staining at the optic nerve head.

Results: An increase in expression of MMP-9 and collagen VI was detected in both ET_B deficient rats and wildtype wistar rats 2 and 14 days post intravitreal ET-1 injection, whereas the deposition of FN was not changed. There was no significant difference MMP-9 and collagen VI immunoreactivity between ET_B deficient rats and wildtype wistar rats.

Conclusions: Changes in ECM expression was demonstrated following intravitreal ET-1 injection. Such ECM remodeling could contribute to the optic nerve changes seen following ET-1 administration and provides additional insight into potentially cellular mechanisms that may contribute to ET-1 induced optic neuropathy.

Introduction

Glaucoma is an optic neuropathy, characterized by cupping of the optic disc, progressive loss of retinal ganglion cells and slow degeneration of optic nerve, resulting in blindness [1, 2]. It is estimated that there are over 70 million people suffering from this disease [3]. The optic nerve head is one of the major sites showing pathological changes in glaucoma. It is reported that the extensive remodeling of the extracellular matrix (ECM) occurs in the optic nerve head in glaucoma patients and animal models [4-8].

It is reported that different MMP and TIMPs expression profiles could contribute to remodeling of the optic nerve head in response to different damages/insults to the optic nerve. For example, in laser-induced glaucoma in primates, there was the increased expression of membrane-type-1 MMP (MT1-MMP) and MMP-1 in reactive astrocytes at the optic nerve head due to elevation of intra ocular pressure (IOP), whereas in a parallel experiment in primates with optic nerve transection, there was increased expression of MT1-MMP, MMP-1, MMP-2, TIMP-1 and TIMP-2 in reactive astrocytes at the transection site [9]. Other investigators have shown that extensive ECM remodeling was correlated with RGC apoptosis and axon loss, and that the increased MMP activity might enhance ECM degradation, including collagen degradation, as a mechanism to facilitate the migration of astrocytes into optic nerve bundles[7, 10, 11]. Astrocytes are the major glial cells in the central nervous system, and they also play an important role in the regulation of extracellular matrix (ECM) components in the brain and eyes as they are a major source of matrix metalloproteinases (MMPs). Recently, endothelin-1 (ET-1) has been

implicated as a potential factor in reactivation of astrocytes, which leads to the induction of astrogliosis [12-14].

ET-1 is not only known as a potent vasoactive peptide, but it is also involved in ECM remodeling by shifting the balance of MMPs/TIMPs [15-17]. In addition, growing evidence from other tissues has shown that ET-1 induces the expression of many types of MMPs and TIMPs as well as ECM protein expression, including collagens, laminin and fibronectin in cell culture and animal models [18-22]. It has been shown that ET-1 levels were elevated not only in the aqueous humor and plasma of glaucoma patients [23, 24] but also in glaucoma animal models, including dogs [25] and rats [26]. Our lab has shown that the increased ET-1 levels in aqueous humor in rats with elevated IOP are correlated with increased GFAP expression in astrocytes and increased ET_B receptor immunoreactivity [26]. Ahmed et al. also demonstrated that there was a significant increase in retinal mRNA levels of ET receptors, TIMP-1, MMP-3, ET-2, fibronectin and GFAP tested by gene microarray analysis and RT-PCR in the elevated IOP in Brown Norway rats [27]. Furthermore, intravitreal injection or perfusion of ET-1 into eyes in many animal models such as primates, rabbits and rats, caused optic nerve head damage similar to that seen in glaucoma, including optic disk cupping, axon loss and astrogliosis [28-33]. Based upon these observations, it's possible that ET-1 is involved in ECM remodeling of the optic nerve head in glaucoma as a result of the astrogliosis and reactivation of astrocytes by ET-1, however, a detailed study of the activity of MMPs and TIMPs by ET-1 has not been delineated.

In the current study, we investigated ET-1-induced ECM remodeling at the optic nerve head of rats, which were intravitreally injected ET-1 into eyes. ECM remodeling was determined by immunoreactivity of collagen IV, collagen VI, fibronectin, MMP-2, MMP-9, TIMP-2 and GFAP.

Materials and Methods:

Animals:

The wildtype Wistar Kyoto rats (*Rattus sp.*) (aged from 5 months-12 months, 200–300 g; Charles River, Wilmington, MA, USA) and ET_B transgenic ET_B sl/sl rats Wistar Kyoto rats (kindly provided by Dr. Yanagisawa) were used in experiments. All procedures complied with the ARVO statement on the Use of Animals in Research and with the guidelines of the UNTHSC Committee on Animal Welfare.

Intravitreal injection procedure:

The rats were anesthetized for surgery by intraperitoneal injection using a standard rat cocktail (1 mg/ml) consisting of a solution of 5 ml ketamine (100 mg/ml), 2.5 ml xylazine (20 mg/ml), 1.0 ml of acepromazine (10 mg/kg), and 0.5 ml sterile water. Topical proparacaine (0.1%) were also administered.

Nine ET_B deficient rats and twelve wildtype rats were used in experiments (Table 1 and 2.). The animals were anesthetized with an *ip* injection of a standard rat cocktail (1 ml kg^{-1}). 4 µl of 500 µM ET-1 (H-6995, Peninsula Laboratories, San Carlos, CA, USA) in HEPES or 4 µl of HEPES (sham control) were injected into vitreous of left eyes of rats. The right eyes without any treatment were served as contralateral controls.

Rats were killed by an overdose of pentobarbital into the heart and their eyes enucleated immediately at 2 and 14 days post-endothelin-1 injection. Four incisions were made on the cornea to facilitate influx of fixation solution. The eyes were fixed in 4%

paraformaldehyde in phosphate buffered saline (PBS) for 6 hours and later embedded in paraffin wax. Five-micron saggital sections of optic nerve head were used in this study.

Immunoflourescent staining:

Slides were de-paraffinized in xylene, re-hydrated using ethanol washes and washed in PBS. After permeabilization using sodium citrate (0.1%) and 0.1% Triton-X, the sections were washed with PBS and non-specific binding was blocked by 5% BSA in PBS for 1 hour. The sections were incubated with combinations of primary antibodies (monoclonal anti-mouse and polyclonal anti-rabbit) for 2 hours at room temperature. The primary antibodies were rabbit anti-MMP-2 (2 μg/ml; Santa Cruz, CA), rabbit anti-MMP-9 (2 μg/ml; Santa Cruz, CA), rabbit anti-collagen IV (2 μg/ml; Santa Cruz, CA), rabbit anti-collagen VI (2 μg/ml; Chemicon) and mouse mono-anti-GFAP (3 mg/ml; Neomarkers, Fremont, CA), mouse anti-TIMP-2 (2 μg/ml; Santa Cruz, CA), mouse anti-fibronectin (2 μg/ml; Sigma, Saint Louis). Control sections were incubated with only secondary antibodies. Slides were rinsed and allowed to incubate with Alexa 488–conjugated donkey anti-mouse antibody (2 μg/ml) and Alexa 633–conjugated donkey anti-rabbit antibody (2 μg/ml) for 1 hour in the dark at room temperature. Coverslips were mounted on slides in antifade medium (FluorSave; Calbiochem, La Jolla, CA) and allowed to dry for 20 minutes in the dark.

Images and Data Analysis:

Slides were viewed and images taken on a Zeiss LSM 410 confocal microscope. Five regions at relative same sites of the optic nerve head in each image was quantitated using NIH ImageJ software. Data obtained by ImageJ were represented as Mean +/- SD (standard deviation of mean). Data were analyzed using one-way analysis of variance (ANOVA) for multiple comparisons. Paired analysis between two groups was performed using Student's *t*-test. Statistical significance was accepted when $p<0.05$.

Results:

No change of fibronectin and collagen IV expression was observed in rats post ET-1 injection

Previously, we found that ET-1 increased the soluble FN expression and FN matrix formation in cultured primary human optic nerve head astrocytes. Astrocytes are the major glial cells at the optic nerve head, therefore, it's important to detect if ET-1's effect in FN expression is also through astrocytes *in vivo*. FN expression was monitored by the immunofluorescent staining. The strong staining of FN was observed at sclera, veins and arteries at optic nerve heads, whereas staining of FN at ONH was relatively weak comparing with staining at sclera. Moreover, there was no increase of FN observed in treatment groups (Fig 1.) including 2- and 14-day treatments except the one eye that the lens was hit by a needle when the eye was injected and acquired a hemorrhage. In this eye, the significant increase in FN, collagen IV was detected and was served as a positive staining control (Fig 2A and 2B). There was very low staining in the negative control without the incubation of primary antibodies (Fig 2C). The immunoreactivity of collagen IV was very slightly increased in some treatment eyes, but remained unchanged in most treated eyes (Fig 1.).

MMP-9 was increased in ET-1-injected rats

Out of 5 eyes of ET_B deficient rats following 2 days post injection of ET-1, there was increased MMP-9 detected in four eyes and unchanged in one eye. Out of four eyes of wildtype (wt) rats 2 days post injection of ET-1, there was increased MMP-9 detected in

three eyes and unchanged in one eye (Table 3). After the images were quantitated by using NIH ImageJ software, the result showed that there was a 50-60% increase in the treated eye compared to the contralateral eyes ($p<0.05$, n=5 in ET_B deficient rats, n=4 in wildtype rats) (Fig. 3.). No significant difference was observed from staining in eyes of ET_B deficient and wildtype rats ($p>0.05$). No difference was found in HEPES-treated eye compared to the contralateral control.

An increased MMP-9 level was detected in three eyes of ET_B sl/sl rats and two eyes of wildtype 14 days post ET-1 injection (Table 3.). One eye of the wildtype rats got a hemorrhage and served as a positive control.

Collage VI was increased in ET-1-injected rats

Out of five eyes of ET_B deficient rats following 2 days post injection of ET-1, there was increased collagen VI detected in four eyes and unchanged in 1 eye. Out of four eyes of wildtype (wt) rats 2 days post injection of ET-1, there was increased collagen VI detected in three eyes and unchanged in one eye (Table 3). A 50-70% increase in collagen VI staining was detected in treated eyes of ET_B deficient rats and wildtype rats ($p<0.05$, n=5 in ET_B deficient rats, n=4 in wildtype rats). There was significant difference compared to contralateral eyes, whereas no difference between two rat types was seen (Fig 4).

Two out of three eyes from ET_B deficient rats and two out of three eyes from wildtype following 14 days post injection of ET-1, increased collagen VI was detected (Table 3). Unchanged collagen VI was detected in one eye from ET_B deficient rat. One eye of wildtype rat got a hemorrhage.

GFAP expression was increased in some treated eyes, but its basal level varied

There were five sl/sl and four wt rats in the 2-day ET-1 injection group excluding the rat with ONH region lost in sections. GFAP immunoreactivity was increased in three out of five ET_B deficient and two out of four wt rats, but unchanged in two of ET_B deficient and two of wt (Table 3). GFAP staining was only seen in ONH region, indicating astrocyte distribution was limited in ONH (Fig. 5.). Another interesting finding was that staining of GFAP greatly varied from rat to rat, indicating the basal level of GFAP was different.

Protein expression varies in different regions of the optic nerve

The immunoreactivity of MMP-9, collagen VI and collagen IV displayed the differential intensity from the anterior of ONH and the posterior region of ONH. The weak staining was observed at the anterior region of ONH, and strong staining at the posterior region (transition zone), which was the corresponding region of the laminar cribrosa in human eye (Fig 6.). However, the staining of FN was unchanged from the anterior to the posterior. The significant staining of MMP-9, collagen VI and collagen IV was along the optic nerve but not sclera and other tissue around the optic nerve. The staining of GFAP displayed the different patterns. In some eyes, there was strong staining of GFAP at anterior regions of ONH (Fig 6.), but the stronger staining observed at posterior regions (data not shown). It may suggest that there are differential stages of astrocyte migration from the anterior region to the posterior region of optic nerve.

Discussion:

Mechanisms leading to apoptosis of RGCs, cupping of optic nerve head and slow degeneration of optic nerve seen in glaucoma can be examined in experimental animal models. Since ET-1 is a very potent vasoconstrictor and there is an elevation of ET-1 levels found in aqueous humor and vitreous of glaucoma patients and glaucoma animal models, a glaucomatous animal model of ischemia has been established using intravitreal ET-1 injection or perfusion in rat, rabbit and primate [28-30, 34, 35]. In addition to ET-1-reduced blood flow at optic nerve head of treated eyes in rabbit and primate [28, 29, 32], the significant RGC apoptosis, cupping of the optic nerve head, loss of axons, a reduction of neurofilament, blockade of the retrograde and anterograde transport and activation of astrocytes were reported in these models [28-30, 32, 34-37]. However, the mechanism of optic nerve cupping and ECM remodeling remains unclear.

Astrocytes are a major source of MMPs and provide extracellular matrix components in term of the regulation of ECM components in the brain and eye, [5]. Reactive astrocytes involved in astrogliosis may be responsible for ECM remodeling in glaucoma. Increased IOP is strongly correlated with elevated endothelin-1 (ET-1) as well as the increase in ET_B receptor expression in astrocytes with marked elevation in GFAP, a marker for astrogliosis [26]. Sprague–Dawley rats intravitreally injected with ET-1 for 14 days[36] showed a significant increase of GFAP in retina. In the current study, the increased GFAP staining in retina as well as optic nerve head was observed in about half of treated eyes of wistar rats. As these were saggital section, the nerve fiber layer of the retina, in which astrocytes are located, was relative thin. It was difficult to observe the intensity of

GFAP staining from this angle, therefore the minor change of intensity was difficult to analyze. It was also reported that GFAP staining at the optic nerve head was attenuated one week after elevated IOP was achieved in rats with hypertonic saline injection, and it was restored 33 days after continuous elevation of IOP in rats[38]. This restored GFAP staining may be due to reactivation of astrocytes in response to increased ET-1 observed in elevated-IOP rats. Therefore, the results in the current study might represent the differential responses of astrocytes, which were in different activation level.

An increase in expression of MMPs and accumulation of ECM molecules including collagen IV, collagen VI, elastin was reported in the elevated-IOP model and in the optic nerve transection model [7, 9-11]. The immunoreactivity of collagen VI was increased at the optic nerve head of ET-1-injected eyes in current study, this result was consistent with the report from elevated-IOP model [38]. In human primary open-angle glaucoma, Hernandez et al demonstrated that there was an elevation of immunoreactivity of elastin and collagen VI detected in the lamina cribrosa as well as increased collagen IV detected around nerve bundle [6], suggesting ECM remodeling occurs during glaucoma progression. The anatomy structure of the optic nerve head in rat is somewhat different than that of human, there is no the lamina cribrosa instead of a transition zone containing the myelinated connective tissue. In our study, the stronger immunostaining was also observed in the transition zone rather than the anterior head region (Fig. 7). However, the similar astrocyte distribution and migration at the optic nerve head were illustrated at untrastructural level between human and rat [8].

MMP-9 is a regulatory MMP that increases in response to a number of stimuli including the elevated IOP, and appears to play a crucial role in inducing apoptosis of RGCs. For example, Fini's group showed that RGC apoptosis may be significantly correlated with the degradation of laminin from the inner membrane and directly related to the increased activity of MMP-9 at the same layer [10]. Zhang also reported that intravitreal injection of kainic acid in mice caused MMP-9 upregulation in the retina as well as activation of astrocytes. The decrease in laminin immunoreactivity in the ganglion cell layer and significant loss of retinal ganglion cells were correlated with increased activity of MMP-9 [39]. Guo et al showed that the elevated-IOP-induced RGC apoptosis was positively correlated with the expression of MMP-9, TIMP-1 and collagen I, but negatively correlated with laminin at the RGC layer [11]. Such observations suggest that ECM remodeling may contribute to the deleterious pathological changes in the retina and the optic nerve head. However, the alteration of MMP-9 activity at the optic nerve head was seldom reported. In the current study, an increase of MMP-9 expression was detected at the optic nerve head of ET-1-induced eyes. The immunoreactivity of MMP-9 was even stronger in the transition zone of optic nerve, indicating that the higher expression of MMP-9 may be in response to the greater accumulation of ECM molecules including collagen IV, collagen VI and elastin. In addition, in agreement with other glaucomatous animal models, there was intensive staining of MMP-9 in RGC layer of the retina and this staining was increased in ET-1-treated eyes (data not shown). The increased MMP-9 in the retina was similar to the response of MMP-9 at the optic nerve head, suggesting that ET-1 appears to upregulate the expression of MMP-9.

An interesting finding in this study is that no differences in MMP expression and accumulation of ECM molecules were found in ET-1-treated eyes of ET_B deficient rats and wildtype rats. The possible explanations are that there are many factors that exert their effects simultaneously in the *in vivo* animal experiments. For example, ET-1, TGF-β, connective tissue growth factor, and neurotrophins, which are all involved in regulation of ECM remodeling, are expressed at optic nerve head [8, 11]. How these factors exert their function and regulate each other is not clear. Perhaps the one-time intravitreal administration of ET-1 is not sufficient to be a predominant factor than other factors in the induction of ECM remodeling. In addition, whether ET_A has the same functions with ET_B at optic nerve head is not clear. If so, ET_A could take the role of ET_B in ET_B-deficient rats. In future study, the expression of ET_A at optic nerve head will be monitored. Furthermore, co-administration of ET-1 with ET_A/ET_B antagonist, bosentan, or ET_B antagonist, BQ788, into vitreous may provide more information about functions of ET-1 and its receptors in ECM remodeling at optic nerve head.

In this study, ECM remodeling has been shown in the model of ET-1-induced optic neuropathy in rats injected with ET-1 into the vitreous. The upregulated expression of MMP-9 and collagen VI was detected in both ET_B deficient rats and wildtype wistar rats, whereas the deposition of FN and collagen IV was not changed. ET-1-induced changes in MMPs and ECM expression could lead to turnover of ECM and contribute to the remodeling often seen in neurodegeneration diseases, such as glaucoma.

Reference:

1. Quigley E, Quigley H, Pease M, Kerrigan L. Quantitative studies of elastin in the optic nerve heads of persons with primary open-angle glaucoma. *Ophthalmology* 1996;103:1680-1685.

2. Clark AF, Yorio T. Ophthalmic Drug Discovery. *Nat Rev Drug Discov* 2003;2:448 -459.

3. Quigley H. Number of people with glaucoma worldwide. *Br J Ophthalmol* 1996;80:389-393.

4. Hernandez M, Pena J. The optic nerve head in glaucomatous optic neuropathy. *Arch Ophthalmol* 1997;115:389-395.

5. Hernandez MR. The optic nerve head in glaucoma: role of astrocytes in tissue remodeling. *Prog Retin Eye Res* 2000;19:297-321.

6. Hernandez M, Andrzejewska W, Neufeld A. Changes in the extracellular matrix of the human optic nerve head in primary open-angle glaucoma. *Am J Ophthalmol* 1990;109:180-188.

7. Johnson EC, Morrison JC, Farrell S, Deppmeier L, Moore C. G., McGinty M. R. The Effect of Chronically Elevated Intraocular Pressure on the Rat Optic Nerve Head Extracellular Matrix. *Exp Eye Res* 1996;62:663-674.

8. Morrison JC, Johnson EC, Cepurna W, Jia L. Understanding mechanisms of pressure-induced optic nerve damage. *Prog Retin Eye Res* 2005;24:217-240.

9. Agapova OA, Kaufman PL, Lucarelli MJ, Gabelt BAT, Hernandez MR. Differential expression of matrix metalloproteinases in monkey eyes with experimental glaucoma or optic nerve transection. *Brain Res* 2003;967:132-143.

10. Chintala SK, Zhang X, Austin JS, Fini ME. Deficiency in Matrix Metalloproteinase Gelatinase B (MMP-9) Protects against Retinal Ganglion Cell Death after Optic Nerve Ligation. *J Biol Chem* 2002;277:47461-47468.

11. Guo L, Moss SE, Alexander RA, Ali RR, Fitzke FW, Cordeiro MF. Retinal Ganglion Cell Apoptosis in Glaucoma Is Related to Intraocular Pressure and IOP-Induced Effects on Extracellular Matrix. *Invest Ophthalmol Vis Sci* 2005;46:175-182.

12. Schinelli S. The brain endothelin system as potential target for brain-related pathologies. *Curr Drug Target CNS Neurol Disord* 2002;1:543-553.

13. Prasanna G, Krishnamoorthy R, Clark AF, Wordinger RJ, Yorio T. Human Optic Nerve Head Astrocytes as a Target for Endothelin-1. *Invest Ophthalmol Vis Sci* 2002;43:2704-2713.

14. Rogers S, Peters C, Pomonis J, Hagiwara H, Ghilardi J, Mantyh P. Endothelin B receptors are expressed by astrocytes and regulate astrocyte hypertrophy in the normal and injured CNS. *Glia* 2003;41:180-190.

15. Nelson J, Bagnato A, Battistini B, Nisen P. The endothelin axis: emerging role in cancer. *Nat Rev: Can* 2003;3:110-116.

16. Grant K, Loizidou M, Taylor I. Endothelin-1: a multifunctional molecule in cancer. *Br J Cancer* 2003;88:163-166.

17. Bagnato A, Natali PG. Targeting endothelin axis in cancer. *Can Treat Res* 2004;119:293-314.

18. Tian X, Tang G, Chen Y. The effects of endothelin-1 and selective endothelin receptor-type A antagonist on human renal interstitial fibroblasts in vitro. *Zhonghua Yi Xue Za Zhi* 2002;82:5-9.

19. Fraccarollo D, Bauersachs J, Kellner M, Galuppo P, Ertl G. Cardioprotection by long-term ETA receptor blockade and ACE inhibition in rats with congestive heart failure: mono- versus combination therapy. *Cardiovascu Res* 2002;54:85-94.

20. Fraccarollo D, Galuppo P, Bauersachs J, Ertl G. Collagen accumulation after myocardial infarction: effects of ETA receptor blockade and implications for early remodeling. *Cardiovascu Res* 2002;54:559-567.

21. Gomez-Garre D, Ruiz-Ortega M, Ortego M, et al. Effects and interactions of endothelin-1 and angiotensin II on matrix protein expression and synthesis and mesangial cell growth. *Hypertension* 1996;27:885-892.

22. Nakamura T, Ebihara I, Tomino Y, Koide H. Effect of a specific endothelin A receptor antagonist on murine lupus nephritis. *Kidney Int* 1995;47:481-489.

23. Noske, WHensen J, Wiederholt M. Endothelin-like immunoreactivity in aqueous humor of patients with primary open-angle glaucoma and cataract. *Graefes Arch Clin Exp Ophthalmol* 1997;235:551-552.

24. Tezel G, Kass M, Kolker A, Becker B, Wax M. Plasma and aqueous humor endothelin levels in primary open-angle glaucoma. *J Glaucoma* 1997;6:83-89.

25. Kallberg ME, Brooks DE, Garcia-Sanchez GA, Komaromy AM, Szabo NJ, Tian L. Endothelin 1 Levels in the Aqueous Humor of Dogs With Glaucoma. *J Glaucoma* 2002;11:105-109.

26. Prasanna G, Hulet C, Desai D, et al. Effect of elevated intraocular pressure on endothelin-1 in a rat model of glaucoma. *Pharmacol Res* 2005;51:41-50.

27. Ahmed F, Brown KM, Stephan DA, Morrison JC, Johnson EC, Tomarev SI. Microarray Analysis of Changes in mRNA Levels in the Rat Retina after Experimental Elevation of Intraocular Pressure. *Invest Ophthalmol Vis Sci* 2004;45:1247-1258.

28. Orgul S, Cioffi G, Bacon D, Van Buskirk E. An endothelin-1-induced model of chronic optic nerve ischemia in rhesus monkeys. *J Glaucoma* 1996;5:135-138.

29. Orgul S, Cioffi G, Wilson D, Bacon D, Van Buskirk E. An endothelin-1 induced model of optic nerve ischemia in the rabbit. *Invest Ophthalmol Vis Sci* 1996;37:1860-1869.

30. Chauhan BC, LeVatte TL, Jollimore CA, et al. Model of Endothelin-1-Induced Chronic Optic Neuropathy in Rat. *Invest Ophthalmol Vis Sci* 2004;45:144-152.

31. Cioffi G, Sullivan P. The effect of chronic ischemia on the primate optic nerve. *Eur J Ophthalmol* 1999;Suppl 1:S34-36.

32. Sasaoka M, Taniguchi T, Shimazawa M, Ishida N, Shimazaki A, Hara H. Intravitreal injection of endothelin-1 caused optic nerve damage following to ocular hypoperfusion in rabbits. *Exp Eye Res* 2006;83:629-637.

33. Taniguchi T, Shimazawa M, Sasaoka M, Shimazaki A, Hara H. Endothelin-1 impairs retrograde axonal transport and leads to axonal injury in rat optic nerve. *Curr Neurovasc Res* 2006;3:81-88.

34. Cioffi G, Orgul S, Onda E, Bacon D, Van Buskirk E. An in vivo model of chronic optic nerve ischemia: the dose-dependent effects of endothelin-1 on the optic nerve microvasculature. *Curr Eye Res* 1995;14:1147-1153.

35. Cioffi GA, Wang L, Fortune B, et al. Chronic Ischemia Induces Regional Axonal Damage in Experimental Primate Optic Neuropathy. *Arch Ophthalmol* 2004;122:1517-1525.

36. Lau J, Dang M, Hockmann K, Ball AK. Effects of acute delivery of endothelin-1 on retinal ganglion cell loss in the rat. *Exp Eye Res* 2006;82:132-145.

37. Stokely ME, Brady ST, Yorio T. Effects of Endothelin-1 on Components of Anterograde Axonal Transport in Optic Nerve. *Invest Ophthalmol Vis Sci* 2002;43:3223-3230.

38. Johnson EC, Deppmeier LMH, Wentzien SKF, Hsu I, Morrison JC. Chronology of Optic Nerve Head and Retinal Responses to Elevated Intraocular Pressure. *Invest Ophthalmol Vis Sci* 2000;41:431-442.

39. Zhang X, Cheng M, Chintala SK. Kainic Acid-Mediated Upregulation of Matrix Metalloproteinase-9 Promotes Retinal Degeneration. *Invest Ophthalmol Vis Sci* 2004;45:2374-2383.

Figure Legends:

Figure 1. No change of fibronectin and collagen IV expression was observed in rats post ET-1 injection:

Collagen IV and FN were determined with immunofluorescent staining. Red: collagen IV; Green: FN. A, C, E: ONH sections from contralateral eyes; B, D: ONH sections from ET-1-injected eyes. F: ONH sections from HEPES-injected eyes. A and B: sections from ET_B-deficient rats. C, D, E and F: sections from wildtype rats.

Figure 2. Increased immunoreactivity of fibronectin and collagen IV in hemorrhaged eye:

Collagen IV and FN were determined with immunofluorescent staining at the optic nerve head section. Red: collagen IV; Green: FN. A: ONH section from contralateral eye; B. ONH section from ET-1-injected eye that got hemorrhaged; C. Negative staining without the incubation of primary antibodies.

Figure 3. MMP-9 staining was increased at ONH in ET-1-injected rats:

Expression of MMP-9 was monitored by immunofluorescent staining. A. histograph shows summary of quantified MMP-9 staining at ONH of rats post ET-1 injection for 2 days. *: $p<0.05$ vs. contralateral eye, student t-test, n=5. B. The representative images showing MMP-9 staining in different condition showed in figure from rats post ET-1 injection for 2 days.

Figure 4. Collagen VI staining was increased at ONH in ET-1-injected rats:

Expression of collagen VI was monitored by immunofluorescent staining. A. histograph shows summary of quantified collagen VI staining at ONH of rats post ET-1 injection for 2 days. *: $p<0.05$ vs. contralateral eye, student t-test, n=5. B. The representative images showing collagen VI staining in different condition showed in figure from rats post ET-1 injection for 2 days.

Figure 5. GFAP expression was increased in some treated eyes, but its basal level varied.

Expression of GFAP was monitored by immunofluorescent staining. A, C, E and G: ONH sections from contralateral eyes; B, D, F and H: ONH sections from ET-1-injected eyes. Red: MMP-9; Green: GFAP

Figure 6. Protein expression varied in different regions of the optic nerve

MMP-9, collagen IV, TIMP-2, FN and GFAP were stained at the transition zone of the optic nerve. A. MMP-9(red)+GFAP(green). B. COL IV (red)+FN (green); C. MMP-9(red)+TIMP-2(green) D. COL VI (red)+FN (green)

Figure 1

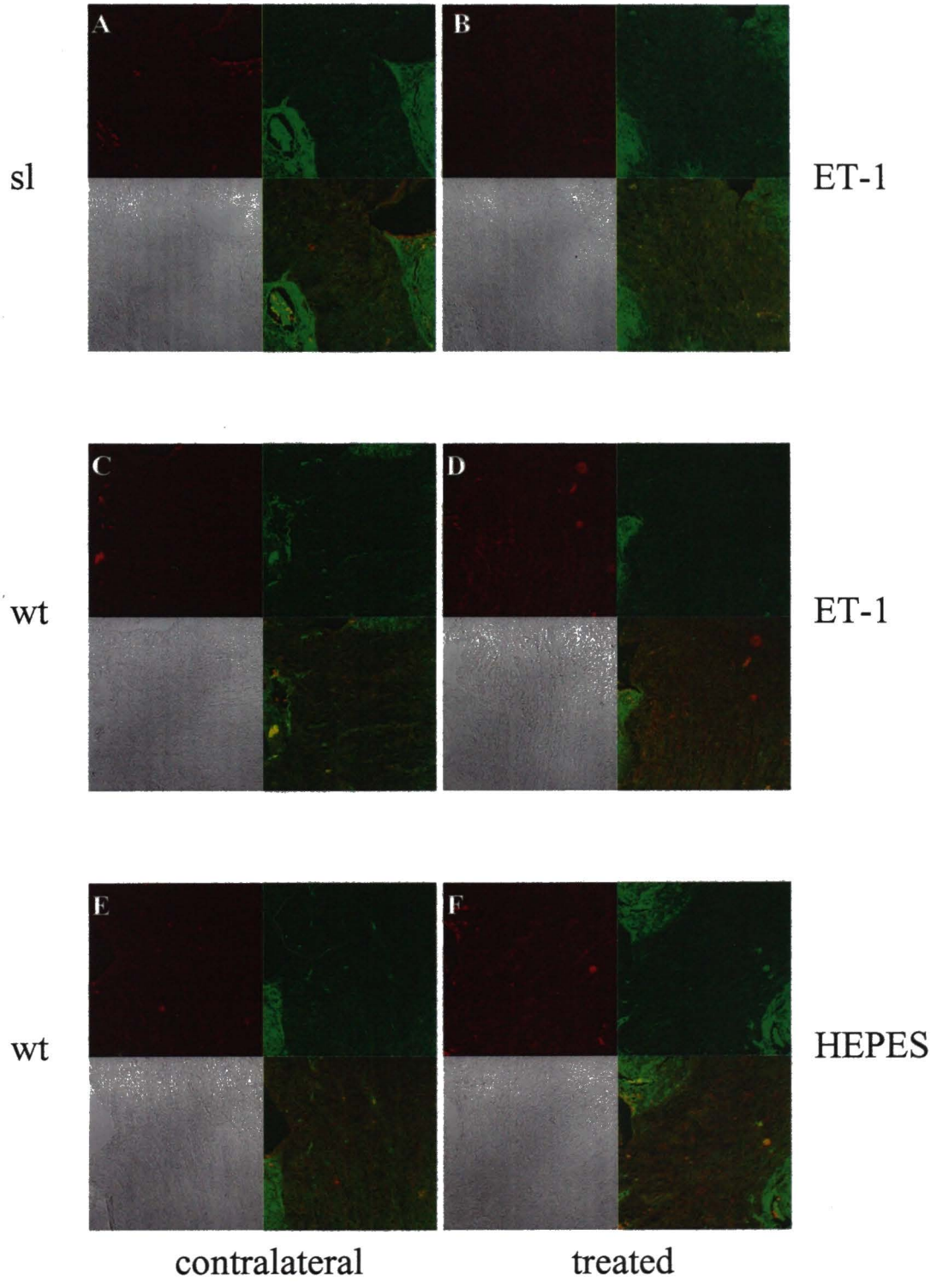

Figure 2

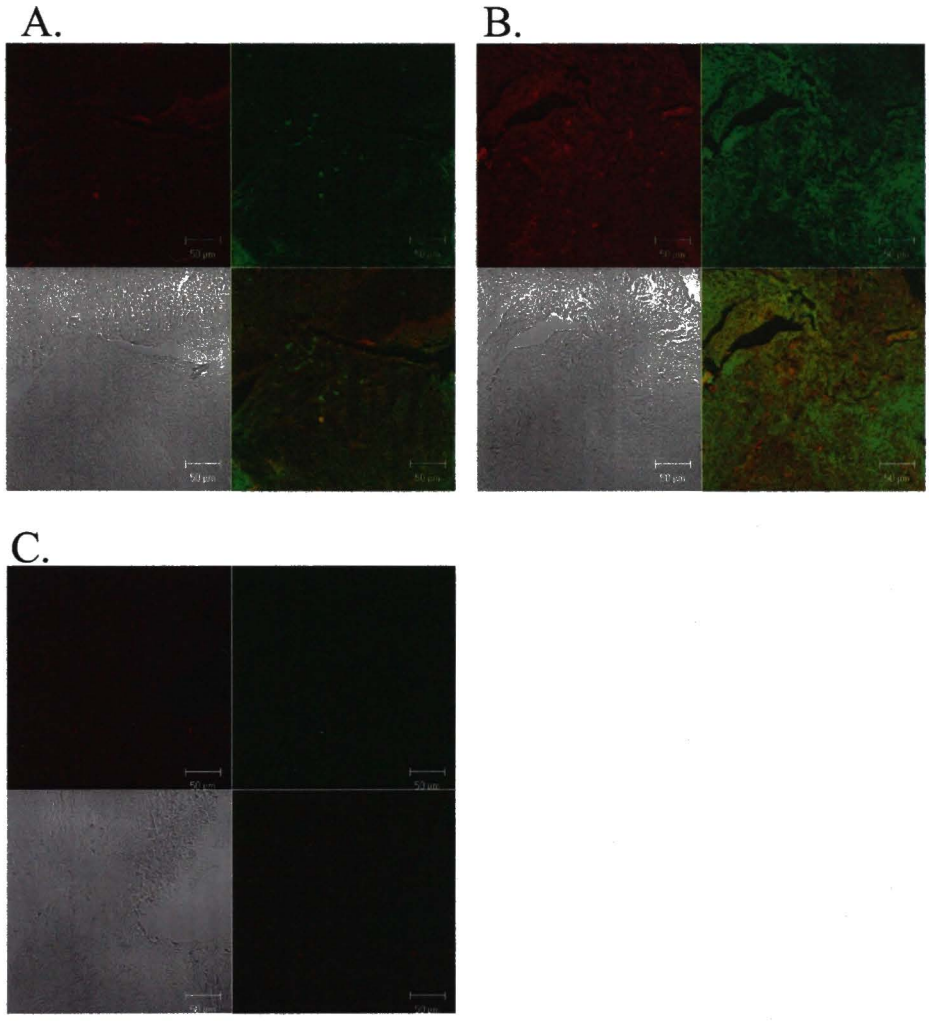

Figure 3

A.

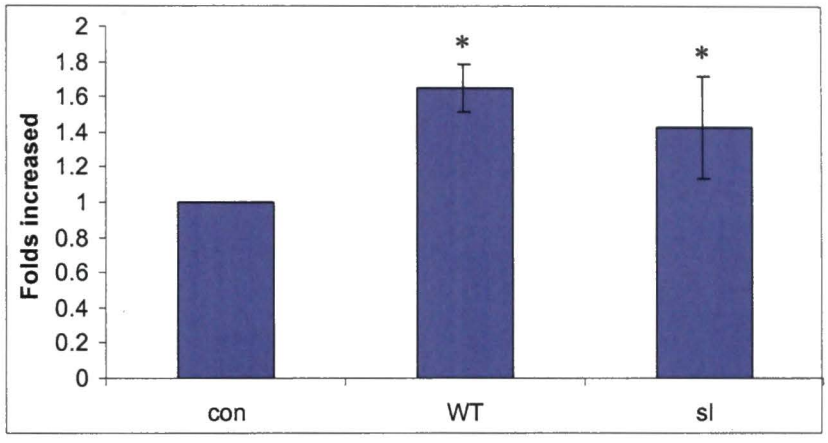
Folds increased
2
1.8
1.6
1.4
1.2
1
0.8
0.6
0.4
0.2
0
*
*
con
WT
sl

B.

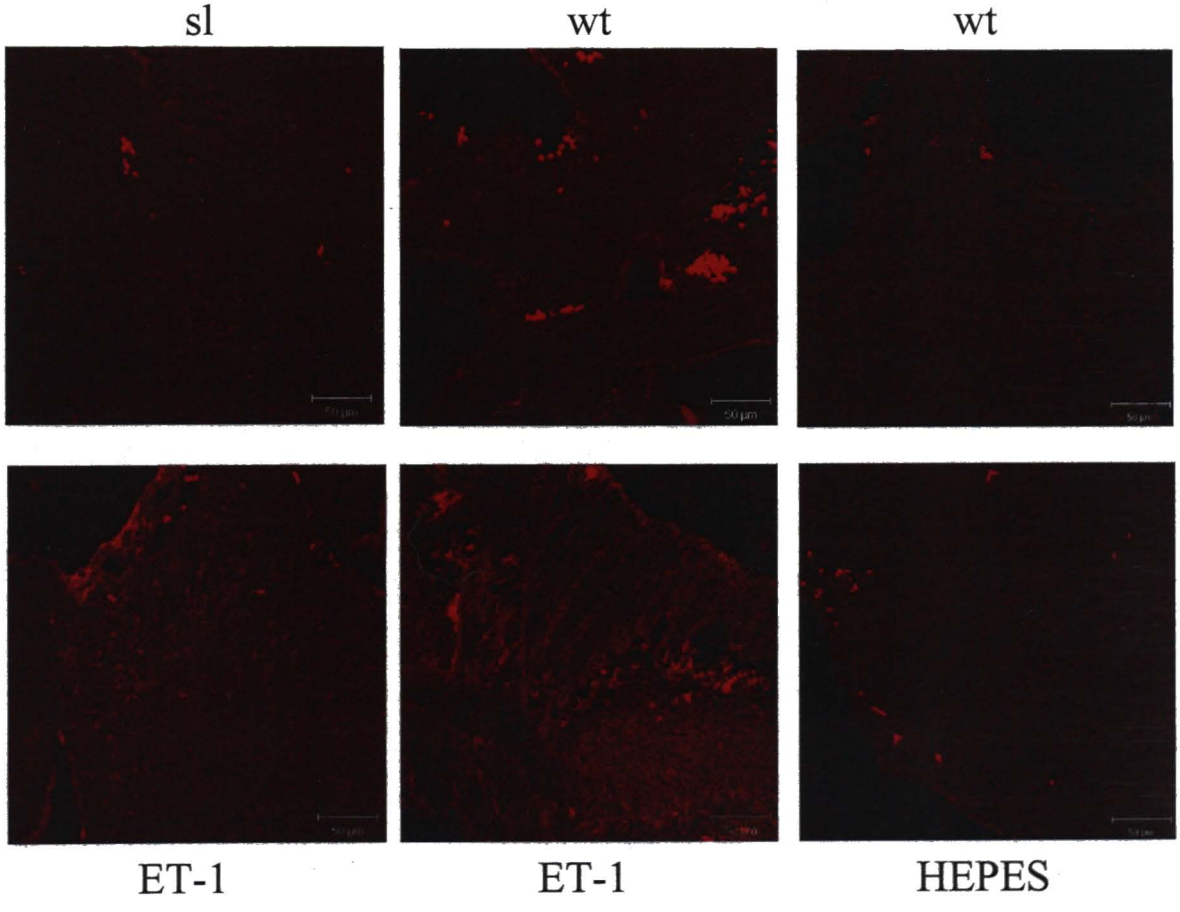
sl
wt
wt
ET-1
ET-1
HEPES

Figure 4

A.

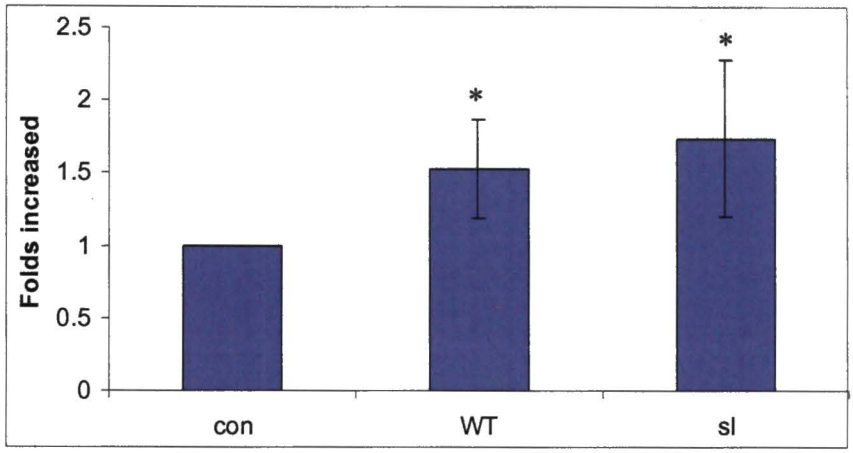

B.

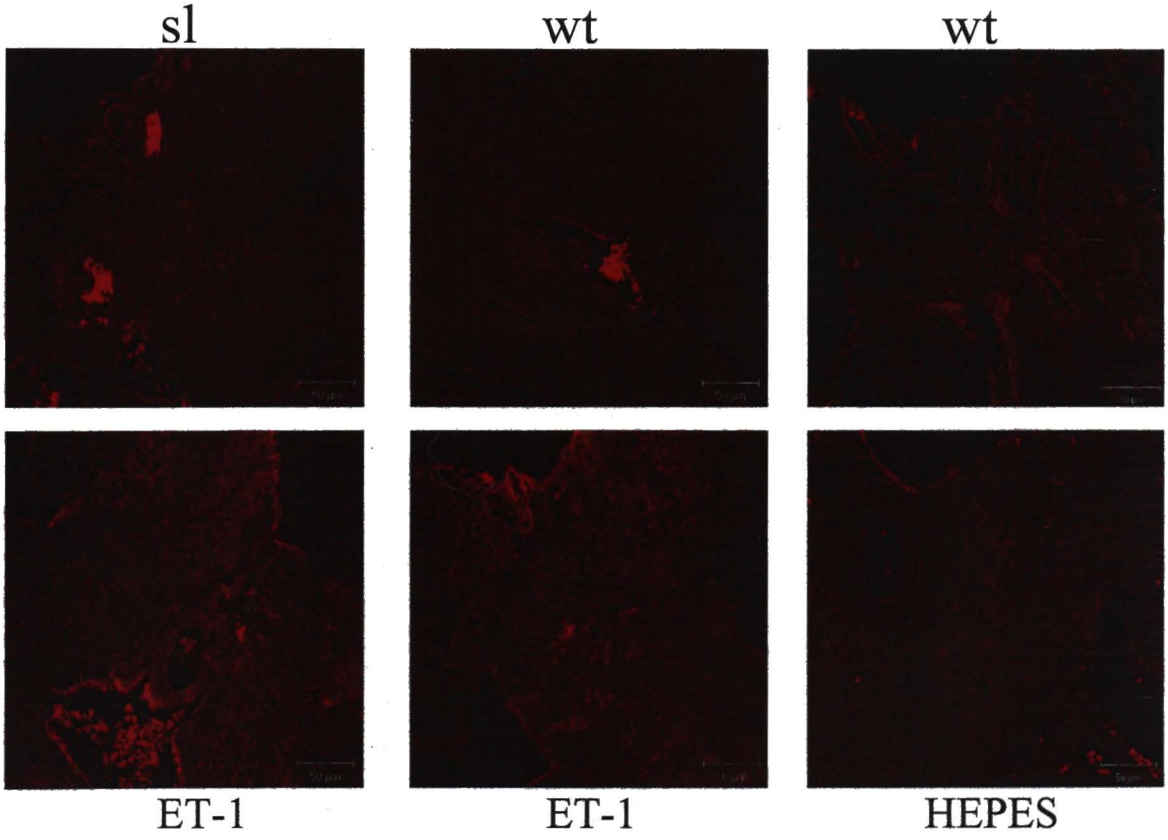

Figure 5

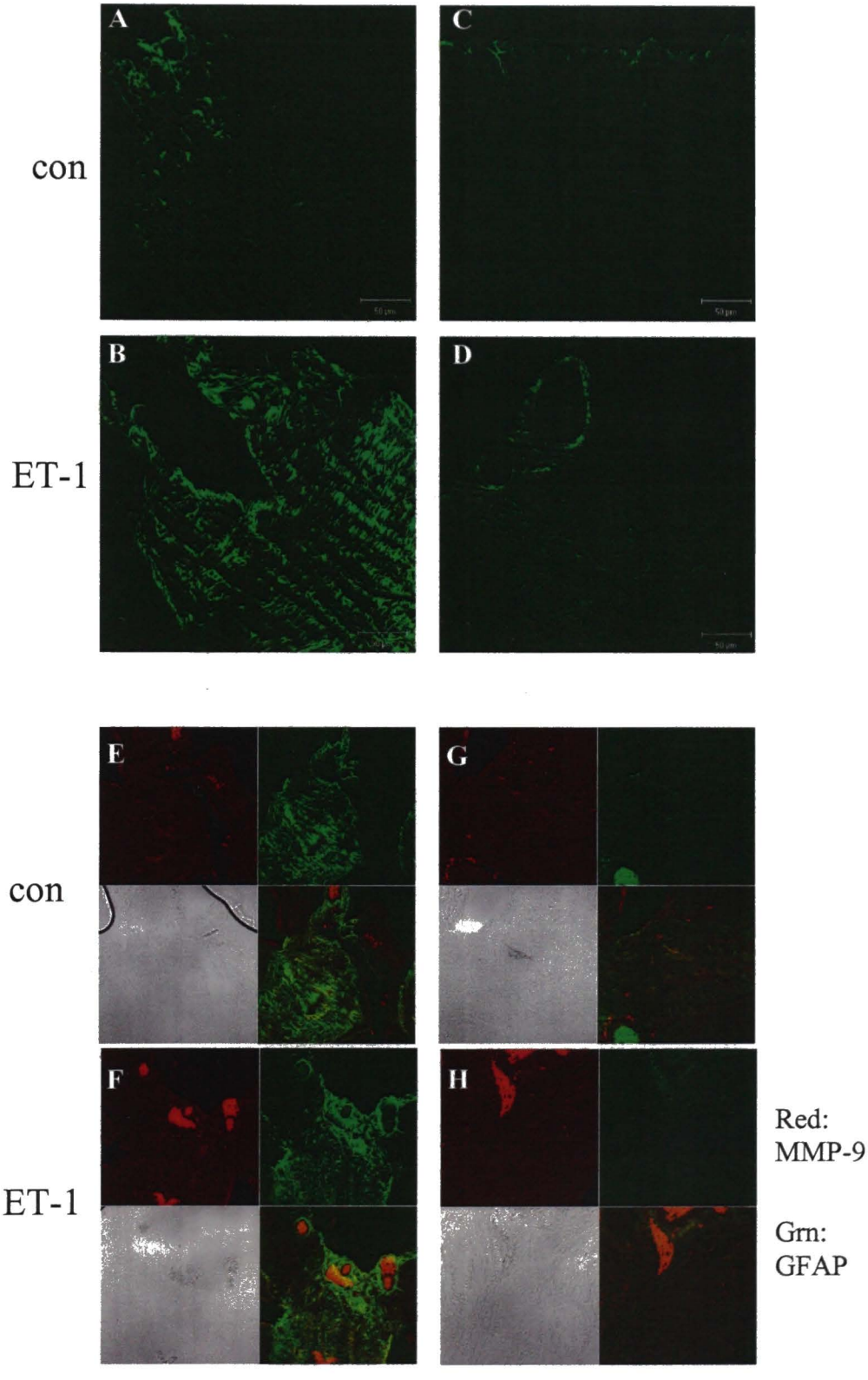

Figure 6

A.

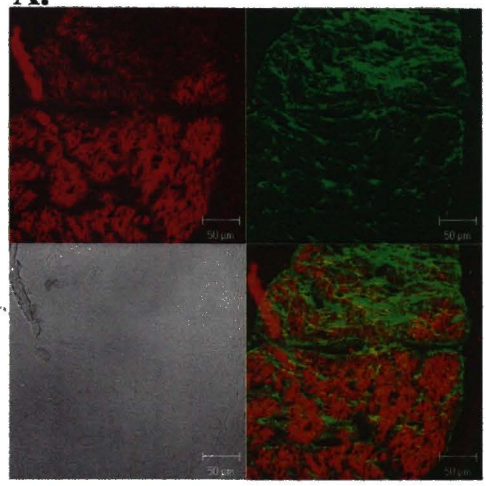

MMP-9(red)+GFAP(green)

B.

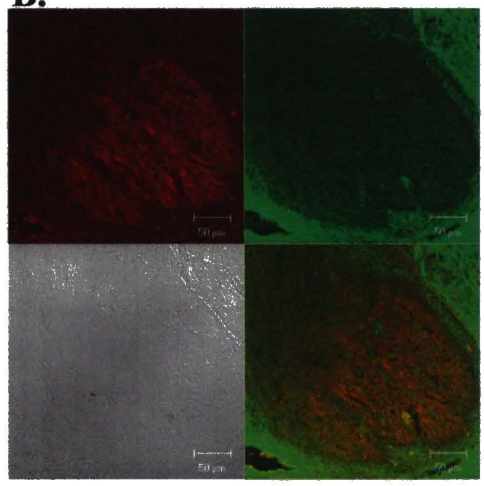

COL IV (red)+FN (green)

C.

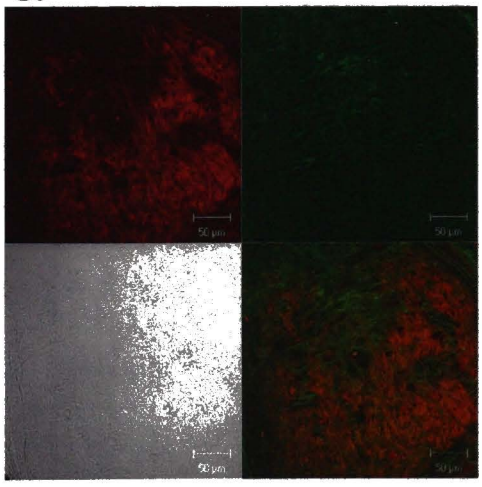

MMP-9(red)+TIMP-2(green)

D.

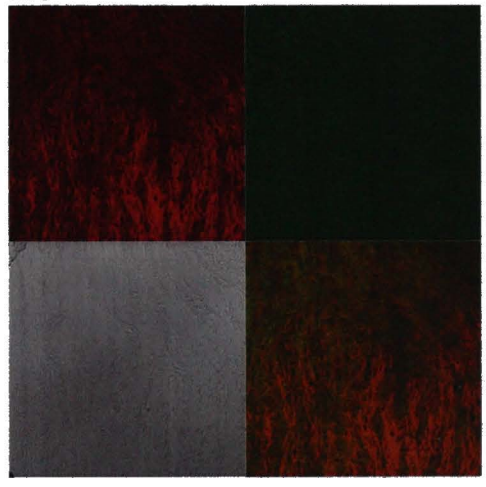

COL VI (red)+FN (green)

Table 1. Rats and ET-1 Injection Condition

(2-day ET-1 injection)

Animal number	Gender	Age	Description	Which eye	Treatment *intra vitreous*
6-12-8	M	10	sl/sl	R	NT
				L	ET-1
19-42-43	F	6	sl/sl	R	NT
				L	ET-1
6-12-9	M	10	sl/sl	R	NT
				L	ET-1
43-49-9	F	5	sl/sl	R	NT
				L	ET-1
43-49-36	F	4	sl/sl	R	NT
				L	ET-1
42-42-20	M	4	sl/sl	R	NT
				L	ET-1
43-49-11	F	5	WT	R	NT
				L	ET-1
43-49-33	M	4	WT	R	NT
				L	ET-1
19-35	F	12	WT	R	NT
				L	ET-1
19-43-44	M	5	WT	R	NT
				L	ET-1
19-42-27	M	8	WT	R	NA
				L	ET-1
19-42-38	F	6	WT	R	NA
				L	HEPES
19-43-26	M	8	WT	R	NA
				L	HEPES

* NT: no treatment

Table 2. Rats and ET-1 Injection Condition

(14-day ET-1 injection)

Animal number	Gender	Age	Description	Which eye	Treatment *intra vitreous*
6-12-5	F	10	sl/sl	R	NT
				L	ET-1
19-42-41	M	6	sl/sl	R	NT
				L	ET-1
6-12-7	M	10	sl/sl	R	NT
				L	ET-1
6-12-4	M	12	WT	R	NT
				L	ET-1
19-43-25	M	8	WT	R	NT
				L	ET-1
19-42-39	F	6	WT	R	NT
				L	ET-1
19-43-47	F	4	WT	R	NT
				L	HEPES
19-43-22	F	8	WT	R	NT
				L	HEPES

* NT: no treatment

Table 3. Summary of immunostaining results of several proteins at ONH in rats with ET-1 intravitreal injection

Protein probed	ET-1 injection days	Rat type and numbers	Increased	Unchanged	ONH lost in section	Hemorrhage or Inflammation
MMP-9	2	sl /6	4	1	1	-
		wt /5	3	1	1	-
	14	sl /3	3	-	-	-
		wt /3	2	-	-	1
Collagen VI	2	sl /6	4	1	1	-
		wt /5	3	1	1	-
	14	sl /3	2	1	-	-
		wt /3	2	-	-	1
TIMP-2	2	sl /6	3	2	1	-
		wt /5	2	2	1	-
	14	Not Tested				
GFAP	2	sl /6	3	2	1	-
		wt /5	2	2	1	-
	14	sl /3	1	1	1	-
		wt /3	1	1	-	1
FN	Unchanged in either sl or wt in two time points					
MMP-2 Collage IV	Very slightly increased in some rats, but no significant difference. Unchanged in most of rats.					

CHAPTER 5

Conclusions and Future Studies

Conclusions:

ET-1-induced signaling pathways linked to astrocyte activation, cell proliferation and ECM remodeling were examined in astrocyte cell culture *in vitro* and in rats following ET-1 intravitreal injection.

U373MG astrocytoma cells were used to investigate ET-1-induced signaling in cell proliferation. This cell line was selected as they are easy to culture and grow rapidly, whereas primary human optic nerve astrocytes grow very slow. Multiple signaling pathways appeared to be involved in ET-1-mediated astrocyte proliferation. Several findings, which were reflective of ET-1's mitogenic potential, were made in U373MG astrocytoma cells. It was determined that three signaling pathways, including ERK1/2, PKC, and PI3 kinase, were involved in ET-1-mediated cell proliferation of astrocytoma cells. Blocking one pathway completely abolished cell proliferation. It appeared that ERK1/2 activation was involved but independent of PKC and PI3 kinase activation by ET-1. It was also determined that the ET_B receptor was the dominant receptor involved in ERK1/2 phosphorylation as well as cell proliferation. Although Ras appeared to be a signaling pathway involved in activation of the ERK-MAPK pathway by ET-1, H-Ras was not, indicating that some other Ras members may be involved. It was also shown that some general protein tyrosine kinases, including c-Src, FAK, etc., were not involved in

ET-1 stimulation in U373MG as has been reported in other cell types. In addition, ERK1/2 phosphorylation was not transactivated by the EGF receptor by ET-1.

These studies also indicated that there was no activation of c/nPKC although PKC was involved in cell proliferation. No activation of PLC and no intracellular calcium mobilization were observed following ET administration provide additional support that c/nPKC were not involved. Therefore, atypical PKCs may play an important role in this event. In U373MG astrocytoma cells, neither c/nPKCs nor PI3 kinase are involved in ET-1-induced ERK1/2 signaling. However, MAPK-ERK, PKC and PI3K pathways appeared to exert their roles in parallel without a direct, apparent "cross-talk". They do, however, appear to activate key components (e.g. common and discrete transcription factors) in the proliferation response, because inhibition of any one parallel pathway blocks proliferation. This parallel signaling is not unlikely as the mitogenic response is dependent on many cellular processes that may be activated simultaneously in the cell proliferation responses and through complex signaling systems and important transcriptional events. Thus a critical component may be activated by each pathway and independent of the others. Therefore, blocking either pathway would exert the same outcome.

Studies with U373MG astrocytoma cells allowed us to map the major ET-1-induced signaling pathways involved in cell proliferation and reactivation of astrocytes. Our findings that the similar pathways exist in primary human optic nerve head astrocytes (hONAs) directed us to investigate the regulation of MMPs/TIMPs and ECM remodeling in ET-1-activated primary human optic nerve head astrocytes. In this aspect

of the study it was hypothesized that ET-1 was involved in ECM remodeling of the optic nerve head, a process seen in glaucoma. It was also proposed that this remodeling occurs as a result of the astrogliosis and reactivation of astrocytes by ET-1. The current results showed that ET-1 induced rapid phosphorylation of ERK1/2 and PKC βI/βII/δ, which played an important role in cell proliferation and reactivation of hONAs. ET-1 increased the activity of MMP-2 and the expression of TIMP-1 and 2 in a time- and dose-dependent manner. However, the expression of TIMP-1 and 2 induced by ET-1 was abolished by inhibitors of MAPK and PKC pathways, therefore, the enhanced activity of MMP-2 was observed due to a shift in the ratio of MMPs/TIMPs. Knock-down of MMP-2 using siRNA not only decreased the activity of MMP-2 but also decreased the expression of TIMP-1 and 2. ET-1 increased the soluble fibronectin (FN) expression as well as FN matrix formation. However, the accumulation sFN didn't enhance FN matrix formation. Unlike ET-1's effects on MMP-2, blockade of MAPK and PKC did not alter the expression and deposition pattern of FN in hONAs. It was suggested that the expression and deposition of FN are MAPK- and PKC-independent, whereas expression and activity of MMPs and TIMPs are MAPK- and PKC-dependent. ET-1-mediated regulation of ECM remodeling in hONA cells was involved in two signaling pathways, ERK-1/2 and PKC, since the blockade of these pathways increased the activity of MMP-2 but inhibited the expression of TIMP-1 and 2. Therefore, the balance of MMP/TIMP was shifted towards increased MMP production and activity. A balance of MMPs/TIMPs may be important not only to regulate the expression of MMPs and TIMPs but also to regulate

ECM remodeling. My current data showed that ET-1 shifted the balance of MMP activity and its substrates such that it may lead to ECM remodeling in activated hONA cells.

ET-1's effects on ECM remodeling at the optic nerve head were also examined following intravitreal ET-1 administration in rats. The upregulated expression of MMP-9 and collagen VI was detected in both ET_B deficient rats and wildtype wistar rats post ET-1 intravitreal injection for 2 and 14 days, whereas the deposition of FN and collagen IV was not changed. There was no significant difference in staining of MMP-9 and collagen VI between ET_B deficient rats and wildtype wistar rats. Such ECM remodeling in the current study provides additional insight into the mechanisms that may explain the glaucomatous changes that can occur in response to ET-1.

In summary (Figure 1), increased ET-1 levels, which may be a result of an elevation of IOP as seen in glaucoma, can activate several signaling pathways at the optic nerve head and this appears to occur through astrocytes. These signaling systems not only induce the activation of astrocytes but also modulated the expression of ECM molecules. This affects ECM turn over and remodeling by shifting the balance of MMPs and TIMPs. Such ECM remodeling could contribute to the pathological changes at the optic nerve head during glaucoma progression. These results also suggest that ET-1 may play a regulatory role in ECM remodeling, particularly during pathological conditions, such as glaucoma.

Figure 1

Hypothetical Actions of ET-1 in ECM Remodeling at the Optic Nerve Head

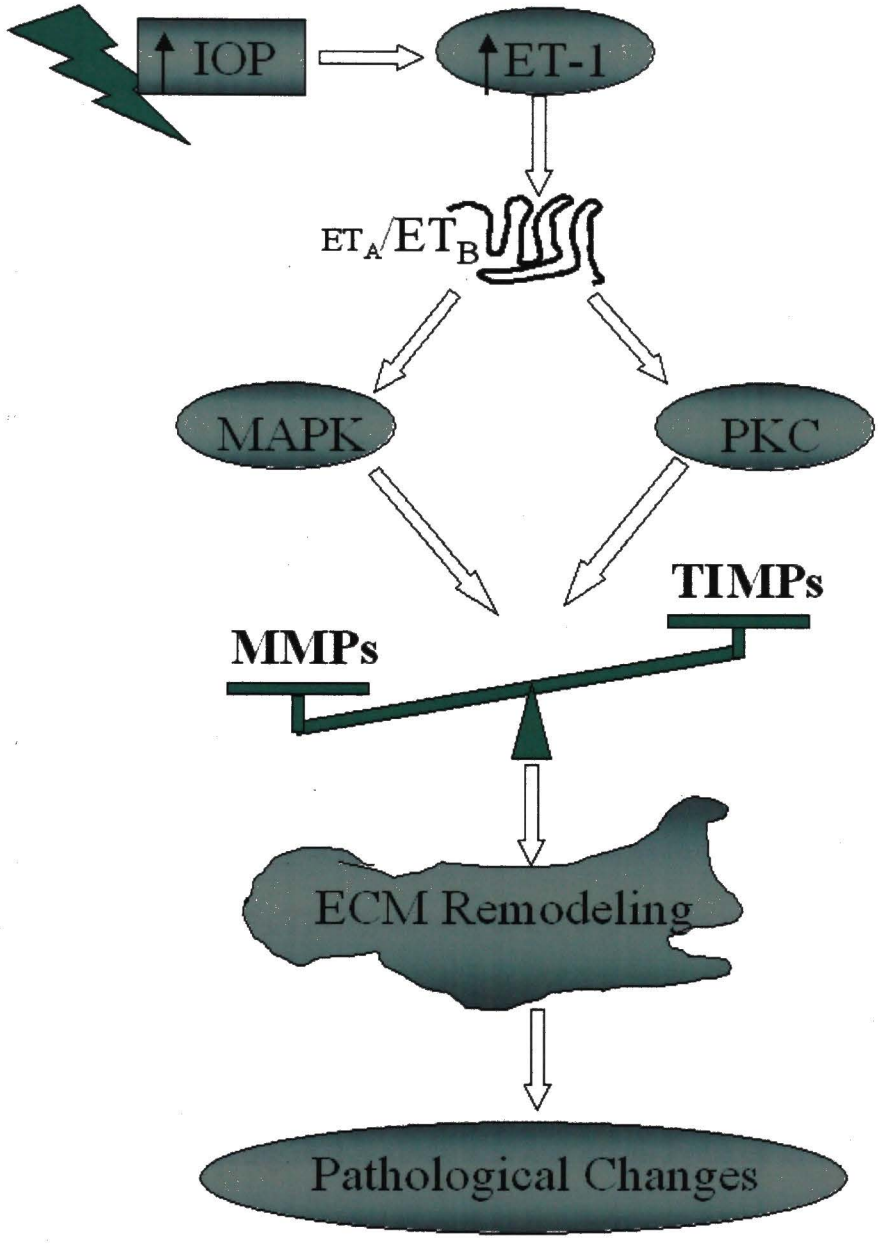

Figure 1. Hypothetical Actions of ET-1 in ECM Remodeling at the Optic Nerve Head. The increased ET-1 levels in response to an elevation of IOP as seen in glaucoma, can activate several signaling pathways including MAPK and PKC pathways. These signaling systems induce ECM turn over and remodeling by shifting the balance of MMPs and TIMPs. Such ECM remodeling could contribute to the pathological changes at the optic nerve head during glaucoma progression.

Future studies:

In order to answer some questions and address some of the uncertainty in the current study, some future experiments are designed.

1. Gene delivery *in vitro* and *in vivo*:

To investigate the regulation of MMPs and TIMPs, we used siRNA of MMP-2 or TIMP-2 to abolish the protein expression in hONAs, but because of the very low transfection efficiency obtained in primary cell culture, it was difficult to demonstrate significant knock-down using western blot analysis. Therefore, the pool of oligonucleotide-based siRNA will be used to enhance the transfection efficiency. Furthermore, overexpression of either MMPs or TIMPs will be designed to investigate the regulation of MMPs and TIMPs *in vitro* and *in vivo*. Adeno-associated virus (AAV) vectors, which provide the very high transfection efficiency, will be used. For the *in vivo* experiment, AAV-based MMP-2 or TIMP-2 can be intravetreally administrated to rats and the expression of MMPs/TIMPS as well as the deposition of ECM molecules can be probed by immunostaining or mass spectrometry.

2. To probe the ET_A and ET_B receptor in the retina and at the optic nerve head:

An interesting finding in this study was that no differences in MMP expression and accumulation of ECM molecules were found in ET-1-treated eyes of ET_B deficient rats and wildtype rats. The possible explanations are that 1) there are too many factors exerting their functions simultaneously in the *in vivo* animal experiments. For example, ET-1, TGF-β, connective tissue growth factor, and neurotrophins, which are involved in regulation of ECM remodeling, are expressed at the optic nerve head [1, 2]. How these

factors exert their function and regulate each other is not clear; 2) the function of ET_A and ET_B at the optic nerve head is not clear. Measurement of the expression of ET_A and ET_B is necessary. In addition, co-administration of ET-1 with ET_A/ET_B antagonist, bosentan, or ET_B antagonist, BQ788, into the vitreous may provide more information about functions of ET-1 and its receptors in ECM remodeling at the optic nerve head.

3. Laser-Capture Microdissection and MASS spectrometry and PCR

Since it's difficult to quantitate the data from immunostaining, 2-Dimension electrophoresis followed by mass spectrometry analysis could provide information to determine ET-1 and its receptors at the retina ganglion cells or the optic nerve head. Laser-capture microdissection is a practical method to isolate the target tissues or cells with less contamination of others. Mass spectrometry will be employed to identify protein levels in cells and tissues isolated by the laser-capture microdissection, and RT-PCR or realtime-PCR to identify the mRNA level of interest genes.

REFERENCE:

1. Guo L, Moss SE, Alexander RA, Ali RR, Fitzke FW, Cordeiro MF. Retinal Ganglion Cell Apoptosis in Glaucoma Is Related to Intraocular Pressure and IOP-Induced Effects on Extracellular Matrix. *Invest Ophthalmol Vis Sci* 2005;46:175-182.

2. Morrison JC, Johnson EC, Cepurna W, Jia L. Understanding mechanisms of pressure-induced optic nerve damage. *Prog Retin Eye Res* 2005;24:217-240.

CHAPTER 6

APPENDIX-Supplemental Data

The following data, which were part of the dissertation, were not included in the other chapters. However, they were important to support the previous results.

Figure 1

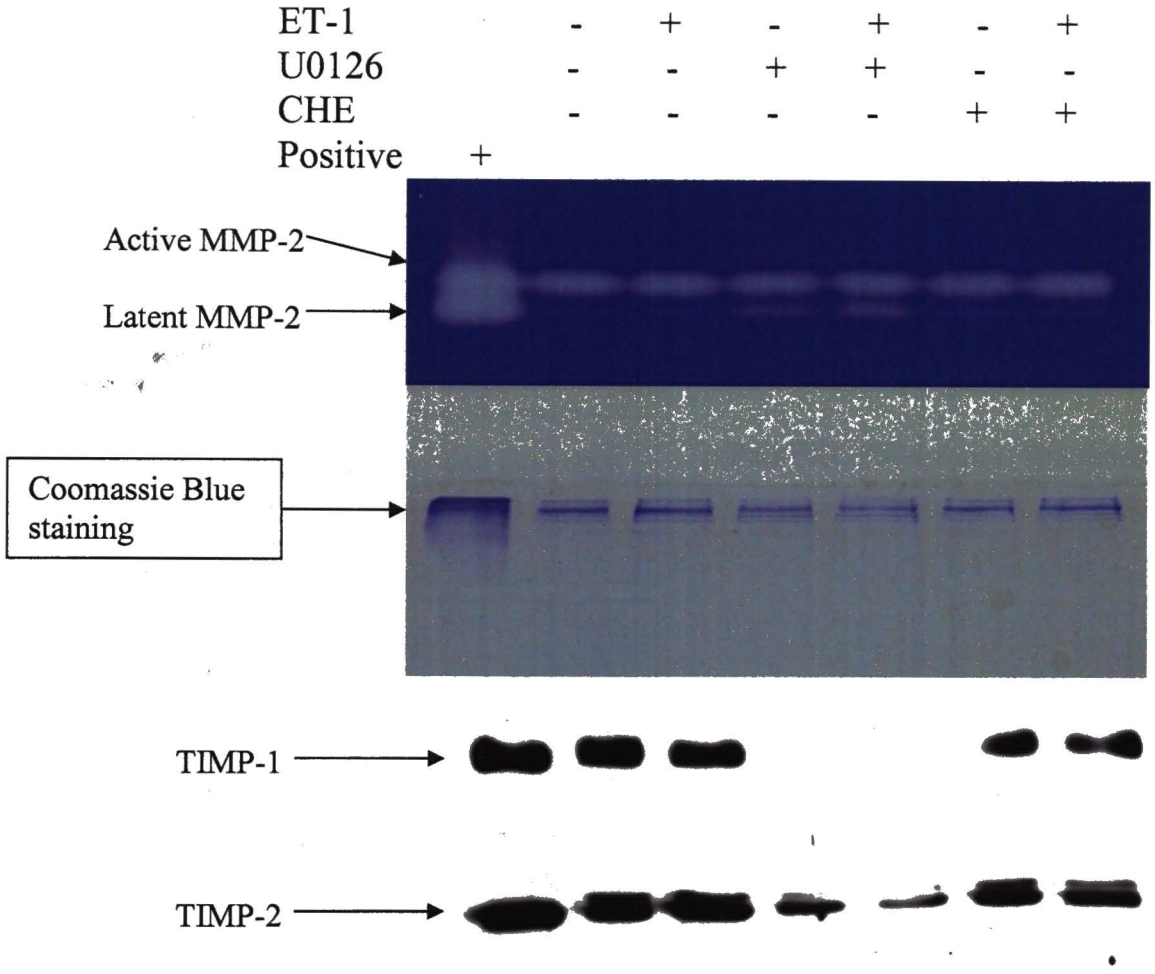

Figure 1. Loading control of proteins in the culture media for zymography assay. 0.1% coomassie blue R-250 were used to stain the SDS-PAGE gels that had be used for transferring protein to nitrocellulose membranes for WB. The proteins left in gels were stained and served as a loading control. We found many protein-staining bands in gels and took several bands with approximately same staining density as normalization controls. (CHE: chelerythrine, a PKC inhibitors; Positive: the positive protein control containing MMP-2, 9, 3 and TIMP-1, 2)

Figure 2

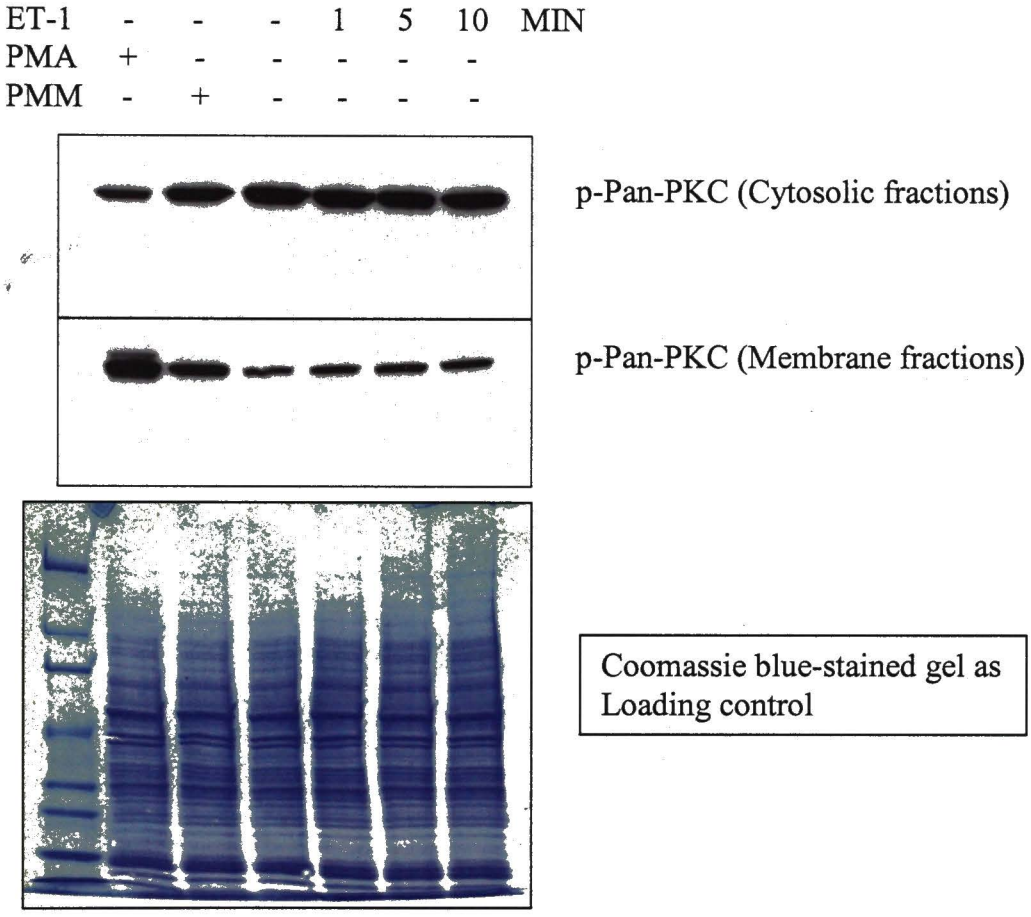

Figure 2. Loading control of PKC translocation assay.
0.1% coomassie blue R-250 Staining of the SDS-PAGE gels was used to normalize the protein loading. The proteins from cytosolic fractions in gels were stained with 0.1% coomassie blue R-250 and served as a loading control for detecting the phosphorylation of PKC isoforms. Western blot showed the phosphorylation of PKC isoforms in the cytosolic and membrane fractions.